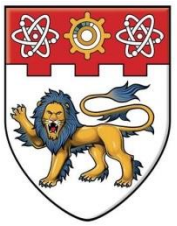

NANYANG TECHNOLOGICAL UNIVERSITY

BIOMECHANICAL ANALYSIS AND MODEL DEVELOPMENT APPLIED TO TABLE TENNIS FOREHAND STROKES

ZHANG ZHIQING

SCHOOL OF MECHANICAL AND AEROSPACE ENGINEERING

2016

BIOMECHANICAL ANALYSIS AND MODEL DEVELOPMENT APPLIED TO TABLE TENNIS FOREHAND STROKES

ZHANG ZHIQING

School of Mechanical and Aerospace Engineering

A thesis submitted to the Nanyang Technological University

in partial fulfilment of the requirement for the degree of

Doctor of Philosophy

2016

Acknowledgement

I would like to take this opportunity to express my sincerest gratitude and appreciation to my supervisor Prof Chou Siaw Meng, my co-supervisor Dr Ben Halkon and my former supervisor Prof Qu Xingda for their invaluable supervision, guidance and advice for this thesis as well as my PhD study during the past four years. I thank them for their patience and encouragement that have carried me through difficult times, and for their insights and suggestions that have helped shape my research skills and results.

Abstract

Table tennis playing involves complex spatial movement of the racket and human body. It takes much effort for the novice players to better mimic expert players. The evaluation of motion patterns during table tennis training, which is usually achieved by coaches, is important for novice trainees to improve faster. However, traditional coaching relies heavily on coaches' qualitative observation and subjective evaluation. While past literature shows considerable potential in applying biomechanical analysis and classification for motion pattern assessment to improve novice table tennis players, little published work was found on table tennis biomechanics. To attempt to overcome the problems and fill the gaps, this research aims to quantify the movement of table tennis strokes, to identify the motion pattern differences between experts and novices, and to develop a model for automatic evaluation of the motion quality for an individual.

Firstly, a novel method for comprehensive quantification and measurement of the kinematic motion of racket and human body is proposed. In addition, a novel method based on racket centre velocity profile is proposed to segment and normalize the motion data. Secondly, a controlled experiment was conducted to collect motion data of expert and novice players during forehand strokes. Statistical analysis was performed to determine the motion differences between the expert and the novice groups. The experts exhibited significantly different motion patterns with faster racket centre velocity and smaller racket plane angle, different standing posture and joint angular velocity etc. Lastly, a support vector machine (SVM) classification technique which was employed to build a model for motion pattern evaluation is addressed. The model development was based on experimental data with different feature selection methods and SVM kernels to achieve the best performance (F_1 score) through cross-validated and Nelder-Mead method. Results showed that the SVM classification model exhibited good performance with an average model performance above 90% in distinguishing the stroke motion between expert and novice players.

This research helps to better understand the biomechanical mechanisms of table tennis strokes, which ultimately benefits the improvement of novice players. The phase segmentation and normalization methods for table tennis strokes are novel, unambiguous and straightforward to apply. The quantitative comparison identified the comprehensive differences in motion between experts and novice players for racket and

human body in continuous phase time, which is a novel contribution to the academic literature. The proposed classification model shows potential in the application of SVM to table tennis biomechanics and can be exploited for automatic coaching.

Table of Contents

ABSTRACT……I

TABLE OF CONTENTS……III

LIST OF FIGURES……VII

LIST OF TABLES……X

LIST OF SYMBOLS AND ABBREVIATIONS……XII

CHAPTER 1 INTRODUCTION……1

1.1 BACKGROUND……1

1.2 MOTIVATION……2

1.3 OBJECTIVES AND SCOPE……3

CHAPTER 2 A REVIEW OF THE STATE AND ART OF RACKET SPORTS BIOMECHANICS……5

2.1 BIOMECHANICS IN RACKET SPORTS……5

2.1.1 Table tennis training and basic strokes……5

2.1.2 Different phases in a stroke……6

2.1.3 Performance analysis……7

2.1.4 Arm motion in racket sports……9

2.2 MOTION PATTERNS IN RACKET SPORTS……13

2.2.1 Phase duration……13

2.2.2 Racket motion……14

2.2.3 Human body movement……15

2.2.4 Variability of motion patterns……23

2.3 MODEL DEVELOPMENT AND CLASSIFICATION……26

2.3.1 Expert system and machine learning……26

2.3.2 Related work in sports biomechanics……29

2.3.3 Support vector machine and related techniques……31

2.4 SUMMARY 38

CHAPTER 3 A NOVEL KINEMATIC MODEL FOR TABLE TENNIS STROKES……..... 39

3.1 QUANTIFICATION OF STROKE MOTION 39

3.1.1 Definitions for the model 39

3.1.2 Measurement and calculations for the model 42

3.2 PHASE SEGMENTATION AND NORMALIZATION 45

3.2.1 Phase segmentation based on racket centre velocity profile 45

3.2.2 Piecewise normalization 51

3.2.3 Visualization for the normalized kinematic model 53

3.3 SUMMARY 53

CHAPTER 4 MOTION PATTERN DIFFERENCES BETWEEN EXPERT AND NOVICE TABLE TENNIS PLAYERS 55

4.1 EXPERIMENT DESIGN 55

4.1.1 Participants 55

4.1.2 Experimental setup 55

4.1.3 Procedure 57

4.2 DATA PROCESSING 57

4.2.1 Data filtering, reduction and normalization 57

4.2.2 Dependent variables 58

4.2.3 Statistical analysis 60

4.2.4 Stroke accuracy 60

4.2.5 Kinematic model visualization 60

4.2.6 Phase durations 62

4.2.7 Racket motion 64

4.2.8 Human motion 68

4.3 DISCUSSION 70

4.3.1 Summary and highlights *70*

4.3.2 For the novice players *71*

4.3.3 Further to individual *72*

CHAPTER 5 CLASSIFICATION MODEL FOR AUTOMATIC IDENTIFICATION OF MOTION QUALITY **75**

5.1 OVERVIEW OF MODEL DEVELOPMENT 75

5.2 DATASETS AND METHODOLOGY FOR MODEL DEVELOPMENT AND OPTIMIZATION 77

5.2.1 Raw dataset *77*

5.2.2 Feature selection *78*

5.2.3 SVM and cross-validation *80*

5.2.4 Tuning SVM parameters C and K *81*

5.3 PRELIMINARY SETTINGS FOR SVM AND RESULTS 83

5.3.1 Effects of different SVM kernels *83*

5.3.2 Effects of different p-threshold *84*

5.4 RESULTS 87

5.4.1 PCA on the dataset *87*

5.4.2 Results by using dataset of ALL *88*

5.4.3 Results for all data subset with and without PCA *90*

5.4.4 All the results on a score table *91*

5.5 CLASSIFICATION MODEL 94

5.5.1 Summary *94*

5.5.2 Implementation of classification model *95*

5.5.3 Framework for coaching system *97*

CHAPTER 6 CONCLUSIONS AND CONTRIBUTIONS **99**

6.1 CONCLUSIONS 99

6.2 CONTRIBUTIONS 100

6.3 FUTURE WORK 101

REFERENCES…..... 102

APPENDIX A: DEFINITIONS OF HUMAN MOTION BASED ON ISB I

APPENDIX B: MOTION PATTERN DIFFERENCES (PART)..... I

APPENDIX C: CLASSIFICATION MODEL PERFORMANCE I

List of Figures

Figure 2-1 Phases of forehands (up) and backhands (down) (Ebrahim, 2010) 6

Figure 2-2 Structure of arm (left) and shoulder complex (right) 10

Figure 2-3 Three-dimensional model for arm motion calculation (Sprigings et al., 1994) 12

Figure 2-4 Contact and peak velocity with tiny time gap but concluded coincident by the author (Bootsma & Van Wieringen, 1990) 14

Figure 2-5 Support Vector Machine illustration in hyperspace x1-x2 32

Figure 2-6 Architecture of Support Vector Machine (Ruiz-Gonzalez et al., 2014) 34

Figure 2-7 Illustration of the sequence of steps in one iteration of the Nelder-Mead method for 2 dimensions (Gavin, 2013) 37

Figure 3-1 Global coordinate system and racket motion 39

Figure 3-2 Rotational movement of human trunk and upper limb 41

Figure 3-3 Marker placement 43

Figure 3-4 Joint coordinate systems for angle calculation 45

Figure 3-5 Phases during a forehand stroke 46

Figure 3-6 Example of distinct trajectories of racket centre between experts and novices 47

Figure 3-7 A typical example of racket centre resultant velocity profile 48

Figure 3-8 Easily identifiable phases time from racket velocity profile 49

Figure 3-9 High speed camera experiment 50

Figure 3-10 Results of high speed camera experiment 51

Figure 3-11 Racket centre velocity before (a) and after (b) alignment for two participants 52

Figure 3-12 Visualized kinematic (right) model from collected data 53

Figure 4-1 Experimental setup 56

Figure 4-2 Body dimension illustration 61

Figure 4-3 Visualized comparison of the posture of experts and novices at racket-ball contact 62

Figure 4-4 Phase durations for each participant 63

Figure 4-5 Comparison result of a) racket centre velocity RCx and b) racket angular velocity RRxz 65

Figure 4-6 Visualized racket centre trajectory with velocity and racket orientation for T_1-T_4 67

Figure 4-7 Comparison of an individual novice with an expert group 74

Figure 5-1 Development and optimization of the classification model 76

Figure 5-2 Architecture of training and testing of the SVM classifier 81

Figure 5-3 Architecture of the cross-validation 81

Figure 5-4 F_1 score with respect to C and K at phase time T_3 for the raw data set (RBF kernel) 83

Figure 5-5 Comparison of different kernel for the raw data 84

Figure 5-6 Results of raw data on different p-threshold 85

Figure 5-7 Results of raw data on different p-threshold with p=1 and p=0.05 highlighted 86

Figure 5-8 Results of different segments when p=1 (up) and p=0.05 (down) 87

Figure 5-9 Results for using ALL dataset without PCA (up) and with PCA (down) ... 89

Figure 5-10 Results for some dataset (D+V) (1st), D (2nd) and V (3rd) without PCA 91

Figure 5-11 Prediction score of trained SVM model 96

Figure 5-12 Desired classification model 96

Figure 5-13 Framework of the coaching system.....97

List of Tables

Table 2-1 Advantages and disadvantages of several methods for measuring coupling 22

Table 2-2 Statistics used for quantifying variability of repeat trials (Mullineaux, 2000) 24

Table 2-3 Comparing classification algorithms (Kotsiantis et al., 2007) 28

Table 2-4 Common SVM kernel functions 33

Table 2-5 Confusion matrix for a two class classifier 34

Table 3-1 Motion of the racket in each DOF 40

Table 3-2 Motion definition of the human kinematic model in each DOF 41

Table 3-3 Marker placement 43

Table 4-1 Number of strokes of each participant 58

Table 4-2 Comparison of body dimensions 61

Table 4-3 Comparison of mean and variability of durations of phases 63

Table 4-4 Comparison of different variables of racket motion on different phase time 65

Table 4-5 Comparison of different variables of human motion at different phase time 69

Table 5-1 Motion Abbr. for SVM input 78

Table 5-2 Basic feature combinations 79

Table 5-3 Percentages of retained the components 88

Table 5-4 Best performance of the model for ALL(D+V) without PCA 89

Table 5-5 F_1 score table showing all the results 92

Table 5-6 Selected feature combinations 95

List of Symbols and Abbreviations

Below lists the frequently-used symbols and abbreviations according to the orders of their appearance in this thesis.

Symbols / abbreviations	Representation
DOF	**Degree of freedom**
JCS	**Joint coordinate system**
ISB	**International Society of Biomechanics**
SVM	**Support Vector Machine**
RC	**Racket centre movement**
RC_x, RC_y, RC_z	Translational movement in *x*-, *y*-, *z*- directions
RC_{2D}, RC_{3D}	Resultant velocity in *2D* (*x*- and *z*-) and *3D* (*x*-, *y*- and *z*- directions)
RR	**Racket rotational movement**
RR_{xy}, RR_{yz}, RR_{xz}	Angular movement against the global *x*-*y*, *y*-*z*, *x*-*z* planes
TC	**Trunk centre movement**
TC_x, TC_y, TC_z	Translational movement in *x*-, *y*-, *z*- directions
T	**Trunk rotational movement**
T_{fe}, T_{ll}, T_{aa}	Flexion/extension; lateral left/right; axial rotation left/right
S	**Shoulder rotational movement**
S_{pe}, S_e, S_{ie}	Plane of elevation; elevation; internal/external rotation
E	**Elbow rotational movement**
E_{fe}, E_{ps}	Flexion/extension; pronation/supination
W	**Wrist rotational movement**
W_{fe}, W_{ru}	Flexion/extension; radial/ulnar flexion
Phase time	Phase time and phases (*Figure 3-5*)
P_{BS}, P_{FS}, P_{FT}	Backswing phase; forward swing phase; follow-through phase
T_1, T_2, T_3, T_4	The phase time between P_{BS}, P_{FS} and P_{FT}
T_x, $T_{x\text{-}y}$ $(1 \leqslant x,y \leqslant 4)$	The moment of phase time *x*, the phase time from *x* to *y*
(Miscellaneous)	
D	Displacement
V	Velocity
ALL	*ALL =(RC+RR+TC+T+S+E+W)*

Chapter 1 Introduction

1.1 Background

Table tennis is one of the most popular sports in the world. There are over 300 million table tennis participants worldwide, making it stand out in the list of the highest participation sports, as is reported by the International Sports Federation (*ISF*). Good motion patterns are essential for table tennis players to achieve good performance. Trainees in professional teams, for example, are instructed to repeat prescribed movement hundreds of times to construct stable motion patterns and develop so-called dynamic stereotype (Pavlov, 1927) for selected techniques. Good motion patterns can help the players keep continuity of hitting, improve overall appearance, and further strengthen, energize and revitalize the body. On the other hand, bad motion patterns may prevent further skill improvement because of interference between old and new learning, which is known as negative transfer (Singley, 1989).

However, trainees do not receive clear or timely feedback on the quality of their technical practice without a personal coach, and therefore they do not know how to improve accordingly. Though the fundamental knowledge and instructions may be available in some books, they lack sufficient details and are not effective enough. In fact, most novice and amateur players remain in a low-skill level and have difficulty in improving their table tennis skill without good assessment and instructions.

Coaches make great contributions to the improvement of players' techniques. They evaluate the trainees' motion patterns by observing and recalling good ones from their experience, and provide specific feedback to trainees to rectify their wrong

motion patterns. This requires the coaches to continuously observe and assess the players. However, such professionals may not always be available and hiring a coach can be costly. On the other hand, the fast flying table tennis ball prevents the coach from accurately observing and noticing all the detailed critical events which are required for a complete understanding or interpretation of performance (Franks & Miller, 1986). This may lead to low-quality instructions. Other factors, such as subjectivity and fatigue, more importantly the skill level and experience of the coach, may also affect the quality of coaching.

1.2 Motivation

Performance analysis (O'Donoghue, 2009) in sports helps develop an understanding of sports to enhance sports performance. Biomechanical research provides knowledge on the basic kinematic and kinetic features of specific athletic movements for performance enhancement, and has been used in a lot of sports-related research. Current biomechanical research on table tennis is limited without complete quantitative descriptions of the whole successive phases of table tennis strokes. In addition, most existing studies only focused on racket motion, and revealed little information on body segment biomechanics (Anglin & Wyss, 2000). The implementation of biomechanical analysis may help table tennis players better understand their motion patterns.

The integration of artificial intelligence techniques into the development of modern sports information systems enables a prompt and automatic evaluation of sport-specific parameters, thereby allowing the establishment of computer-based feedback and interventions (Baca et al., 2009). Unlike human, a computer system or algorithm is able to process a huge amount of data in a short time for objective and timely assessment of motion quality. The application of techniques in sports biomechanical

analysis has received little attention (R Bartlett, 2006), but has the potential in solving the problem since reviewed work (i.e. Section 2.3.2) presented good model performance in sports biomechanics.

The investigation on table tennis playing has found that very few reviewed biomechanical analysis work has been done on table tennis. This research aims to study the motion of racket and racket arm for the most basic forehand stroke by applying the methods of biomechanical analysis and model development in order to give better assessment of table tennis motion patterns.

1.3 Objectives and scope

This research has three major objectives:

1) To quantify the movement of table tennis forehand strokes.
2) To identify the differences in motion patterns between novice and expert players.
3) To further build a model for automatic evaluation of the motion quality of table tennis players for an individual.

The scope of the work includes different stages:

- Determination of the variables for quantification of the kinematic motion of racket and human body. Finding a method to measure data and calculate these kinematic variables from experiment with different phases distinguished between the beginning and the end of a stroke.
- Design an experiment and recruit table tennis players, including experts and novices, and collect their movement data of forehand strokes. Process the

experimental data with proposed method, and use statistical analysis to determine the differences between experts and novices.

- Develop a model for automatic evaluation of player motion quality for individuals. Tuning the settings and parameters of the model, and validate the model performance using available data from previous stages.

Chapter 2 A review of the state and art of racket sports biomechanics

2.1 Biomechanics in racket sports

2.1.1 Table tennis training and basic strokes

Technical practice is essential for table tennis trainees, especially low-level players. During technical practice, the feeding of balls is fixed or with certain variations so that players focus on improving their strokes and build so-called dynamic stereotype (Pavlov, 1927), which is a type of integral activity by the cerebrum of higher animals and man and manifested by a fixed succession of conditioned reflexes.

Multi-ball is a frequently used training method for table tennis technical practice. During multi-ball training, the feeder continuously sends the balls to the trainees, and the trainee repeats a specific technique multiple times in a short period. The feeder can be either a player, a coach, or even a robot. The robot is a useful aid for improving strokes and footwork, especially if a human feeder is not available. Training robots are available on the market and can provide precise control of the feeding parameters (e.g. angle and speed) of table tennis balls.

Beginners are recommended to start with the "big six", which includes the four basic striking techniques, plus serve and serve return. The four basic skills of strokes are forehand counterhit, backhand counterhit, forehand push, backhand push (Lee, 2001). Among the strokes, forehand counterhit is used to return any long balls and to hit high balls, and is the foundation of all forehand topspin strokes; backhand counterhit is similar to forehand counterhit but the reverse side of the racket is used, and is used to return top-spin balls as the foundation of all backhand topspin strokes.

This thesis focuses on the technical practice of the basic forehand stroke, as an

example study for the biomechanics of table tennis strokes.

2.1.2 Different phases in a stroke

Ballistic sports movement can be biomechanically subdivided into different phases. Roger Bartlett (2007) presented a general viewpoint of three phases: preparation phase, action phase and recovery phase. Mülling and Peters (2009) divided a table tennis stroke cycle into awaiting stage, preparation stage, hitting stage, finishing stage. Alexander and Honish (2009) segmented the cycle into preparatory movement, backswing phase, force producing phase, critical instant and follow-through. There are other examples that are not included here. Despite the fact that different phases or names of phases are used in different research studies, they actually referred to similar partial movements. A general decomposition into four phases was chosen for this thesis: preparatory phase, backswing phase, forward swing phase, and follow-through phase, as illustrated in *Figure 2-1*.

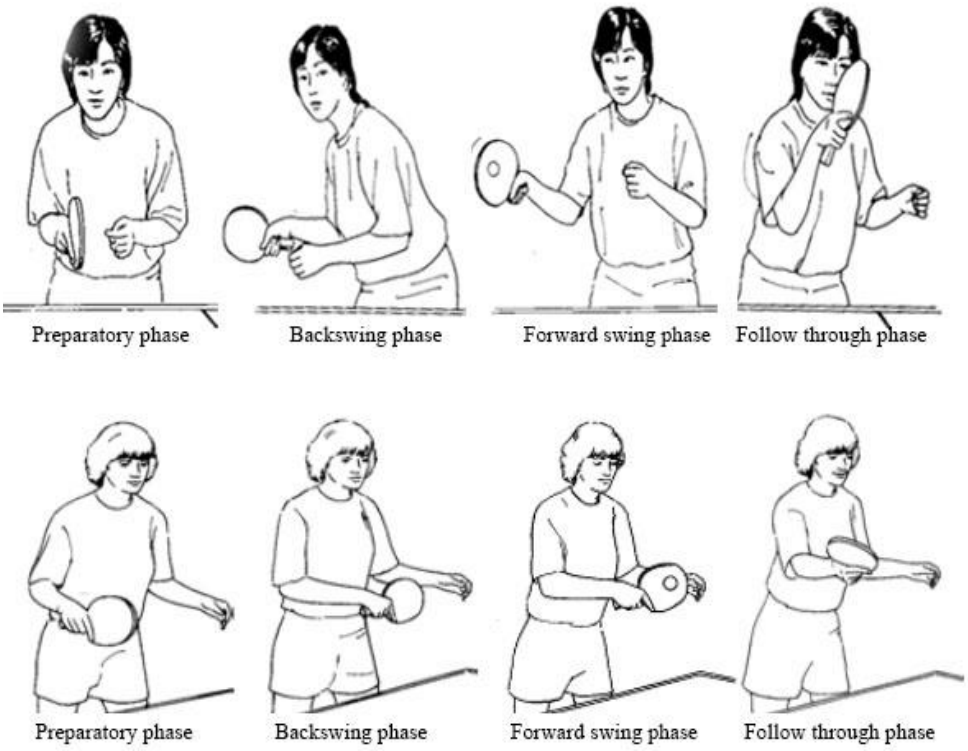

Figure 2-1 Phases of forehands (up) and backhands (down) (Ebrahim, 2010)

A complete table tennis stroke goes through all the four phases, and each involves a series of complex motions, especially the racket arm (the arm that controls the racket and intercepts the ball). The motions of racket and human body in different phases are qualitatively understandable through *Figure 2-1*. However, quantification is essential for further analysis on motion data in order to get a deeper understanding of the stroke, which can help players improve their performance.

2.1.3 Performance analysis

Performance analysis of sports, which is the investigation of actual sports in training or competition, aims to understand the complexities and dynamic nature of sports. Two different disciplines are connected with analysis and improvement of players' movement performance in racket sports— biomechanical analysis and notational analysis (Hughes & Bartlett, 2002).

Biomechanical analysis is the study of structures and functions of biological systems by means of "methods of mechanics". The laws of mechanics are applied in order to gain a greater understanding of athletic performance through mathematical modeling, computer simulation and measurement. Biomechanical analysis includes both kinematic (e.g. motions of bodies with respect to time, displacement, velocity, and speed of movement either in a straight line or in a rotary direction) and kinetic (e.g. forces associated with motion, including forces causing motion and forces resulting from motion) assessments trying to identify mechanical characteristics of performance.

Notational analysis (O'Donoghue, 2009) collects data like positions, actions, time and outcomes that can quantify critical events in a game. Notational systems such as Labanotation provide rich descriptions of the kinematic and also non-kinematic features of body movement (Foroud & Whishaw, 2006). These qualitative or

quantitative features can be further used to evaluate movement, tactical and technical performance (Ivan et al., 2011; Lees, 2003). Notational analysis can be used in evaluation or application of tactical analysis, technical analysis, movement analysis, development of a database and modeling, and educational use with coaches and players (Nevill et al., 2008).

Both biomechanical analysis and notational analysis involve the measurement of performers' movement based on "performance indicators". Systematic observation techniques are used by both methods, with a concern for data validity and reliability, and strong theoretical links with other sports science (particularly the dynamical system approach of ecological motor control) (R Bartlett, 2001). Both biomechanical analysis and notational analysis emphasize feedback to coaches and performers, and may assist the coaches by helping them understand the characteristics of certain sports or players. Yet there are many differences between them. Biomechanical analysis studies fine details of performance in individual sports thus involves technique analysis; while notational analysis usually uses gross tactical and technical indicators and is applied to team sports analysis, concerned mainly with strategies and tactics. Performance indicators for notational analysis and biomechanical analysis are also different: biomechanical analysts focus on kinematic and kinetic parameters; in contrast, notational analysts use match, tactical and technical performance indicators. Biomechanical analysis identifies performance indicators that relate to good and bad techniques; notational analysis identifies performance indicators that relate to good and bad team performance like tactics (Hughes & Franks, 2004).

According to the above reviews of characteristic differences between biomechanical analysis and notational analysis, this research, however, focuses on the technical skills of table tennis players therefore the biomechanical variables are studied. The

discipline of tactical indicators is not to be considered though may also contribute to the performance of players in the progressive training. Specifically, this thesis involves only the kinematic variables for the biomechanical analysis since the human body only interacts with the ground, with the kinematic movement of human body doing the major contribution to the movement of racket, and subsequently the table tennis ball, directly. The measurement of forces on the feet, on the other hand, requires additional equipment (e.g. force plate) which involves kinetic and inverse kinematic calculation including estimated mass of body segments and/or kinematics of lower limb, which may introduce additional errors. Therefore, the force measurement of feet is not applied in this thesis to simplify the study.

2.1.4 Arm motion in racket sports

To apply biomechanical analysis, the definitions of the kinematic movement of human body should be defined unambiguously. The human arm includes different segments and joints (*Figure 2-2* left), making it a complex subject in biomechanical analysis. Among these segments and joints, the shoulder is one of the most complex joints since it has a structure of three bones (clavicle, scapula and humerus), and a combination of 30 muscles, 5 joints and many tendons and ligaments (*Figure 2-2* right).

It is an onerous task to describe the motion of these bones considering their shapes and anatomical positions. Another difficulty lies in the measurement for the shoulder motion. It is hard to track the scapula and clavicle rotation using traditional marker-based method because of the large amount of under-skin movement and relatively small geometrical shape of the clavicle. Current available methods use magnetic markers and related apparatus to measure acromion, scapula ridge or appropriate landmarks with a scapulohumeral regression equation (Anglin & Wyss, 2000). These methods were quite complex to use.

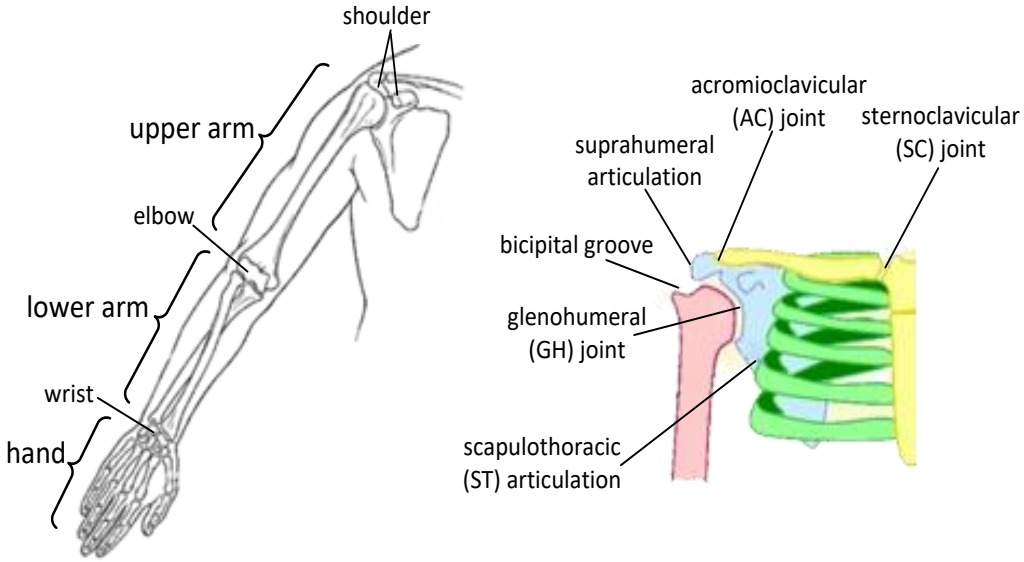

Figure 2-2 Structure of arm (left) and shoulder complex (right)

Most of the papers reviewed in biomechanics (e.g. citations in this thesis), however, did not include detailed definitions for the clavicle and scapula, but instead they simplified the motions of shoulder complex as relative movement of humerus with respect to the thorax. Existing researchers tended to put more effort on the motion of the entire arm during specific motion rather than the clavicle and scapula bones. Only in pathology and rehabilitation research it is confirmed that the shoulder component is very important. The simplification is also easy to understand clinically and accessible in daily living activities (Anglin & Wyss, 2000). The simplification also avoids complex measurement of clavicle and scapula, therefore is adopted in this research.

However, different researchers (e.g. Anglin & Wyss, 2000; Cheung et al., 2009; Sprigings et al., 1994; etc) have used different terms to describe arm movement without a unified definition especially for the shoulder motion, for example: flexion, abduction/adduction, horizontal abduction/adduction (Sprigings et al., 1994), vertical abduction/adduction etc. The different terminologies made it difficult to perform quantitative comparison between different studies. It is mainly due to the

difficulty in describing three-dimensional movement with many *DOF*s since there are multiple methods (e.g. vector-based methods, Cardan angles) and reference systems (e.g. sagittal plane, coronal plane, or any axis). Although none of them is wrong, there is no explicit conclusion that one is definitely the best.

Among the multiple methods applied to quantify arm motion including the shoulder, some are oversimplified as they only considered limited segments or did not involve enough *DOFs*. For example, some models were planar (e.g. Van Gheluwe et al. (1987)), some just included two segments (e.g. Putnam (1993), some ignored certain *DOF*s (e.g. Feltner (1989) assuming velocity around the longitudinal axis of each segment as zero). These relatively early research did not have the modern motion capture systems that most researcher use today.

Sprigings et al. (1994) used a three-dimensional computation method for capturing and calculating arm motions in their work, which included segment rotations about all the *DOF*s. It was also used by other researchers in similar racket sports studies (Elliott et al., 1995; Iino et al., 2008; X. Liu et al., 2009; Rodrigues et al., 2002). This was a vector-based method for the anatomical rotation of the upper arm, lower arm, and hand. Two marker points were located at each articulation *(Figure 2-3*). The movement of these marker points was captured by optical motion capture system. The centre of each segment and corresponding vectors were calculated from the marker points. The coordinate system of each body segment was then established based on vector arithmetic. Particularly, this model made calculation of the rotations around longitudinal axis possible. However, there are also some concerns about this method as vectors are sensitive to the directions (X. Liu et al., 2009). The errors may lead to negative vectors, which totally inverse the vectors and cause mistakes in calculating angular velocities.

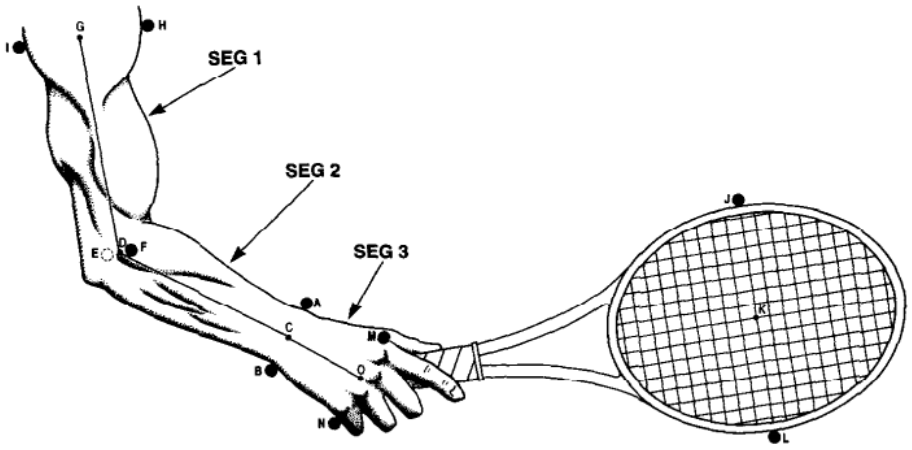

Figure 2-3 Three-dimensional model for arm motion calculation (Sprigings et al., 1994)

The International Society of Biomechanics (*ISB*) also provided recommended definitions of joint coordination systems and motions for human body (G. Wu et al., 2005). It provides fine details regarding the definitions for human body segments with the bony landmarks, and uses the sequences of Cardan angles to describe the rotation of joints. *ISB* included all the possible motions, even those rarely reported *DOF*s (e.g. the change of the carrying angle of elbow joint, which is the angle between the longitudinal axis of the ulna and the plane perpendicular to the flexion/extension axis). This method is relatively new and provides standards for unambiguous definitions compared to others.

Therefore, a typical human arm kinematic model with fine details would be established for motion analysis of table tennis players with the definitions according to *ISB* recommendation (G. Wu et al., 2005). Particularly, the simplification of shoulder motion may be adopted, which means movement of the humerus with respect to the thorax will be studied without more details of clavicle and scapula. This is because measurement of the clavicle and scapula requires additional complex equipment and no research revealed they were indispensable. In addition, the simplification is common in current racket sport research.

2.2 Motion patterns in racket sports

This section is organized according to different types and subjects of measures, including phase duration, racket motion, human body motion, and variability. Previous work and analytical methods on both table tennis and other racket sports were reviewed in the current section.

2.2.1 Phase duration

Phase time duration is the time spent during each phase of a table tennis stroke. Existing research showed a negative correlation between skill level and forward swing phase duration in table tennis playing, as reviewed by Ebrahim (2010): complete novices (*239 ± 38.3 ms*), low-skill players (*165 ± 52.2 ms*), highly skilled players (*150 ± 47.6 ms*), elite players (*139 ± 11.7 ms*). Investigation into duration of downswing phase (i.e. backswing) was conducted. Early work of Tyldesley and Whiting (1975) reported remarkably constant downswing time for a variety of shots in experts' forehand drive. Such consistency is clearly different between expert performers and novice performers (Bootsma et al., 1986; Tyldesley & Whiting, 1975). Later Bootsma (1988) claimed that variability existed. Ebrahim (2010) reported in his study the downswing phase of movement took from *89-284 ms* for loop and *67-151 ms* in smash, which were comparable to *128-164 ms* (Tyldesley & Whiting, 1975) and *92-179 ms* (Bootsma, 1988). Ebrahim (2010)'s work did not support the constant downswing time hypotheses and the simple proportional duration model. From the reviews on previous studies, it is more convincing that variability may exist on all the four phases. Note that the durations, however, did not have an unambiguous definition for their exact moments for phase starting and phase ending, therefore it is not clear if their data can be compared to others' work.

2.2.2 Racket motion

Moment of ball-racket contact

The critical moment of ball-racket contact was commonly studied in table tennis biomechanics research. The critical moment is when the ball velocity changes from positive to negative. Researchers concluded that racket speed reached its maximum value at the moment of impact (Bootsma & Van Wieringen, 1990; Ramanantsoa & Durey, 1994; Sheppard & Li, 2007). In some research (e.g. Sørensen et al., 2001), ball-racket contact time was directly defined from raw acceleration data as the moment when acceleration changes from positive to negative. The intrinsic mechanics of such coincidence may lie in how human motor control and coordination work. Queries may be raised that existence of human motion variability cannot make the overlap mathematical truth. In fact, examination on figure reported by Bootsma and Van Wieringen (1990) showed a small time gap of approximate 10 *ms* between contact and peak velocity (Figure 2-4). This visually gap was ignored by the author because it is comparable to errors like the motion capture system resolution. Such small gap between contact and peak velocity time is common in racket sports. For example, the average peak velocity of the centre of the racket head was recorded with a mean just *0.005 s* prior to impact at tennis serve (Elliott et al., 1995).

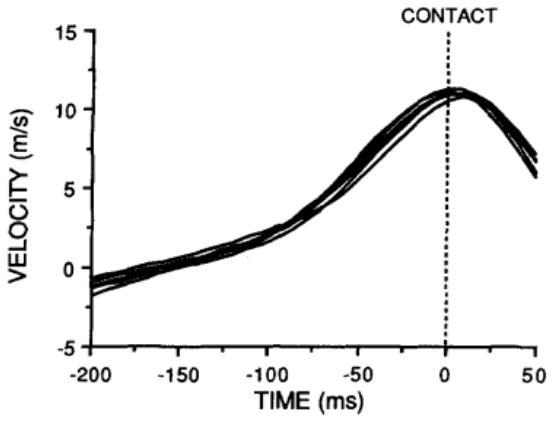

Figure 2-4 Contact and peak velocity with tiny time gap but concluded coincident by the author (Bootsma & Van Wieringen, 1990)

Research on racket motion

Racket motion was importantly concerned in reviewed research studies because players intermittently control and adjust their rackets movement to hit the oncoming balls (Allen, 1996). The movement of the racket directly affects the trajectory of the ball. In addition, the effectiveness of the stroke technique may also be represented by racket motion by the ratio of the striking speed to the amplitude of movement (Barchukova & Voronov, 1998). Bootsma and Van Wieringen (1990) studied the direction of travel of the racket at the moment of ball-racket contact on the transversal plane, although no statistical comparison was performed. The authors reported that the variability in the direction of travel of racket decreased during a stroke. Sheppard and Li (2007) compared kinematics of the racket during the time period around ball-racket contact in forward swing between expert and novice players. In their study, they found that the racket movement differed significantly between the two groups. Compared to novice players, expert players showed greater velocity, more rightward direction and more downward orientation.

2.2.3 Human body movement

To precisely control the racket, motions are transferred through the whole body segment in the kinematic chain to the hand. In fact, the racket is considered as an acquired body part, namely an extension of the player's body (Aldrich, 1937). Little reviewed work attempted to provide mechanisms of biomechanical construction of a full table tennis strokes. Ramanantsoa and Durey (1994) tried to build a stroke construction model for table tennis by applying Bernstein's theory (Bernstein, 1967) and reported some interesting results that expert players performed better by reducing their *DOF*s during movement. Only one participant was involved in the experiment and there was no quantitative comparison between different levels of players. Therefore, this section reviews motion patterns and analytical methods in

other racket sports.

Joint angular displacement and angular velocity

Joint angular displacement and angular rotation are the most basic movement. Iino et al. (2008) reported some data of joint angular velocities of the upper limb rotation during table tennis backhands against topspin and backspin. However, since the author focused on the contribution of the upper limb, there was no comparison on the joint angular velocity data. This was the same as another work of Iino and Kojima (2009), which also included some joint angular velocity data, but aimed to compare the contribution pattern of joint rotations. Their definitions of arm motion have been reviewed in the previous section (Section *2.1.4*). However, the inconsistency of definitions (especially shoulder, Section *2.1.4*) and measurement across different research made the reported data of angular displacement less meaningful.

Range of motion

Range of motion (*ROM*) refers to the movement of a joint from full flexion to full extension, or the existing amount of motion around a joint (Günal et al., 1996). It is expressed in degrees of joint angle. Each joint has an established *ROM*. Therapists often prescribe specific range of motion exercises of each joint. Research on injuries rehabilitation shows interest in ROM, because injuries of soft tissues surrounding a joint may reduce ROM. ROM is closely related to flexibility, which can be improved by exercises. Skilled athletes are characterized by a larger range of motion in their shots in most sports (Alexander & Honish, 2009). For example, skilled players show greater forward trunk flexion, which helps to keep balance, helps the trunk to rotate in muscle level, and increases racket head speed. Skilled players also have longer backswings and longer follow-throughs, which make the shots more powerful (Alexander & Honish, 2009). However, work of Alexander and Honish (2009) has only qualitative conclusion without quantitative and experimental support.

Joint motion contribution to racket speed

In racket sports, the spatial motion of racket is an important factor contributing to success of play. Producing racket speed relies both on the angular velocity of segment's axis rotation and the spatial position of racket with respect to segments. The contribution pattern studies the effectiveness and importance of human body segments in producing racket speed. It is represented as the ratio of the partial speed of the racket caused by each joint/segment motion to the total racket speed. For example, the elbow internal rotation and wrist flexion both lead to the forward movement of the racket, and they do different contributions. A typical method (Sprigings et al., 1994) including modeling arm and calculation of contribution pattern was reviewed in the arm motion analysis method section (Section *2.1.4*). Related findings in other racket sports like badminton, squash, and tennis are described below.

In badminton, the linear velocity of racket head during smash was significantly contributed by the wrist compared to the elbow and shoulder joints (Rambely & Osman, 2008; Tsai et al., 2000). In addition, the rotational contribution of the wrist is much larger than the translational component (Kwan et al., 2011). With a more detailed model (Sprigings et al., 1994) regarding separate contributions in terms of different rotational *DOF*s of joints, X. Liu et al. (2009) reported that in badminton overhead smashes, internal rotation of upper arm is the most important, followed by internal rotation of forearm and hand flexion. Their conclusions are similar to previous research by Gowitzke and Waddell (1991) who reported that during power strokes in badminton, world class players used pronation of forearm and lateral rotation of upper arm to produce high speed.

In squash forehand drive, Elliott et al. (1996a) reported that internal rotation of the upper arm at the shoulder joint, hand flexion at the wrist joint and forearm pronation

at the radioulnar joint made the major contribution to the mean racket-head speed at ball-racket impact. Forearm pronation at the radioulnar joint and extension at the elbow joint both played a significant role in generating racket velocity in the period prior to moment of impact.

In tennis serve, the internal rotation of upper arm was the major contributor to racket head velocity, followed by flexion of wrist and horizontal adduction, according to different researchers (Elliott et al., 1995; Sprigings et al., 1994; Tanabe & Ito, 2007). Although forearm pronation had the highest angular velocity, it was only reported as making a fourth contribution due to the position of the racket with respect to axis of rotation (Sprigings et al., 1994). Elliott et al. (1995) also included the contribution of lower body and trunk apart from upper arm, forearm and hand, as his results showed that shoulder and lower limb ranked fourth in contribution. In their experiment, forearm extension at the elbow joint played a negative role and reduced the forward velocity of the centre of the racket at impact. Tanabe and Ito (2007) concluded with the same order of upper arm internal rotation first and wrist flexion second, although the calculated percentages were different from Elliott et al. (1995). Tanabe and Ito (2007) also researched on slow serve and found movements like forearm pronation/supination might have different functions between fast and slow serves.

Limited work has been done in table tennis. Iino et al. (2008) did such work in comparison between topspin backhands against coming balls with topspin and backspin. The upper arm external rotation, wrist dorsiflexion and elbow extension were the largest contributors to the racket velocity for both activities. With an in-depth analysis by decomposing the velocity into forward and upward components, they concluded that elbow extension contributed most in forward direction and upper arm external rotation contributed most in upward direction. This was true for

both against topspin and against backspin without significant difference, although their contribution percentage values differed. Wrist dorsiflexion had the largest angular velocity, followed by upper arm external rotation and elbow extension. Neal (1991) built a model of three-linked system of arm, forearm, and hand/racket. However, his result showed equivocal evidence for the summation of speed principle.

Sequencing of joint motions

Sequencing concerns the timing of movement of multi-segment open-linked kinematic chain. Human body segments are assumed to be actuated in certain sequence during a complex motion so that the best performance is achieved. Sequencing is also interpreted as a time accumulation of contribution history to distal end speed. For instance, the linear velocities of proximal segment may not provide large kinematic contribution to the final speed of the most distal end, but their motion histories make the achievement of speed possible (Putnam, 1993). Therefore, it is essential to study the sequencing pattern of arm movement.

One principle of optimal partial momenta coordination argues that the angular speed of all segments should simultaneously reach to maximum to achieve maximal speed at the distal terminal (Van Gheluwe & Hebbelinck, 1985). Although this is observed in some movements such as the volley and forehand ground stroke in tennis, most throwing or striking actions typically do not match this principle(Putnam, 1993).

Another principle of proximal-to-distal sequencing raised more interest among researchers. Quite a lot of studies reported the proximal-to-distal sequencing in throwing and kicking movements. For example, it was reported that in javelin showing, the velocities of all segments of elite players showed a proximal to distal order of reaching of their maximum values (Campos et al., 2004; H. Liu et al., 2010). The most influential principle underlying the description of proximal-to-distal

sequencing in sports movement is the summation of speed principle (Bunn, 1972). According to this principle, each segment starts its motion at the instant of greatest speed of the preceding segment and reaches a maximum speed greater than that of its predecessor. Thus the speed of distal end is built up by summing up all the speeds of individual segments by sequence of proximal to distal, although the mechanical interpretation of how it is achieved in not mentioned by this principle.

Sequences are often described in terms of the linear velocities of the segment endpoints, joint angular velocities or segment angular velocities (Putnam, 1993). Linear velocities of segment endpoints provide a clear description of the instantaneous contribution to distal end speed. However, the linear velocity of one segment terminal alone has a limited value. Joint angular velocity and segment angular velocity both present intuitive description of segment movement and provide a clear description of proximal-to-distal sequencing.

Research on different racket sports shows different conclusions. In underarm power strokes in badminton, elite players were reported to combine hip and trunk rotation with shoulder flexion at first (Gowitzke & Waddell, 1991). When the rackets were approximately opposite the side of the players, they laterally rotate shoulder and supinate forearm while they were still driving their hand forward. This action biomechanically help players produce the maximum speed (Gowitzke & Waddell, 1991). In squash forehand drive, trunk and upper limb were synchronized within 200ms or less to produce high speed (Elliott et al., 1996a). In baseball, internal rotation of upper arm happened late but its peak velocity was synchronized approximately with the ball-racket contact (Sakurai et al., 1993). In tennis, the peak angular velocity occurred very late in the forward swing sequence (approximately 10ms prior to impact) together with palmar and ulnar flexion of the hand and later than other movements about the shoulder and elbow joints. This sequencing was

generally common across flat, topspin and topspin lob forehand ground strokes (Elliott et al., 1996b).

Other methods

There were several other approaches to describe the coordination between limbs (interlimb coupling) or between segments within a limb (intersegmental or interjoint coupling) (Tepavac & Field-Fote, 2001), as presented in the literature (e.g. Glazier et al., 2003; Hamill et al., 2000; Lees, 2002; Wheat & Glazier, 2005). A review of several methods will be introduced, and some of their advantages and disadvantages are highlighted in *Table 2-1* (Wheat & Glazier, 2005).

Variable-variable plots is a qualitative method to analyze the motion of one joint relative to the motion of another joint (angle-angle plot) or the angle of one joint relative to the angular velocity of that joint (phase-plane plot)(Glazier et al., 2003). The angle-angle plots illustrate the spatial and spatial coupling, and the phase-plane plots illustrate the spatial and temporal coupling. Variable-variable plots display the relationship between two variables graphically. However, they do not formally quantify the coordination. Coordination can only be quantified by the subsequent implementation of other analysis techniques such as continuous relative phase analysis, cross-correlation and vector coding.

Continuous relative phase (CRF) between two joints are defined as the difference between the respective phase angles of each segment (Hamill et al., 2000). At first, the time series data of the displacement and velocity data are normalized to construct a phase-plane portrait (normalized angular velocity versus normalized angular displacement) for each joint. Then the phase angle can be obtained by calculating the four-quadrant arctangent phase angle from a phase-plane plot of each joint. The continuous relative phase is calculated by subtraction of the phase angles of the two

joints. Continuous relative phase can show the relationship (in-phase or anti-phase) between a pair of joints and its relative amount.

Cross-correlation is a generalization of standard linear correlation (Wheat & Glazier, 2005). It introduces the time lags between data sets and calculating the corresponding correlation coefficients to obtain an indication of the type of relationship between body segments (in-phase or anti-phase), the degree of linkage between body segments, and the stability of coordination patterns when applied to repeated trials (Temprado et al., 1997). However, the cross-correlation is based on the assumption that linear relationship exists between two sets of kinematic time-series data. Therefore, it may lose efficacy when used in determining the degree of linkage between body segments that have a nonlinear relationship (Sidaway et al., 1995).

Vector coding is based on the chain-encoding technique, which involves using a superimposed grid to transform the data curve from an angle-angle plot or a position-time plot into a chain of digits (Wheat & Glazier, 2005). Each of the digital elements that comprise the chain is given a weighting based on the direction of the line formed by the frame-to-frame interval between two successive data points. The chain of digital elements can then be cross-correlated with a chain of digital elements obtained from another angle-angle plot or position-time plot to obtain a recognition coefficient, which is the peak value of the cross-correlation function. The recognition coefficient can then be interpreted in much the same way as the cross-correlation coefficient outlined previously.

Table 2-1 Advantages and disadvantages of several methods for measuring coupling

	Advantage	**Disadvantage**
Variable-variable plots	Show straightforward info	Qualitative rather than quantitative
Continuous	Include temporal information	Assume the two oscillating segments

relative phase	More sensitive measurement of coordination variability; continuous measurement throughout the entire movement	are of a one-to-one frequency ratio and they exhibit a sinusoidal time history; hard to relate to conceptually
Cross-correlation	No normalization procedure needed if data are linear; provide only one measure per movement cycle	Assume the linearity exists between segments or joints; hard to distinguish between phase lag and phase lead
Vector coding	Provide only spatial information therefore limit the sensitivity to variability	Data converted from ratio scale to the nominal scale, may lose important info and limit types of statistical methods that can be applied; data points need to be equally spaced

These different approaches were used by different researchers. For example, Glazier et al. (2003) reviewed work on fast bowling, which integrates many throwing, kicking and striking activities. Lees (2003) reviewed work on racket sports focusing mainly on tennis. However, no such work has been done on table tennis. Though these methods help analysis in providing different insights, they raise additional complexity when analyzing the relationship among a lot of variables. The lack of previous research makes it difficult to apply the complex methods without comparable work. This thesis, therefore, will select the basic motion patterns which are also easy for the table tennis players to understand and apply adjustment to improve their skills, like phase duration, angular displacement, etc.

2.2.4 Variability of motion patterns

Movement variability

Variability are ubiquitous in all animal movements, including human in sports. Even elites athlete were unable to produce invariant motion patterns after many years of practice (Davids et al., 2003). However, sports research has not shown a great deal of interest in movement variability until recent years.

Quantification of variability

Variability can be qualitatively assessed by inspecting plots of repeat trials. To further quantify the variability, several approaches are available as tabulated in Table *2-2*. In the table, the first three techniques are non-normalized methods and the last two techniques are normalized by sample mean. All the techniques are similar but have differences with each other: for certain trial size, the magnitude of the variability is fixed for n≤3(*RMSD*<*s*<*95%CI*), n=4(*RMSD*<*95%*<*s*) and n≥5 (*95%CI*<*RMSD*<*s*); for normalized techniques, *RMSD* provides a smaller value for variability than *%CV* for all trial sizes (Mullineaux, 2000; Mullineaux et al., 2001). Mullineaux (2000) pointed out that normalized techniques might only be used when the means were similar, otherwise it might be misleading. In our studies, the typical sample standard deviation will be used, and others may be alternative techniques according to experimental data.

Table 2-2 Statistics used for quantifying variability of repeat trials (Mullineaux, 2000)

Statistic	**Abbr.**	**Equation**
sample standard deviation	*s*	$\sqrt{\sum_{i=1}^{n}(\bar{x}-x_i)^2/(n-1)}$
root mean square difference	*RMSD*	$\sqrt{\sum_{i=1}^{n}(x_c-x_i)^2/n}$
95% confidence intervals	*95%CI*	$1.96s/\sqrt{n}$
percentage coefficient of variation	*%CV*	$100s/\bar{x}$
percentage RMSD	*%RMSD*	$\frac{100\mathrm{RMSD}}{\sqrt{\sum_{i=1}^{n}(x_c)^2/n}}$

Equation: mean ($\bar{x}$); variable (x_i); sample or trial size (n); criterion value (x_c)

Role of variability

Interestingly, variability receives different views from different motor control paradigms (R Bartlett et al., 2007): cognitive motor control theorists traditionally

consider variability as undesirable system noises or error; on the other hand, ecological motor control specialists consider variability as functional in human movement on dynamic system perspective.

From the point of view of cognitive motor control theorist, variability is simply considered to play a redundant role and must be eliminated. Therefore in their opinion, skill learning is the process of reducing variability because the learner freezes unwanted degrees of freedom (*DOF*) in the kinematic chain (R Bartlett et al., 2007).

In dynamic system theory, the variability plays functional roles. Not until recently did sports biomechanists explore functional roles of variability. One point of view suggested that variability in movement is necessary for change in the coordination, such as from walking to running or vice versa (DeLeo et al., 2004). The second point argues that variability in movement provide a broader distribution of stress among different tissues, potentially reducing the cumulative load on internal structures of the body. Furthermore, some experimental evidence exists to support the "variabilit*y*-overuse injury hypothesis" (James, 2004). A third opinion is that variability is seen as coordination change and it gives flexibility to effective adaptation to environmental change. This motor control group sees skill learning and practice as an exploration of the "perceptual-motor workplace". In a multi-*DOF* kinematic chain, variability is greatest for individual because movements that are practiced many times allow the individual to relax the *DOF*s involved to find more flexible solutions to the task (R Bartlett, 2013).

Contradictions may occur while different explanations on the role of variability are applied. An example lies in the debate on whether high speed may lead to large variability during arm motions. Harris and Wolpert (1998) supported that high speed

will lead to bigger final position variability. The noise in the neural control signal was assumed independent of the control signal, and increased with the mean level of the signal. Since moving as rapidly as possible required large control signals, it would increase the error thus increase the variability in the final position. As the resulting inaccuracy of movement may lead to task failure or require further corrective movements, moving very fast becomes counterproductive. On the other hand, another perspective argued that high speed would lead to smaller variability. According to impulse-variability principle (Schmidt et al., 1985), the variability in impulses leaded to variability in trajectories. The execution of a maximal or near maximal velocity movement would tend naturally to be more consistent than a lower velocity drive (Bootsma & Van Wieringen, 1990), therefore less variability was supposed to be found in a high-speed motion. An experiment reported by Bootsma (1988) seems to support latter one by stating that execution of an attacking forehand drive in table tennis with a lower velocity was associated with an increase in movement time variability.

2.3 Model development and classification

2.3.1 Expert system and machine learning

The integration of machine-aided intelligence into the development of modern sport information systems enables a prompt and automatic evaluation of sport-specific parameter values, thereby allowing the establishment of computer-based feedback and intervention routines (Baca et al., 2009). Two terms are reviewed for the systems which make decisions analogous to human: the expert system and machine learning system.

Expert system (Buchanan et al., 1983), as a branch of the artificial intelligence (*AI*), is a computer system that uses reasoning capabilities to reach conclusions or to

perform analytical tasks that emulates the decision-making ability of a human expert. The development of computing capability has enhanced the applicability from data measurement to AI-based modeling techniques for automatic evaluation purpose. An expert system is typically made up of two major components, the knowledge base and the inference engine (Waterman, 1986). The knowledge base contains specific knowledge in a domain. The inference engine is an expert system shell which makes use of knowledge base in order to draw conclusion.

The idea of expert system can be easily applied into sports application. For instance, H. Zhang et al. (2011) utilized computer-aided game analysis to compute technique and tactic indexes into winning probability for net sports prediction. Xiao et al. (2006) proposed an outlook idea of applying the living creature feedback to the technique training of table tennis. The test data was converted into signal hints of sound and light directly to the athlete so that the athlete can make the reaction right away after receiving a signal, and then can adjust the range, strength, speed of motion more easily.

Machine learning is a type of *AI* with the study and design of intelligent agent (Poole et al., 1998). Machine learning involves the construction of algorithms that can learn from existing data and make predictions therefore exhibited human-like intelligence. Machine learning includes both supervised learning and unsupervised learning for the cases that labels of data are known and unknown respectively. Classification is a type of supervised machine learning. With a set of data of different categories, the classification identifies a new observation with the categories.

Many classification algorithms are available (Han et al., 2006; Kotsiantis et al., 2007), for example, the decision trees, the artificial neural networks (*ANN*), the naïve byes, the k-nearest neighbors (*kNN*), the support vector machine (*SVM*) and so on.

Kotsiantis et al. (2007) gave a comparison of these classification algorithms (Table *2-3*). As can be seen from the table, *SVM* has an overall good performance. For this reason, the *SVM* was used in this thesis as a representative example for the classifiers. SVM and related methodologies were reviewed in the following section (Section 2.3.3).

Table 2-3 Comparing classification algorithms *(Kotsiantis et al., 2007)*

	Decision Trees	Neural Networks	Naïve Bayes	kNN	SVM	Rule-learners
Accuracy in general	**	***	*	**	****	**
Speed of learning with respect to number of attributes and the number of instances	***	*	****	****	*	**
Speed of classification	****	****	****	*	****	****
Tolerance to missing values	***	*	****	*	**	**
Tolerance to irrelevant attributes	***	*	**	**	****	**
Tolerance to redundant attributes	**	**	*	**	***	**
Tolerance to highly interdependent attributes (e.g. parity problems)	**	***	*	*	***	**
Dealing with discrete/binary/continuous attributes	****	***(not discrete)	***(not continuous)	***(not directly discrete)	**(not discrete)	***(not directly continuous)
Tolerance to noise	**	**	***	*	**	*
Dealing with danger of overfitting	**	*	***	***	**	**
Attempts for incremental learning	**	***	****	****	**	*
Explanation ability/transparency of knowledge/classifications	****	*	****	**	*	****
Model parameter handling	***	*	****	***	*	***

Note: **** *stars represent the best and* * *star the worst* performance

The expert system and machine learning techniques share the same goal to achieve human-like targets. Expert systems was some of the first truly successful forms of *AI* software (Russell et al., 2003). Some expert systems may be carefully constructed by specific rules for decision making, and the rules are designed based on the knowledge of human experts. Machine learning is more of referring to the algorithms that do with learning from data to construct the rules, therefore able to make decisions based on training data.

Despite the fact that *AI* has raised much interest in research or application to solve real problems, the application of *AI* in sports biomechanics was little (R Bartlett, 2006). The biggest problem with applying *AI* in sports may be because of the high complexity of sports performance. The performance for a specific sport may not be well defined, and multiple factors may contribute to a good performance. Therefore, it may take plenty of time and efforts to seek and quantify the factors. Lapham and Bartlett (1995) pointed out that *AI* application on sport performance analysis lacked advantage when compared to *AI* application in gait analysis, which was a confined expert domain with commonplace laboratory-based automatic marker tracking system and abundant data. In addition, research into sport performance may not be well funded because coaches and sports scientists are expensive.

In summary, this thesis attempts to overcome the problem by utilizing *AI* on the model development. The *SVM* classification technique was selected and related work were specifically reviewed in the following section.

2.3.2 Related work in sports biomechanics

The implementation of *AI* in sports area can help with the development of systems and models for better performance. With a review of table-tennis-related systems, two main types of work on system development exist as corresponding to two different performance analysis methods (*Section 2.1.1*): the first type involves the application of notational analysis, which generally focuses on tactics and teamwork to improve players' performance; the second type regards robot table tennis, which focuses on trajectory generation and movement adaptation of anthropomorphic arm. The notational systems get source data from, for example, video camera to retrieve tactical related information therefore predicts the competition results. However, the notational analysis does not analyze details into biomechanical analysis. These systems are quite different from the proposed system which could perform

biomechanical motion pattern analysis, for table tennis strokes. Currently there is no existing papers or market products which can directly assess table tennis players' biomechanical movement patterns. Therefore, in this section, some examples of related works on other sports that tried to perform assessment from biomechanical perspective are reviewed.

J. Wu and Wang (2008) investigated a combination of *PCA* (Principal component analysis) with *SVM* to classify the reaction force of gait patterns between *30* young and *30* elderly participants, with the results showing that the accuracy was on average *90%*. Fukuchi et al. (2011) utilized *SVM* on *31* kinematic data of the lower extremity of *17* young and *17* elderly during running to distinguish different age groups. The results show different accuracies of different kernel methods with the linear kernel performing the best. The performance rate can be up to *100%* with the forward feature selection algorithm. Begg and Kamruzzaman (2005) applied the *SVM* with six different kernel functions (linear, polynomial, radial basis, exponential radial basis, multi-layer perceptron and spline) on the data of basic temporal/spatial, kinetic and kinematic during a gait in order to classify *12* young participants and 12 elderly participants. The overall accuracy was *91.7%*. Therefore, the *SVM* demonstrated considerable potential on the biomechanical features and presented good performance, it could provide an effective tool for similar biomechanical classification in other applications.

In addition, the *AI* based system will also increase its power by connecting with an automated motion capture system. The idea of a tracking system has appeared in a lot of research. The researchers built powerful or convenient systems for collecting better measurement of biomechanical variables. For example, Ahmadi et al. (2009) used gyroscope sensors to measure the peak angular velocity of internal upper arm rotation, wrist flexion, and shoulder rotation for skill assessment and acquisition of

a tennis player during the first serve. Davey et al. (2008) used a platform of the tri-axial accelerometer at the sacrum to record swimming motion to retrieve the information of wall push-off, stroke type and stroke count metrics. Guggenmos (2007) proposed a snowboarding assistant for beginners, which used force sensitive resistors, bend sensors, *3D* accelerometers, and gyroscopes to diagnose weight distribution, knee flexion, trunk inclination and counter-rotation. Ghasemzadeh et al. (2009) described a system that analyze the golf driver swing using a body sensor network of accelerometers and gyroscopes. The sensors listed in the examples are quite light and portable, and measured the interested biomechanical variables, thereafter can be input into the *AI* system for data processing for objective and quantitative assessments.

2.3.3 Support vector machine and related techniques

This section reviews and lists the key concepts regarding the *SVM* and related techniques that is a potential tool for solving the problems in the current research, as to be applied in *Chapter 5* of this thesis.

2.3.3.1 Support vector machine

Support Vector Machine (*SVM*) (Cortes & Vapnik, 1995) is a supervised learning model for classification or regression purpose developed from the statistical learning theory. *SVM* constructs a hyperplane in a high or infinite dimensional space and maps data to the hyperplane in order to maximize the margin to classify samples (*Figure 2-5*). *SVM* is widely used in many fields and it generally performs better than other classifiers (Table *2-3*).

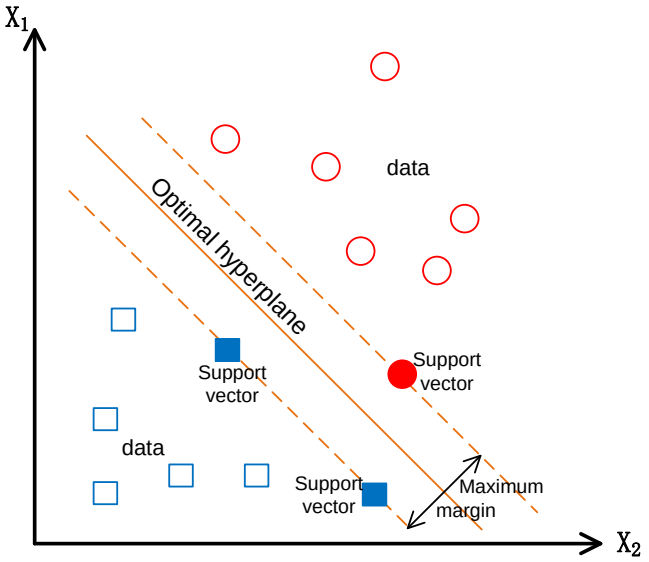

Figure 2-5 Support Vector Machine illustration in hyperspace x1-x2

The development of a *SVM* is to find the maximum margin in hyperspace, which can be simplified into a mathematical optimization problem as shown in *Equation (2-1)*. Note the latter part of the target function is introduced for allowing misclassification. The *C* is the weight for slack variables: when *C* increases the optimization attempts to make a stricter separation between classes; on the other hand, less weight on *C* means misclassification is less important. Specifically, a binary *SVM* has two classes, noted as y_i where $y_i \in \{-1, +1\}$. The data input are vectors noted x_i where $x_i \in R^p, i = 1,2, \dots, N$.

$$\min_{\omega,b,\zeta} \frac{1}{2}\omega^T\omega + C\sum_{i=1}^{N}{\zeta_i}^2$$
$$\text{subject to } y_i(\omega^T\phi(x_i) + b) \geq 1 - \zeta_i \qquad (2\text{-}1)$$
$$\zeta_i \geq 0, \ \mathrm{i} = 1,2 \dots \mathrm{N}$$

where ω is the weight vector, b is the intercept term, ζ_i are the slack variables. C is capacity constant, $\phi^T(x_i)\phi(x_j) = K(x_i, x_j)$ is the kernel function.

The common kernel functions include linear kernel, polynomial kernel and Radial Basis Function (*RBF*) kernel, as listed in *Table 2-4*. The linear kernel is the simplest

one which maintains the features in linear space; the polynomial kernel and RBF kernel transform features to a higher dimension to attain better ability of classifying complex features. *RBF* is a relatively more common kernel. In general, all the kennels may have an additional coefficient parameter: the kernel scale *K*. Therefore, a *SVM* classifier with a determined kernel has two unknown parameters: *C* and *K*. Changing these two parameters may change the model performance therefore a better set of their values should be determined.

Table 2-4 Common SVM kernel functions

Kernel	Math expression
Linear kernel	$K(x_1,x_2)=K*x_1'x_2$
Polynomial kernel	$K(x_1,x_2)=K*(1+x_1'x_2)^p$
RBF kernel	$K(x_1,x_2)=K*\exp(-\lvert x_1-x_2\rvert^2)$

The architecture of the *SVM* is illustrated in *Figure 2-6*. For any input vector x, the *SVM* produces the prediction result by calculation using the kernel functions. When the actual classes are known (e.g. training and testing) for input data, the results y are used to compare with the actual results to tuning parameters (e.g. ω, b, ζ during training) and evaluate the classifier (e.g. testing); when the class label is unknown (i.e. application of trained *SVM*), the *SVM* gives prediction result.

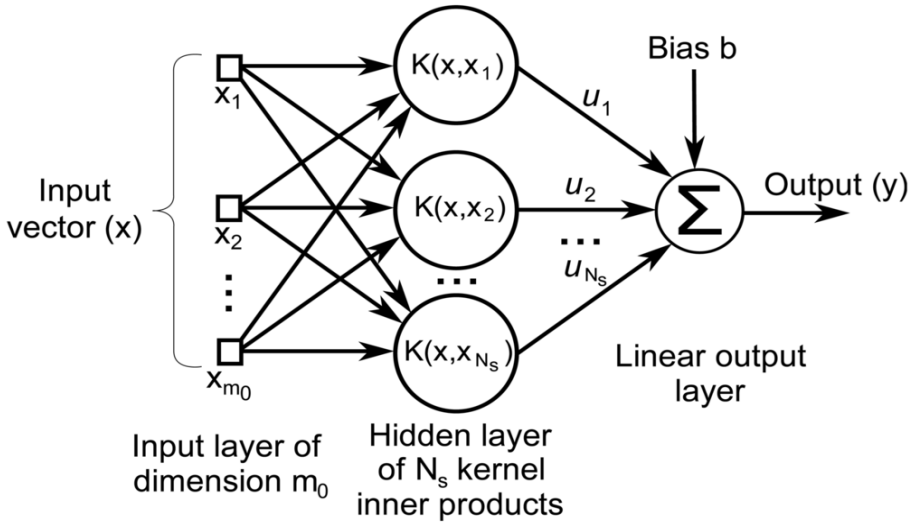

Figure 2-6 Architecture of Support Vector Machine (Ruiz-Gonzalez et al., 2014)

2.3.3.2 Confusion matrix and model performance

A confusion matrix (Kohavi & Provost, 1998) contains the information about actual and predicted classifications which are output from a classification. The confusion matrix contains the basic information of true positive, false positive, false negative and true negative (*Table 2-5*). Then performance of a classifier, including accuracy, precision, recall and F_1 score etc., is calculated based on the confusion matrix.

Table 2-5 Confusion matrix for a two class classifier

		Actual		
		Actual positive	Actual negative	
Predicted	Predicted positive	True Positive (TP)	False Positive (FP)	Positive predictive value $(PPV) = \frac{TP}{TP+FP}$ Precision
	Predicted Negative	False Negative (FN)	True Negative (TN)	
		True positive rate $(TPR) = \frac{TP}{TP+FN}$ Recall		

The accuracy is the proportion of the total number of predictions that were correct:

$$Accuracy = \frac{TP + TN}{TP + TN + FP + FN} \quad (2\text{-}2)$$

The precision is the proportion of the predicted positive cases that were correct:

$$Precision = \frac{TP}{TP + FP} \quad (2\text{-}3)$$

The recall, aka sensitivity, is the proportion of positive cases that were correctly identified:

$$Recall = \frac{TP}{TP + FN} \quad (2\text{-}4)$$

F_1 score (Powers, 2011) is the harmonic mean of precision and recall. It is calculated as:

$$F_1 = 2 \times \frac{Precision \times Recall}{Precision + Recall} \quad (2\text{-}5)$$

The accuracy, precision and recall each on its own may not be adequate to measure the performance. For example, accuracy may still be good when the number of negative cases is much greater than the number of positive cases and all the cases are predicted as negative (Kubat et al., 1998). F_1 score combines both precision and recall therefore is a better way to measure the overall performance of the model. Therefore, F_1 score is generally better than others to represent the model performance.

2.3.3.3 Cross-validation

Cross-validation is a model assessment technique used to evaluate a machine learning algorithm's performance in making predictions on new datasets that it has not been trained on. This is done by partitioning a dataset and using a subset to train the algorithm and the remaining data for testing. Cross-validation does not use all of the data to build a model therefore prevents overfitting during training. Common

cross-validation techniques include *k*-fold, leave-one-out and repeated random subsampling etc.

The *k*-fold cross-validation partitions data into k randomly chosen subsets (or folds) of roughly equal size. One subset is used to validate the model trained using the remaining subsets. This process is repeated k times such that each subset is used exactly once for validation. The leave-one-out cross-validation is a special case of k-fold by using one observation as the validation set and the remaining observations as the training set. This is repeated for all the observations to segment the original sample for validation set of one observation and a training set. The repeated random subsampling cross-validation performs Monte Carlo Repetitions of randomly partitioning data and aggregating results over all the runs.

2.3.3.4 Nelder-Mead Method

The Nelder–Mead method (Nelder & Mead, 1965) is a commonly applied numerical algorithm used to find the minimum or maximum objective function in a high-dimensional space. It is one of the best known algorithms for multidimensional unconstrained optimization without derivatives (Singer & Nelder, 2009). Nelder-Mead method is simplex-based by searching for the better objective function values gradually. In addition, it requires only one or two function evaluations at each step. For a two-dimensional case, an initial set of *3* points are used as seeds and during each step of iteration the worst point is replaced with a better point. The step sequences in one iteration is shown in *Figure 2-7.*

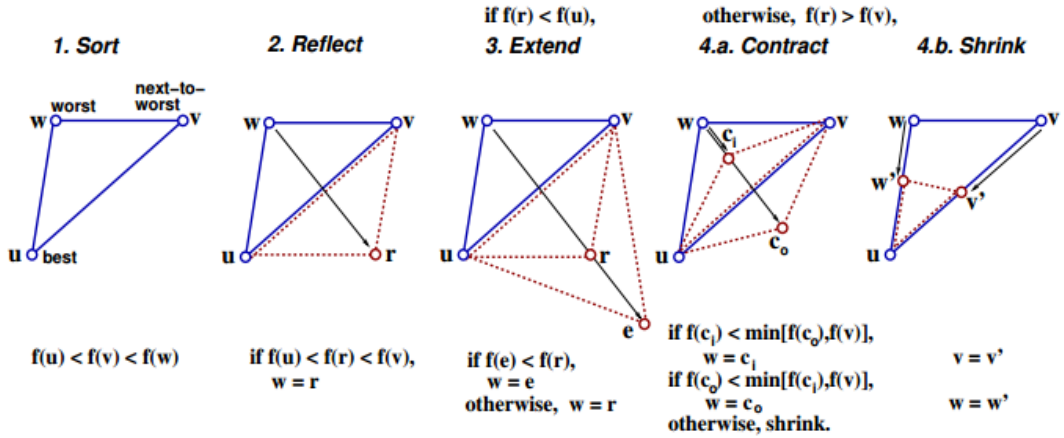

Figure 2-7 Illustration of the sequence of steps in one iteration of the Nelder-Mead method for 2 dimensions (Gavin, 2013)

2.3.3.5 Principal component analysis

The Principal component analysis (*PCA)* (Jolliffe, 2005) is discussed here as a feature selection method. *PCA* uses orthogonal transformation to convert a set of observations of possibly correlated variables into a set of values of linearly uncorrelated variables. The components with higher variances can be selected as principal components. The equations for *PCA* are listed in Equation (*2-6*).

$$
\begin{aligned}
w_{(1)} &= \arg\max_{\|w\|=1}\left\{\frac{w^T X^T X w}{w^T w}\right\} \\
\hat{X}_{k-1} &= X - \sum_{n=1}^{k=1} X w_{(n)} w_{(n)}^T \\
w_{(k)} &= \arg\max_{\|w\|=1}\left\{\frac{w^T \hat{X}_{k-1}^T \hat{X}_{k-1} w}{w^T w}\right\} \\
T &= XW
\end{aligned}
\tag{2-6}
$$

where X is the matrix of dataset with each column as a feature, $w_{(k)}$ is the *kth* component or the eigenvector of X^TX. T is the full principal components decomposition of X. W is the matrix whose columns are $w_{(k)}$.

2.4 Summary

This chapter reviewed literature related to the proposed research objectives. *Section 2.1* focused on the basic biomechanics of basic strokes and phases, biomechanical analysis and arm motion analysis. *Section 2.2* reviewed the motion patterns in racket sports, including the previous work results and analytical methods for motion quantification. *Section 2.3* reviewed model development and classification, which included machine learning techniques, related work and *SVM*-related concepts. According to the literature review above, some key scientific knowledge is missing.

Firstly, the quantification of table tennis basic strokes was essential for a better investigation of players' motion, but was not comprehensively conducted. There were no unambiguous quantification methods for table tennis stroke motion, especially for the arm motion and different phases.

Secondly, the motion pattern differences between expert and novice players need to be quantitatively investigated therefore for performance improvement of novice players. However, most existing studies only focused on the motion of the racket on limited moments, and revealed little about human body segment biomechanics.

Thirdly, the application of *AI* techniques into sports biomechanics has considerable potential but there is no reported application in table tennis. Therefore, it is a challenge to apply AI classification technique to achieve the automatic assessment of players' motion patterns.

To fill in the gaps and overcome the problems to achieve the assessment of players' motion patterns, *Chapter 3* to *Chapter 5* below describe the work carried out to achieve the specific research objectives.

Chapter 3 A novel kinematic model for table tennis strokes

3.1 Quantification of stroke motion

3.1.1 Definitions for the model

A global coordinate system is defined with its origin *O* in the centre of the table tennis table's short edge, with its *x*-axis pointing to the opponent's side, *y*-axis pointing upward and *z*-axis pointing rightward (*Figure 3-1*). The racket centre has three translational *DOF*s (RC_x, RC_y and RC_z) with respect to the origin *O*; the racket plane, which is the plane parallel to the racket surface, has three rotational *DOF*s (RR_{xy}, RR_{yz} and RR_{xz}) with respect to each of the global planes (plane *x-y*, *y-z*, *x-z* respectively). These notations to describe the movement of the racket are tabulated in *Table 3-1*.

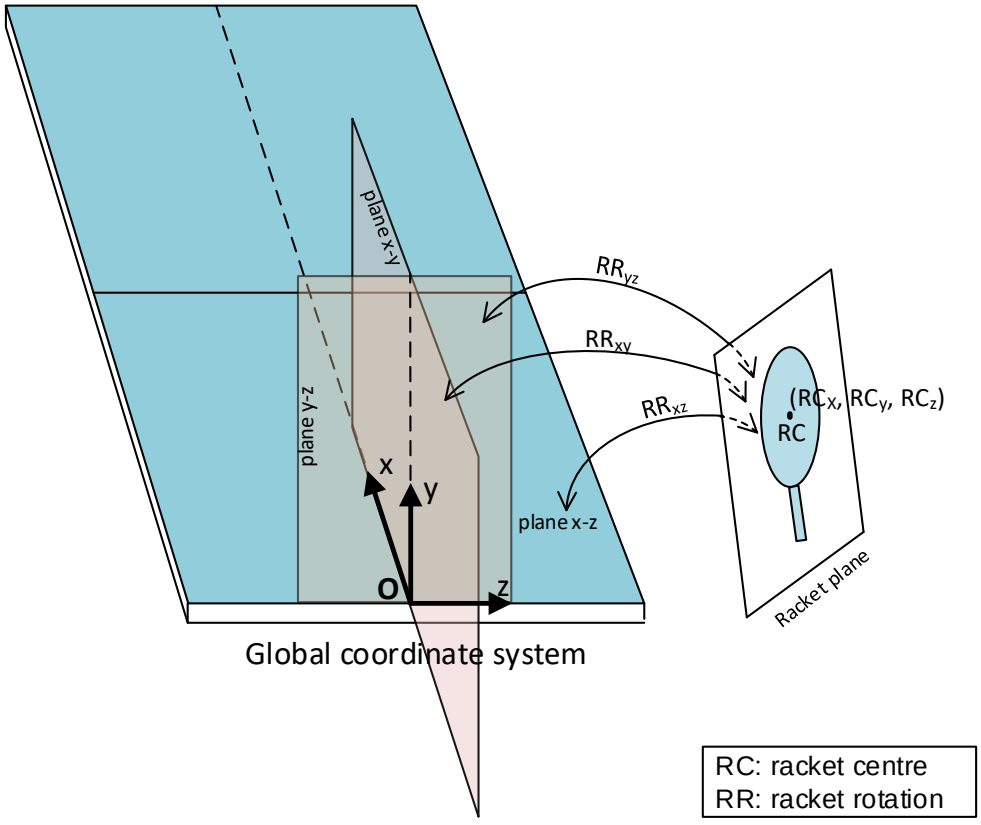

Figure 3-1 Global coordinate system and racket motion

Table 3-1 Motion of the racket in each *DOF*

Racket	***DOF***	**Notation**	**Displacement of each *DOF***
Racket centre (translational)	3	RC_x	displacement along *x*-axis of the global system
		RC_y	displacement along *y*-axis of the global system
		RC_z	displacement along *z*-axis of the global system
Racket (rotational) *	3	RR_{xy}	angle between racket plane and the global *x*-*y* plane
		RR_{yz}	angle between racket plane and the global *y*-*z* plane
		RR_{xz}	angle between racket plane and the global *x*-*z* plane

Note: * angles between the racket plane and the respective global planes range within *0°~180°*

The human trunk and upper limb function as a multi-segment open-linked kinematic chain to transfer the motion to the racket. Their complex motion patterns are the consequence of the high *DOF*s of the human body in *3D* space. To quantitatively describe the movement of human body, the definitions of *ISB* (G. Wu et al., 2005) were followed. The rotational *DOF*s for each segment and joint are illustrated in *Figure 3-2*. In the model, the trunk has three rotational *DOF*s. The upper limb has *7 DOF*s with *3*, *2*, *2 DOF*s for the shoulder, elbow and wrist joints respectively. In addition, the trunk centre has three translational *DOF*s, as tabulated in *Table 3-2*.

According to *ISB*, each of the local joint coordinate system (*JCS*) is defined precisely using bone landmarks thereafter the relationship between two adjacent *JCS* was calculated (i.e. a rotation matrix), which is further converted into three sequential rotational angles (Euler angles) to describe segment/joint rotations. For example, the motion of the elbow joint is the relative movement of the lower arm coordinate system with reference to the upper arm coordinate system. This relationship matrix is converted to three Euler angles in *Z-X-Y* order: the first rotation is defined as flexion/extension, the second is defined as abduction/adduction of the radius, and the third is pronation/supination. Since the second rotation is negligible and usually

considered in rehabilitation studies only, the elbow is assumed to have 2 *DOF*s (Table 3-2) in the current research. The detailed definitions for each of the human rotational *DOF*s are listed in *Appendix A*. All of these rotations have a value of zero when the person is in the anatomical reference position.

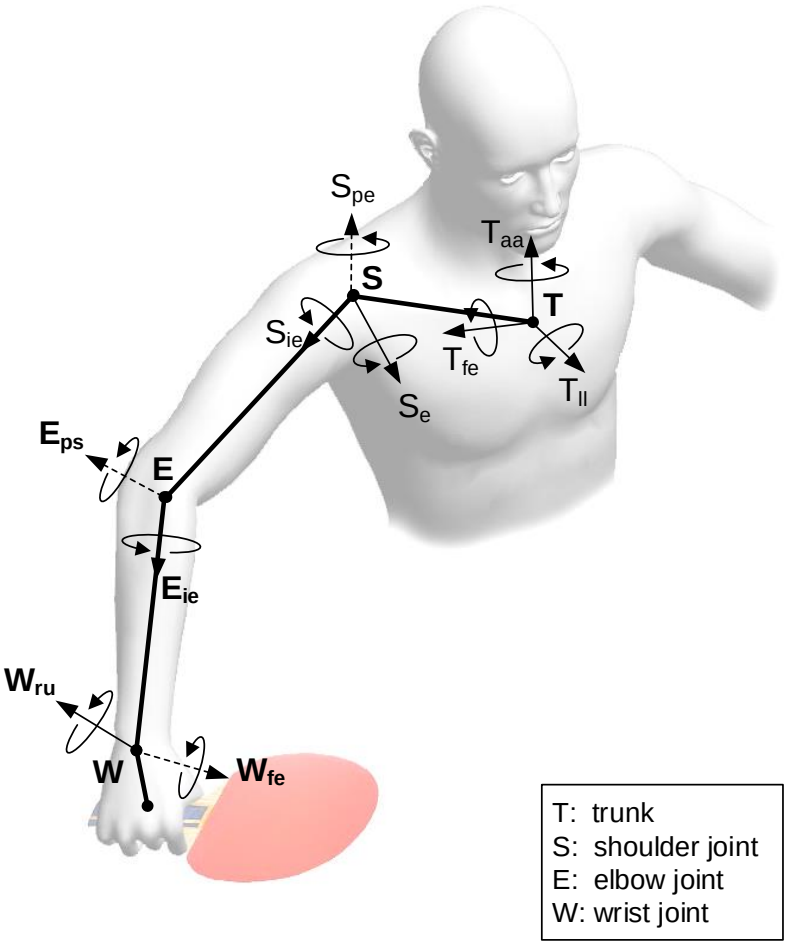

Figure 3-2 Rotational movement of human trunk and upper limb

Table 3-2 Motion definition of the human kinematic model in each *DOF*

Segments/Joints	***DOF***	**Notation**	**Each *DOF***	**Range of motion***
Trunk centre (translational)	3	TC_x	forward (+) /backward (-)	-
		TC_y	upward (+) /downward (-)	-
		TC_z	leftward (-) /rightward (+)	-

Trunk (rotational)	3	T_{fe}	flexion (-) /extension (+)	-
		T_{ll}	lateral left (-) /right (+)	-
		T_{aa}	axial rotation right (-) /left (+)	-
Shoulder joint	3	S_{pe}	plane of elevation (-/+)	-45.5° ~ +140.7°
		S_e	elevation (-)	-180.0° ~ -0.0°
		S_{ie}	internal (+) /external (-) rotation	-180.0° ~ +180.0°
Elbow joint	2	E_{fe}	flexion (+) /hyperextension (-)	-0.6 °~ +142.9°
		E_{ps}	pronation (+) /supination (-)	+7.9 °~ +165.8°
Wrist joint	2	W_{fe}	flexion (+) / extension (-)	-74.9° ~ +76.4°
		W_{ru}	radial (-) /ulnar (+) deviation	-21.5° ~ +36.0°

Note: * normal amplitude of active motion of human joints (Boone & Azen, 1979); shoulder data is partly missing (due to different definitions of the coordinate system) therefore is estimated.

3.1.2 Measurement and calculations for the model

To capture the kinematics of the human body and racket with an optical motion capture system (which will be used during the experiment as described in the next chapter), the placements of reflective markers are shown in *Figure 3-3* and also tabulated in *Table 3-3*.

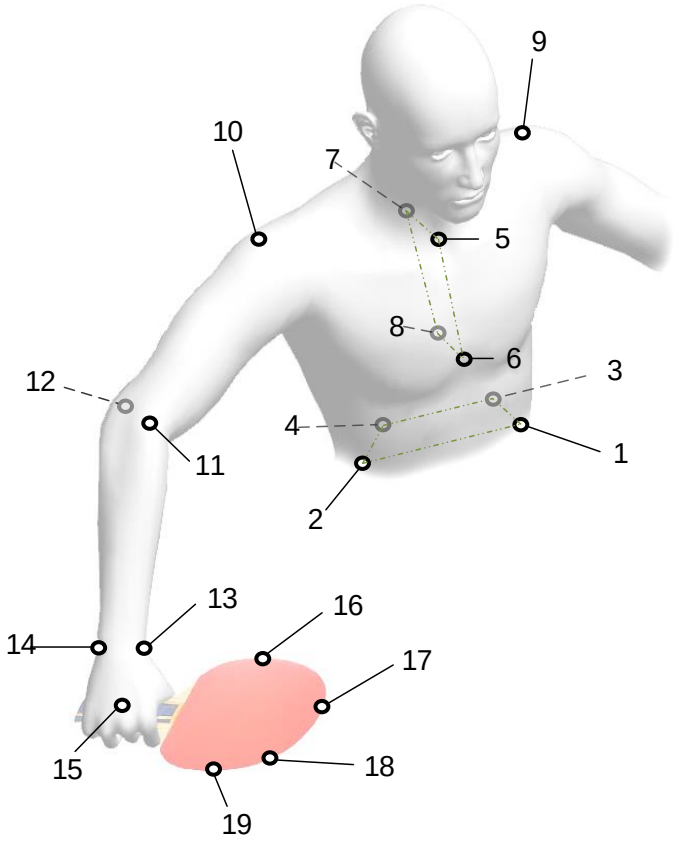

Figure 3-3 Marker placement

Table 3-3 Marker placement

Marker No.	**Marker location**	**Abbr.**
1	Left *ASIS* (Anterior Superior Iliac Spines)	*ASISL*
2	Right *ASIS*	*ASISR*
3	Left *PSIS* (Posterior Superior Iliac Spines)	*PSISL*
4	Right *PSIS*	*PSISR*
5	Jugular Notch where clavicles meet the sternum	*IJ*
6	Xiphoid process of the Sternum	*PX*
7	Spinous process of the *7th* cervical vertebrae	*C7*
8	Spinous process of the *8th* thoracic vertebrae	*T8*
9	Left acromion	*GHL*
10	Right acromion	*GH*

11	Right lateral epicondyles of humerus	*EL*
12	Right medial epicondyles of humerus	*EM*
13	Right styloid processes of radius	*WR*
14	Right styloid processes of ulna	*WU*
15	*3rd* metacarpophalangeal (*MCP*) joint	*H*
16	Racket left *90* °edge	*RL*
17	Racket head	*RH*
18	Racket right *45* °edge	*RHR*
19	Racket right *90* °edge	*RR*

Among the markers *16-19* on the racket, the marker *16* (*RL*) and *19* (*RR*) are used to calculate racket centre and its related translational movement; with the additional marker *17* (*RH*), the vector normal to the racket plane can be obtained therefore for racket rotational movement calculation. The marker *18* (*RHR*) is only used to help shape an asymmetrical distribution in order to make the racket easily identifiable by the motion capture system.

The markers *1-15* are attached on the bony landmarks (Table *3-3*) to ensure that the related definitions of the *JCS* are identical to those defined by *ISB*. The markers *1-4* are not used in the current study but only as an extension for potential future work (inclusion of the investigation of lower trunk motion). Specifically, the maker *10* (*SR*) is attached to the acromion to estimate the centre of humeral head centre. An offset of equivalent size of the radius of the upper arm was applied to *SR* parallel to the sagittal plane of trunk, in order to compensate the distance from humeral head centre to marker centre. Similarly, to estimate the metacarpophalangeal joint centre from marker *15* (*H*), the *H* is offset by half of the thickness of the hand. For the definitions of the humerus *JCS*, the *ISB* alternative method was used: the *z*-axis of the upper arm coordinate system is derived from the vector normal to the plane made

up of *GH*, the midpoint of the line between *EL* and *EM* and the midpoint of the line between *WR* and *WU* (*Figure 3-4*). Note that some coordinate systems are translationally shifted in *Figure 3-4* (compared to *Appendix A*) to make them easier to understand , which do not change any rotational relationship. This alternative method is preferred due to the high error sensitivity in the direction connecting *EL* and *EM* (i.e. the other method), due to the relatively short distance between *EL* and *EM*. The trunk centre is simplified as the centre of 4 markers: *IJ*, *PX*, *C7* and *T8*. The rest can be found in *Appendix A*.

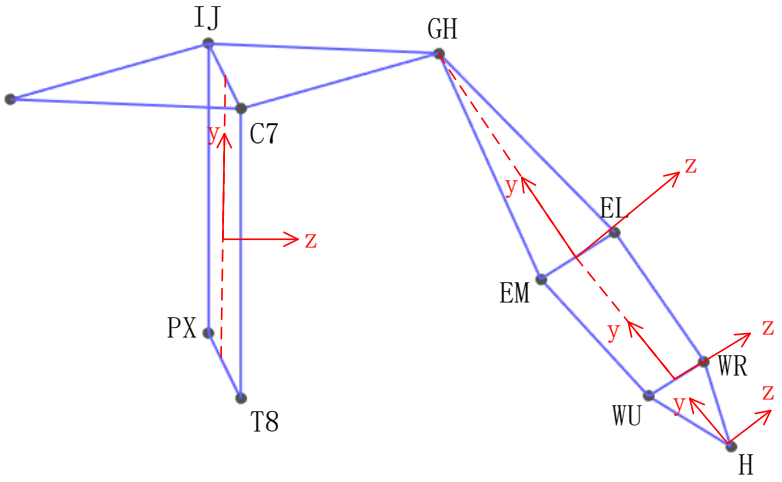

Figure 3-4 Joint coordinate systems for angle calculation

3.2 Phase segmentation and normalization

3.2.1 Phase segmentation based on racket centre velocity profile

There are *4* phases in a table tennis forehand cycle: preparatory (*PR*), backswing (*BS*), forward swing (*FS*) and follow-through (*FT*), as illustrated in *Figure 3-5*. The critical septal moments between the phases are marked as T_0, T_2, T_3 and T_4 respectively.

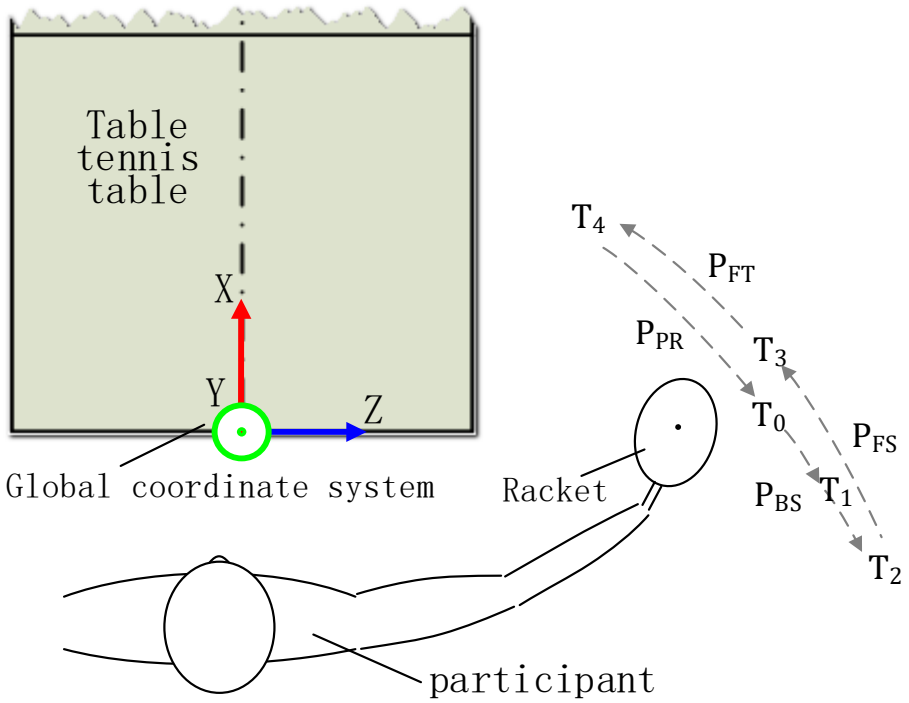

Figure 3-5 Phases during a forehand stroke

To identify the phases of a stroke, a direct method by using displacement profile may be taken into consideration. For example, to find out T_2, a maximum backward point (i.e. along the global -*y* axis) on the displacement trajectory may indicate this phase time, or a more reasonable vertex on the trajectory curve between T_0 and T_3, which better adapts to curved shapes in different directions. However, individual differences may exist and prevent easy identification of curve vertices. An example of such cases (*2* experts and *2* novices) from the preliminary experiment is shown in *Figure 3-6*. Whenever the magnitude of curvature is small (e.g. large radiuses at backswing end of expert *1* and follow-through end of novice *1* in *Figure 3-6*), it is hard to find out the curve vertex, which leads to less accuracy in determining the phases. Therefore, another method based on racket centre velocity profile (Z. Zhang et al., 2016) is preferred .

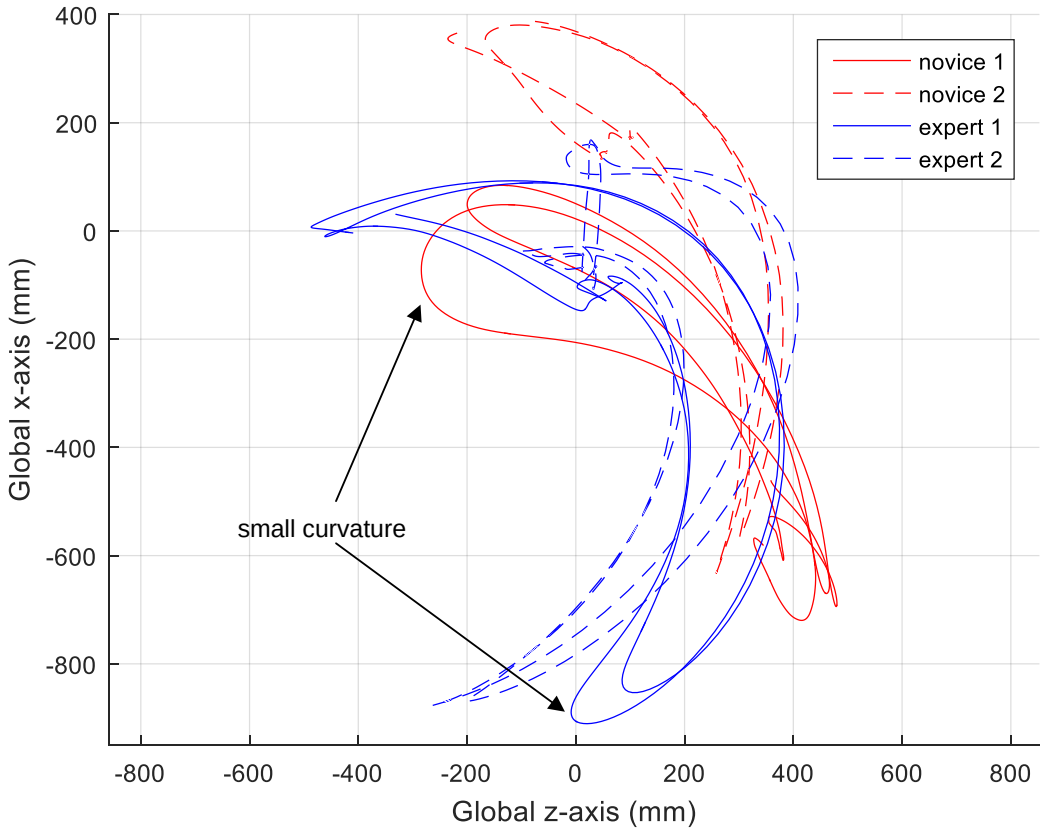

Figure 3-6 Example of distinct trajectories of racket centre between experts and novices

Interestingly, the velocity profiles of the racket centre of different people show similar patterns according to our motion capture, therefore the profiles are utilized for phase identification. The general shape and process of identification is illustrated in *Figure 3-7*: the *T*s are first identified from the racket velocity curve, with the phases then readily retrieved. Note that there is an additional T_1 which is also marked in *Figure 3-5*. With the curve of the racket velocity— the resultant speed of forward and leftward velocity of the racket centre (i.e. projected velocity on the ground floor plane, as the motion relative to this plane is of the most interest), the *T*s can be determined from the time points with velocity values at local maximum or minimum. In other words, all the *T*s are generally located where the acceleration is zero. This method identifies the phases using only the information of racket centre velocity, and the processing is unambiguous and much more straightforward than the

displacement-based identification method.

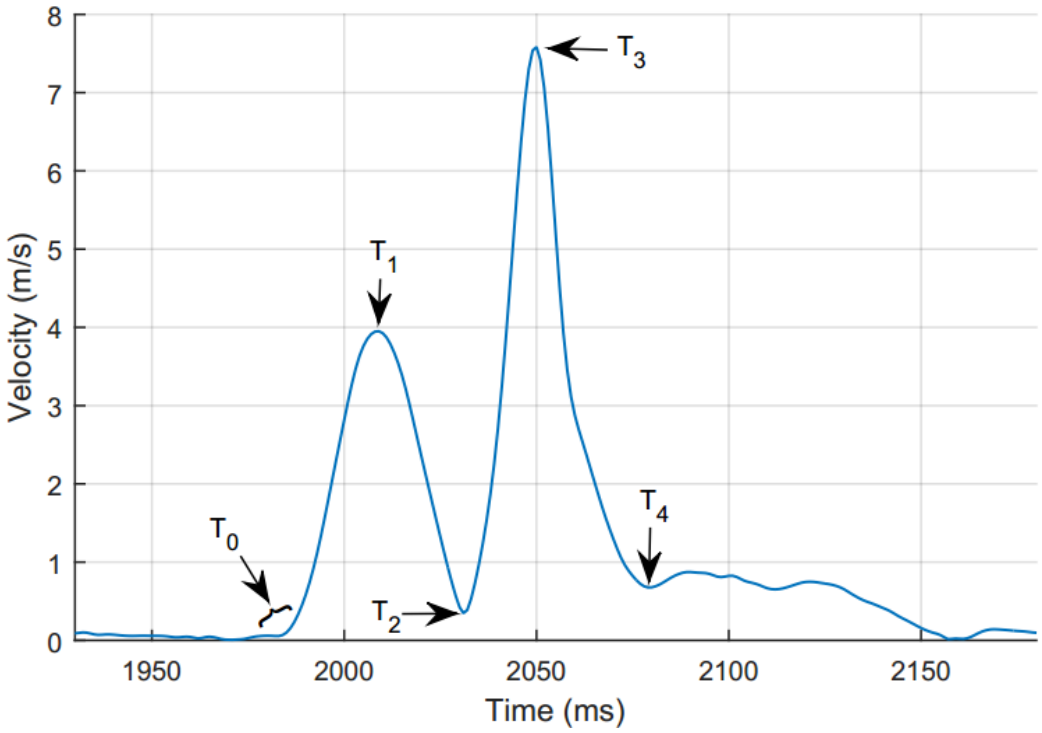

Figure 3-7 A typical example of racket centre resultant velocity profile

The velocity-based method identifies the *T*s which are different from those identified from displacement profiles on the trajectory curve. For example, the captured samples show that T_2 may have a bias up to *0.02s* between velocity profile and vertex method from displacement profile (when the vertex is identifiable). The gap is quite short in time yet considerable in the short phases. However, the situations of misidentification or failure of identification from the displacement profile may result in errors times or tens of times (e.g. *0.1*s) of the gap. Therefore, the velocity-based method shows advantages in minimizing the identification errors. According to the data from the preliminary experiment, however, T_0, where the player (and therefore the racket) starts to move from a relatively stationary pose, was generally challenging to identify reliably. This can be seen by inspection of the typical example data shown in *Figure 3-7*. A common solution to this is to set a speed threshold value. Whenever the backswing speed exceeds that value (e.g. like toe-off event in gait),

then that point is regarded as the beginning of P_{BS}. However, such a value is generally somewhat arbitrarily defined and may therefore affect T_0 in turn to a significant extent (Z. Zhang et al., 2016). This bias may be especially large when it comes to a racket sport like table tennis, because the phases are all relatively short in time. In fact, *Figure 3-7* shows two parts under the backswing phase: T_0 - T_1 and T_1 - T_2, where the T_1 is defined as the moment with the maximum backswing speed. Since T_0 is not sufficiently reliably identified from the velocity data, the duration T_1 to T_2 was used for the definition and alias for the backswing phase P_{BS} in the remainder of this thesis.

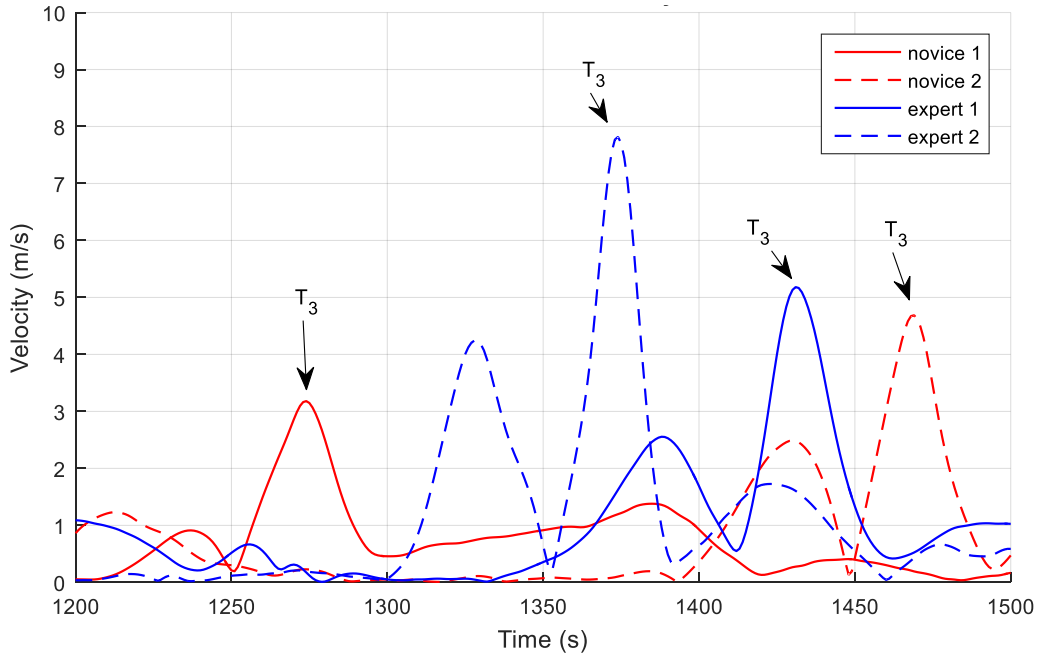

Figure 3-8 Easily identifiable phases time from racket velocity profile

The prominent T_3 is coincident with or very close to the moment when the racket and ball come into contact, as supported by previous research (Bootsma & Van Wieringen, 1990; Ramanantsoa & Durey, 1994; Sheppard & Li, 2007). It is quite convenient and fast to identify T_3 based on racket velocity profiles (*Figure 3-8*) as compared to the method based on the table tennis ball, which requires an extra

motion capture device (e.g. high speed camera).

In addition, an experiment (*Figure 3-9*) was conducted to investigate and verify the coincidence of maximum racket speed and racket-ball contact moment for T_3 for participants of different skill levels under the experimental setting of this thesis. Based on the data of several participants (*2* experts and *2* novices, *15+* strokes for each) by high speed camera, the left and right edge (*RA* and *RB*) of the racket and the centre of the ball (*RC*) are highlighted for all the captured frames. The position data of the racket edges and ball center were retrieved frame by frame, and their velocities were calculated as the first derivative of the position data. The displacement and velocity curves were aligned above the axis of time. The results show that the maximum speed of the racket centre generally occurs within *30 ms* after the racket-ball contact. This is relatively negligible considering the errors and the duration of the phases. An example of one captured stroke is shown in *Figure 3-10*.

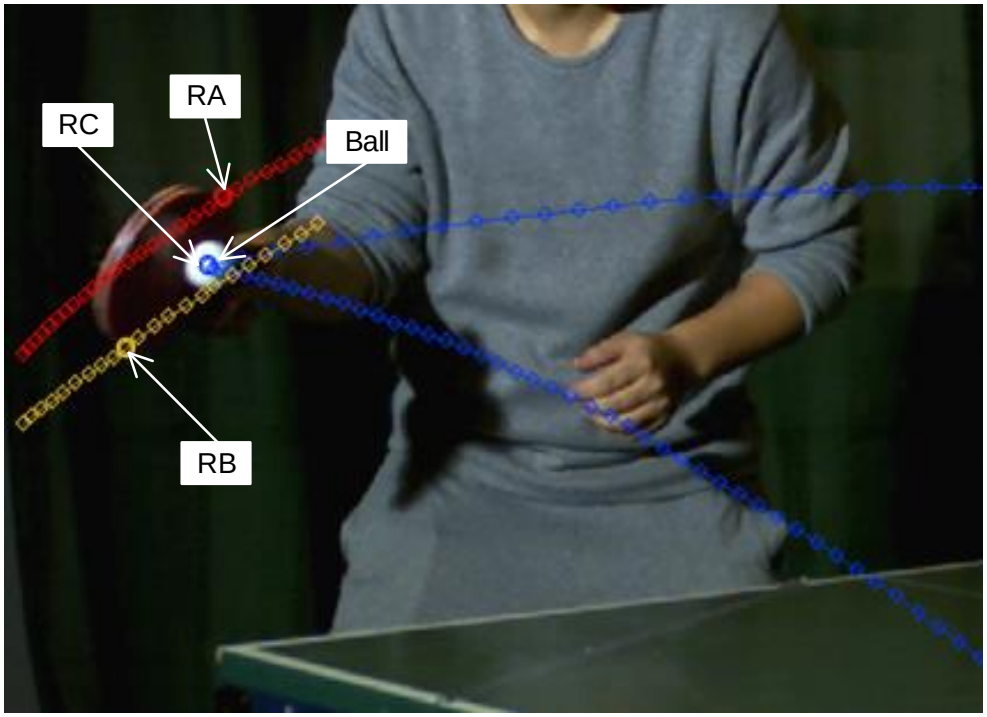

Figure 3-9 High speed camera experiment

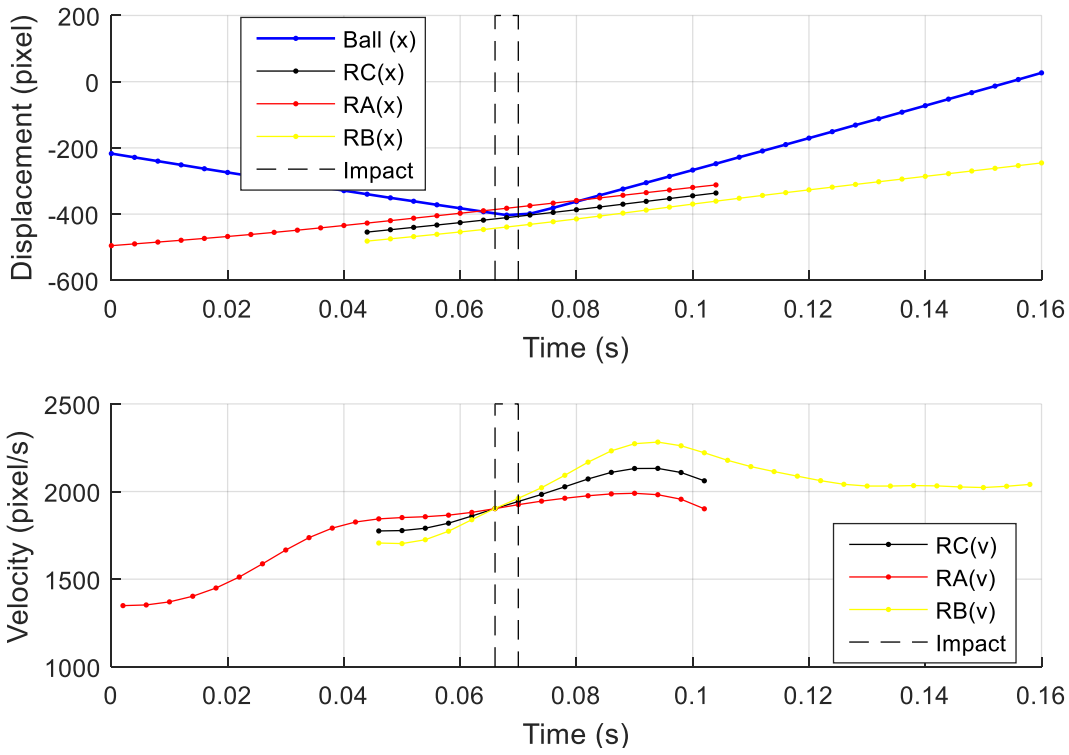

Figure 3-10 Results of high speed camera experiment

Therefore, the method based on racket centre velocity profile would be applicable for the unambiguous segmentation of the important phases P_{BS} (T_1 to T_2), P_{FS} (T_2 to T_3) and P_{FT} (T_3 to T_4).

3.2.2 Piecewise normalization

Each stroke of each player may have different time duration, which make analysis difficult on the time series data (e.g. trunk rotation during forward swing). Therefore, the piecewise alignment normalizes movement data based on the phases, in order for easier comparison between different strokes of different players. The detailed steps are explained below.

After the various phases (i.e. T_1, T_2 and T_3 for P_{BS}, P_{FS} and P_{FT}) of a stroke are identified, all the displacement and velocity variables are aligned by assigning new time labels: each original time series data keep their values unchanged but the

respective time labels T_{before} are replaced by T_{after} based on *Equation (3-1)*. P_{PR} is not of interest and therefore not presented.

$$T_{after} = \begin{cases} \frac{T_{before} - T_1}{T_2 - T_1} + 1, T_1 \leq T_{before} \leq T_2 \\ \frac{T_{before} - T_2}{T_3 - T_2} + 2, T_2 \leq T_{before} \leq T_3 \\ \frac{T_{before} - T_3}{T_4 - T_3} + 3, T_3 \leq T_{before} \leq T_4 \end{cases} \quad (3\text{-}1)$$

The normalized data is based on aligned phase time $1-4$, where T_1 to T_4 are aligned to phase time *1* to *4* respectively. In other words, the segmentation of phases is not changed but the data is aligned within each phase. Missing data can be interpolated where the respective phase time T is not measured. *Figure 3-11* is included to illustrate the phase alignment. Since every stroke has a different total duration, all the strokes were aligned to the moment of racket-ball contact (i.e. to maximum velocity) as shown in *Figure 3-11a*; once phase aligned, the curves were completely aligned over T_1 to T_4 as shown in *Figure 3-11b*.

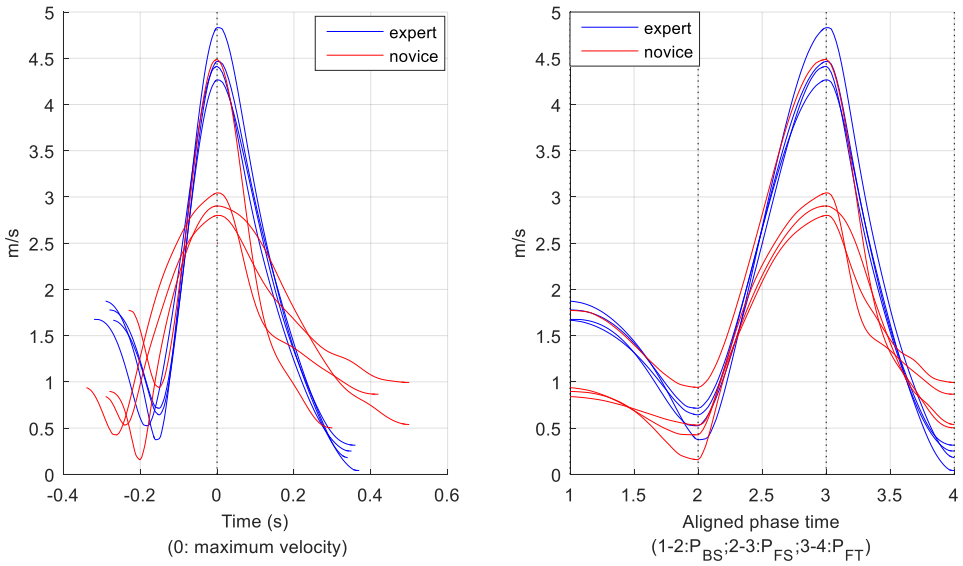

Figure 3-11 Racket centre velocity before (a) and after (b) alignment for two participants

3.2.3 Visualization for the normalized kinematic model

The collected kinematic data can be visualized (*Figure 3-12*) to assist the analysis of the strokes. The position of the human body in the figure is reconstructed reversely using the data of the kinematic model (e.g. displacement of the trunk and angular displacement of joint angles).

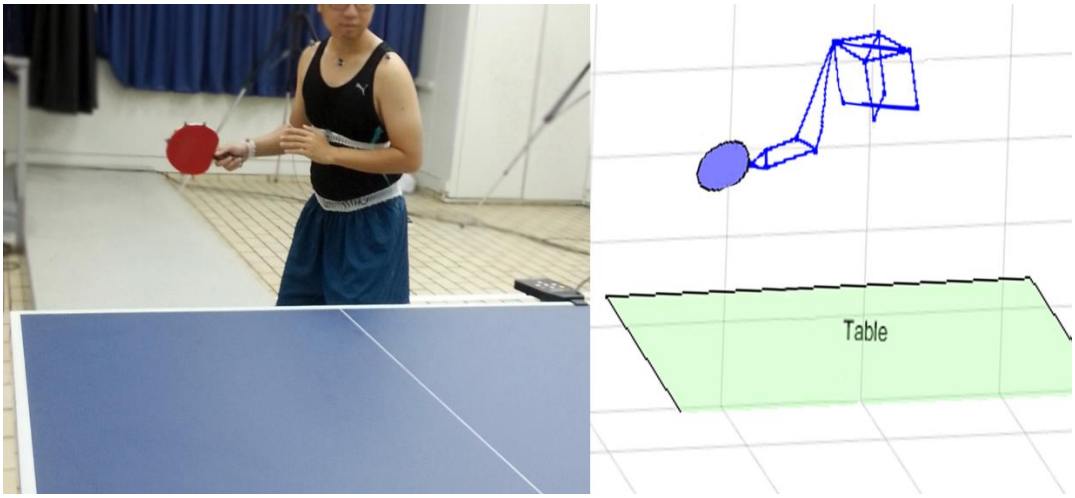

Figure 3-12 Visualized kinematic (right) model from collected data

The visualized *3D* animation takes advantage of the multi-angle viewports as compared to the recorded video resources. The stroke data can be displayed either partly or in multiple phases to highlight the motion of specific segments or joints. In addition, the introduction of the phase segmentation and piecewise normalization makes it possible to display multiple strokes of the same figure for visual comparison. Other beneficial information can also be added to the figure to aid understanding, such as the direction of the racket, or tabulated values of certain joint angular velocity, etc.

3.3 Summary

This chapter described the work of the quantification of the kinematic model for

racket and human body during a forehand stroke, and the phase segmentation and normalization methods for these time series variables. The definitions of the variables on different *DOF* were based on *ISB* recommendation. The measurement and calculation methods for these variables were also proposed. The quantification is comprehensive and unambiguous. The novel racket center velocity profile was used to segment phases, which presents smaller errors and is more straightforward than using displacement. The normalized variables can be aligned and visualized to assist data analysis. These methodologies is the basis for data processing and quantified comparison in the subsequent chapters.

Chapter 4 Motion pattern differences between expert and novice table tennis players

4.1 Experiment design

4.1.1 Participants

A sample of *20* table tennis players (*10* experts and *10* novices) were recruited as participants for the experiment. These participants were male and right-handed shakehand-grip table tennis players. None of them had any current or recent musculoskeletal disorders or other medical conditions. The *10* experts were higher-level players recruited from professional teams or clubs. They had received training from coaches from they were beginners. The *10* novices were beginners recruited from the general university population. The inclusion criteria for the novice were that they play table tennis less than one hour per week and had never received formal training from coaches or other professionals. The protocol was approved by *NTU IRB* (Institutional Review Board) before the experiment began. The sample size was more than previous study (e.g. *9* advanced *vs. 8* intermediate players by Iino and Kojima (2011)) and power was preliminarily checked by using data of several participants with power analysis (power = *0.8*).

4.1.2 Experimental setup

The experiment was conducted indoors. The apparatus and their locations are illustrated in *Figure 4-1*. A standard table tennis table (2.74×1.525×0.76 m) was placed in the room. A ball-feeding machine (Robo-Pong, Newgy, *USA*) was set up on side of the table opposite the player. The ball-feeding machine was set to propel the balls from the centre of the table edge every *3* seconds to land approximately *480 mm* from the right table edge and *71*0 mm from the near side table edge, and

bounced with a speed of about *4 m/s*. A piece of rectangular *A5*-size white paper was located on the ball-feeding machine side of the table, about *380 mm* to the left table edge and *450 mm* to the front table edge, which functions as participants' hitting target. An ordinary video camera was used to record the whole table tennis play during the experiment. The participants were provided a standard shakehand-grip racket. An optical eight-camera motion capture system (Motion Analysis Eagle System, *Santa Rosa, CA*, *USA*) was used to capture data at the sampling rates of *100 Hz*.

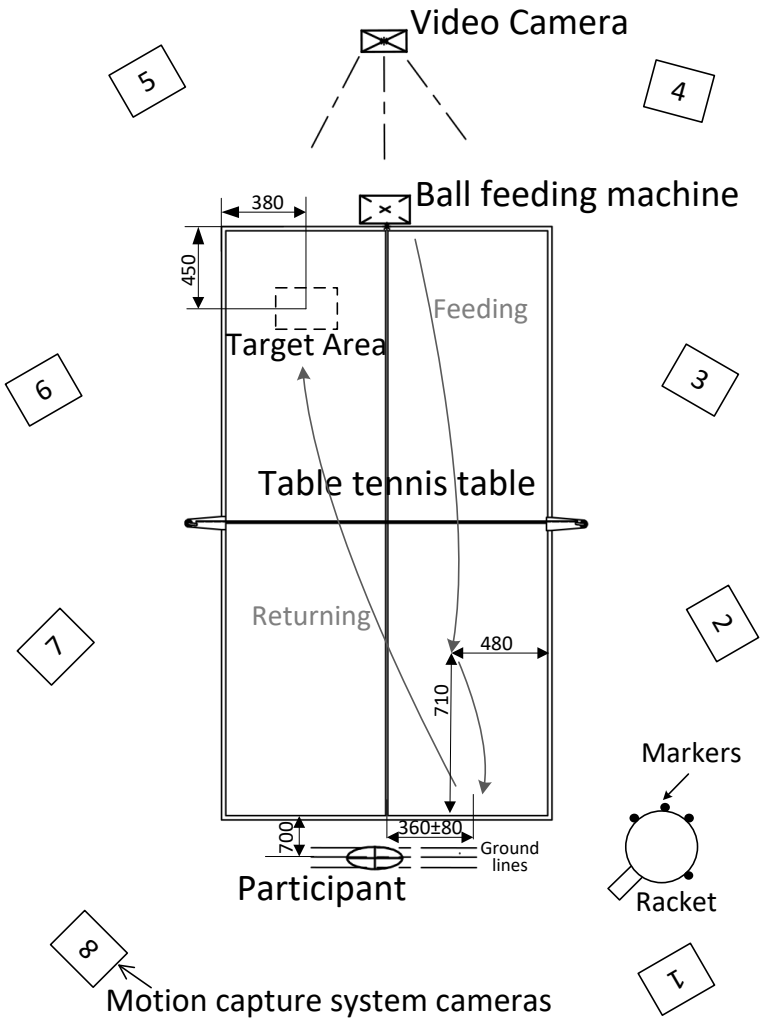

Figure 4-1 Experimental setup

4.1.3 Procedure

The whole experiment took about a maximum of one hour for each participant, including 30 minutes of warming up. Each participant's personal data was collected at the beginning. Several anthropometric dimensions including body height and weight, sizes of trunk, upper arm, lower arm, and hand, were then measured using human body anatomical landmarks for logging purpose. Written consent was sought after the procedures had been fully described. Before the experiment, the reflective markers were attached onto the racket and participants' body as described in the previous chapter (Section *3.1.2*). The participants warmed-up for *30* minutes by practicing the forehand counterhit to familiarise with the environment and equipment, during which they adjusted their body movement and tried to find their preferred speed to hit the ball towards the target as accurately and as quickly as possible. During the experiment, participants used the forehand counterhit technique with their preferred speed to repeatedly return the balls towards the target while standing on the marked ground lines (no restriction on the side standing position) without any initial foot movement (*Figure 4-1*). Motion capture started when participants could perform consistently based on the experimenter's observation and lasted for *3* minutes. In other words, a total number of *60* feedings was recorded for each participant.

4.2 Data processing

4.2.1 Data filtering, reduction and normalization

The data from the motion capture system were subjected to the low-pass Butterworth filter (Butterworth, 1930) of cut-off frequency varying from *9.3-13.9 Hz* based on the residual analysis (Pezzack et al., 1977).

By reviewing the recorded video, successful and failed strokes were identified. A

failed stroke refers to a stroke when a participant did not successfully return the ball to the target. Only the data of successful strokes of each participant were used for further analyses (*Table 4-1*). Here, a stroke accuracy was calculated as the percentage of the successful strokes in all strokes for each player.

Table 4-1 Number of strokes of each participant

	Number of stroks of each expert										Number of stroks of each novice									
	.	.	.	.	.	.	.	.	.	.	.	.	.	.	.	.	.	.	.	.
recorded	59	59	59	59	59	60	59	60	59	60	59	59	60	59	60	59	59	59	59	59
hitting target	51	59	53	54	46	46	40	46	39	60	30	36	39	26	39	33	24	30	21	18
final	39	57	48	36	43	26	39	46	39	59	29	34	38	25	38	29	24	26	19	18

There were also incomplete data due to failure motion capture (e.g. missing marker etc.). To make results more accurate, these strokes were removed rather than interpolated by software. Final data of each stroke (Table 4-1) were used to obtain the kinematic variables with the method described in *Section 3.1*, then segmented and piecewise-normalized with the method described in *Section 3.2*.

4.2.2 Dependent variables

The dependent variables for the statistical analysis were based on the above-mentioned processed kinematic variables. They covered the majority of the kinematic variables of table tennis basic strokes including motion of the racket and the human body as defined in *Table 3-1* and *Table 3-2* respectively. These variables involved all the available *DOF*s and therefore were able to describe the movement of the racket and human trunk and upper arm. Both of the mean of the displacement and velocity among different motions for each participant were included. In addition, the phase time was also taken into consideration since the normalization removed the duration information of time from the original data. The dependent variables were defined and categorized as below.

1. Phase

    a) Phase durations

    This is the time elapsed during the three considered phases in a stroke—backswing phase P_{BS}, forward swing phase P_{FS}, and follow-through phase P_{FT}. They are calculated as the time intervals between adjacent T_i (i =1~4).

2. Racket motion (refer to *Table 3-1*)

    a) Racket centre linear movement

    It includes the racket centre displacement and velocity with respect to the origin of the global coordinate system. In addition to the racket centre velocity in the three directions, RC_{2D} and RC_{3D} are specifically raised for investigation in the current chapter. RC_{2D} is the projected racket centre velocity on the ground plane (the global plane *x*-*z*), which is also the resultant velocity of the racket centre in *x*- and *z*- directions; RC_{3D} is the racket centre velocity in *3D* space, which is also the resultant velocity in *x*-, *y*- and *z*- directions.

    b) Racket spatial orientation

    Three components of the racket plane orientation with respect to the axis planes of the global system are compared under each of the three phases, which are time-series variables.

3. Human motion (refer to *Table 3-2*)

    a) Translational movement of the trunk centre

    It is the translational movement of the human trunk centre, including the displacement and velocity of the trunk centre with respect to the origin of the global coordinate system.

    b) Rotational movement of the trunk, shoulder, elbow and wrist

    It is the rotational movement of the trunk, shoulder, elbow and wrist joints.

Both angular displacement and angular velocity were investigated.

4.2.3 Statistical analysis

The two-sample Student's *t*-test was used for the comparison between expert and novice players with the level of significance set at *0.05*. For the time series variables, the *t*-test was performed at *50* equally spaced intervals (e.g. step of *0.02* for P_{FS}, or T_2, $T_{2.02}$, $T_{2.04}$, . . . , T_3) within each phase. Welch's *t*-test (unequal variances *t*-test) was used instead if two groups of data had significant different variances based on Levene's test. This modification was based on the assumption test on preliminary data of several participants, which showed that the variances of the data of experts and novices were not always the same on different phase time.

4.2.4 Stroke accuracy

Results shows that the stroke accuracy for hitting the target of the expert players was significantly higher ($p < 0.001$) than their novice counterparts (83.55 ± 11.92 % versus 49.95 ± 12.10 %).

4.2.5 Kinematic model visualization

This section describes the visualization of the normalized kinematic model (*Section 3.2.3*) of the stroke by applying the player's segment dimensions and the collected kinematic data. Before the reconstruction, the body dimensions of the players were obtained through calculation from the markers (and verification from direct measurement), as illustrated in *Figure 4-2*. The *t*-test comparison was conducted on the data. The results are tabulated in *Table 4-2*. There were no significant differences between the body dimensions of experts and novices except the hand height, which is the distance from racket centre to the wrist joint along the handle of racket. This indicated that the experts held the racket deeper than the novices.

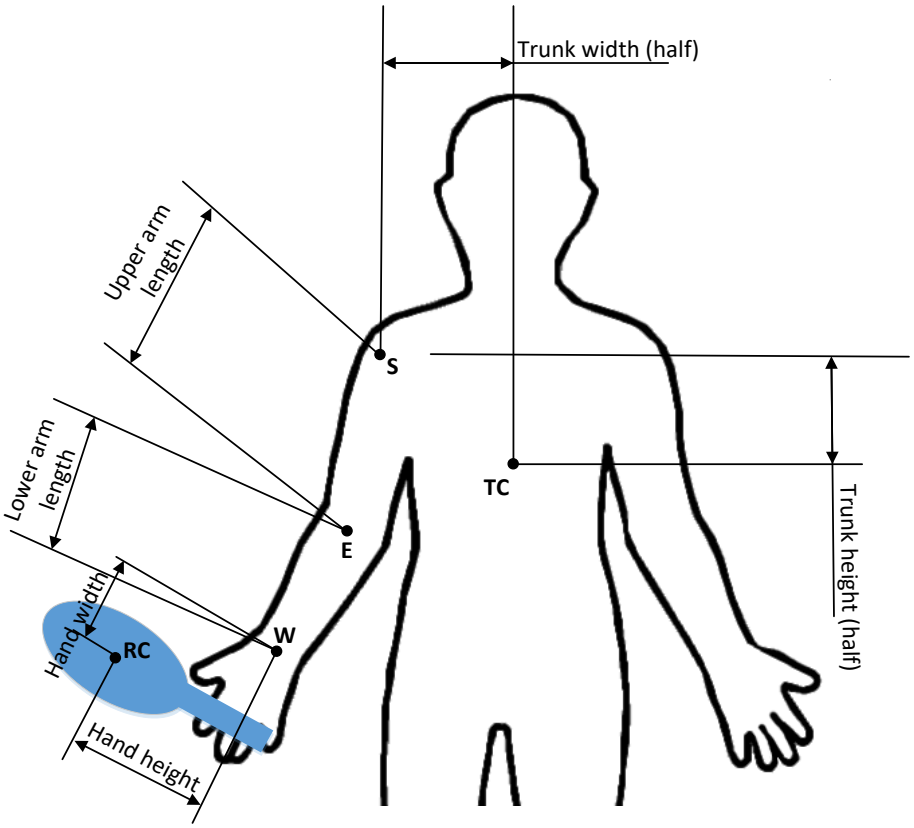

Figure 4-2 Body dimension illustration

Table 4-2 Comparison of body dimensions

	Experts	**Novices**	***p*-value**
Upper Trunk height (half)	78.06 ±15.78	80.25 ±16.69	0.77
Upper trunk width (half)	148.91 ±12.33	156.18 ±8.85	0.15
Upper trunk depth (half)	-4.36 ±8.49	-8.42 ±12.77	0.41
Upper arm length	273.69 ±16.89	283.69 ±13.64	0.16
Lower arm hand	232.78 ±14.60	243.19 ±14.75	0.13
Hand height	166.11 ±10.34	185.88 ±17.24	0.01*
Hand width	38.20 ±15.96	34.78 ±19.92	0.68
Hand depth	35.15 ±9.69	38.66 ±12.11	0.48

The motion data was used to rebuild the kinematic model. Since the body dimensions do not differ significantly, it allowed the implementation with unified

and averaged body dimensions for each segment, therefore allows the visualization of the differences for highlights on motions rather than body dimensions. The segment and joint motion were applied to the respective position in the model. It was then visualized as a *3D* animation to show the group differences during a stroke, which allowed investigation from multi-angles in any of the phases. *Figure 4-3* illustrated the different posture of the experts and novices at the moment of racket-ball contact. The directions of the racket were added and it is apparent from the figure that experts were pointing their racket more in the downward direction compared to the novices. Since the figure works as an assistive tool, further detailed results are listed in the following sections with the statistical analysis.

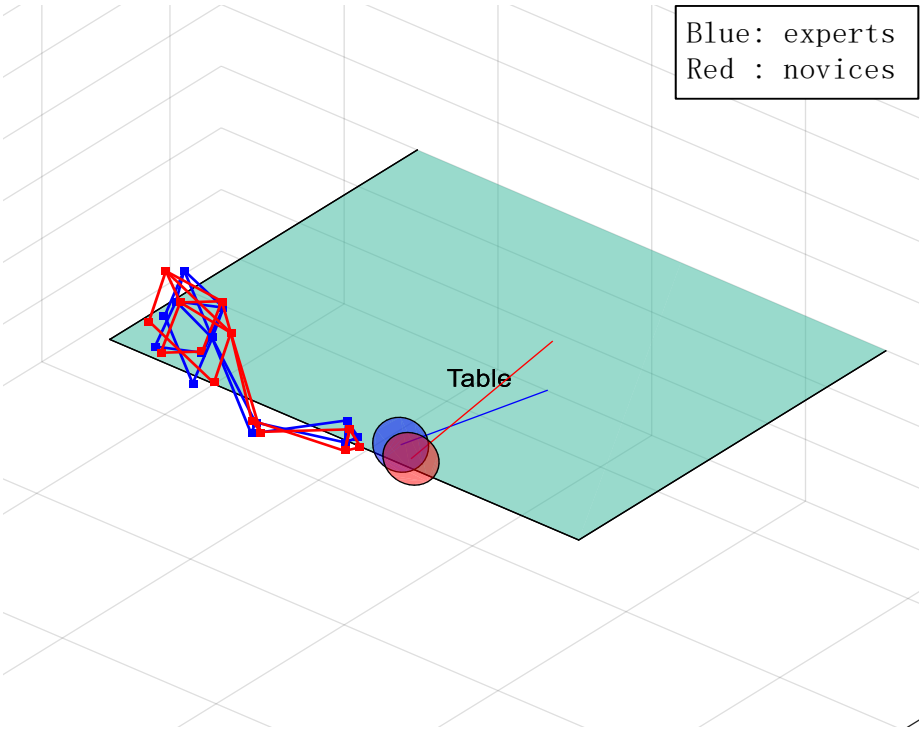

Figure 4-3 Visualized comparison of the posture of experts and novices at racket-ball contact

4.2.6 Phase durations

The durations of each phase, the backswing phase P_{BS}, the forward swing phase P_{FS} and the follow-through phase P_{FT} of each participant are shown in *Figure 4-4*, as the

mean ± variability (standard deviation) for the error bar charts. Student's *t*-test was performed and the results are tabulated in *Table 4-3*. The total duration of the three phases "$P_{BS}+P_{FS}+P_{FT}$" is also included in the table.

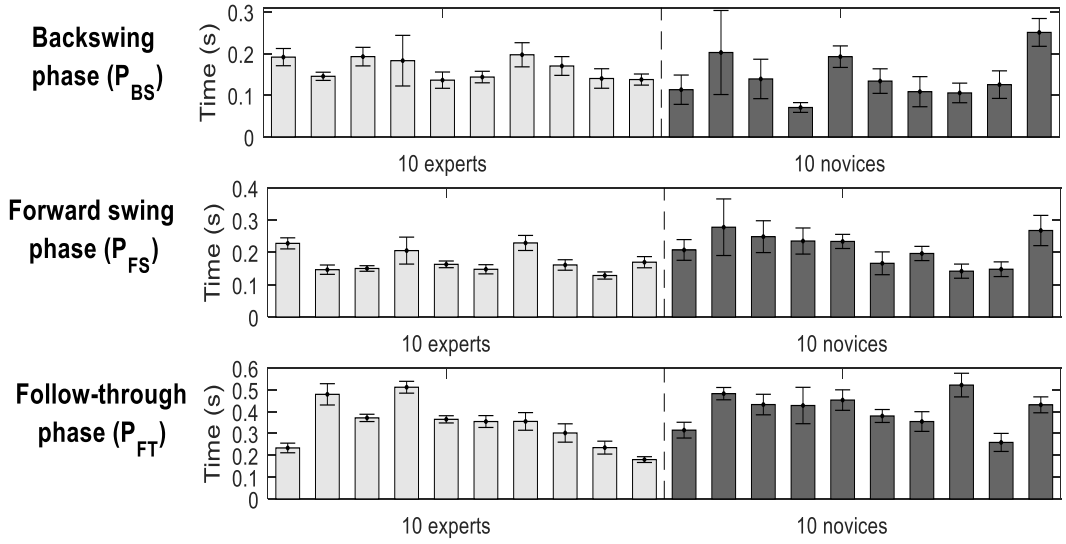

Figure 4-4 Phase durations for each participant

Table 4-3 Comparison of mean and variability of durations of phases

	Phases	Experts	Novices	p-value
Mean	$P_{BS}+P_{FS}+P_{FT}$	0.68 ± 0.12	0.76 ± 0.14	0.162
	P_{BS}	0.16 ± 0.03	0.14 ± 0.05	0.319
	P_{FS}	0.17 ± 0.04	0.21 ± 0.05	0.053**
	P_{FT}	0.34 ± 0.11	0.41 ± 0.08	0.126
Variability	$P_{BS}+P_{FS}+P_{FT}$	0.07 ± 0.03	0.12 ± 0.04	0.003*
	P_{BS}	0.02 ± 0.01	0.04 ± 0.02	0.128
	P_{FS}	0.02 ± 0.01	0.04 ± 0.02	0.010*
	P_{FT}	0.03 ± 0.01	0.04 ± 0.02	0.017*

Note: ∗ indicates significance ($p < 0.05$); ** indicates marginal significance ($0.05 < p < 0.1$).

The duration of each stroke for each participant varied to a different extent; experts

also displayed certain variability across different strokes in each of the phases, though relatively smaller than those of the novices (*Figure 4-4*). From *Table 4-3*, there are no significant difference on the total time between experts and novices ($p = 0.162$). There are no significant differences on the duration of backswing phase ($p = 0.319$) and follow-through phase ($p = 0.126$) though experts spent longer time in backswing phase and shorter time in follow-through phase. During the forward swing phase, experts spent a little less time as compared to novices by marginal significance ($p = 0.053$). Experts had significantly smaller variability over the duration of all phases ($p = 0.003$), the forward swing phase ($p = 0.010$) and the follow-through phase ($p = 0.017$).

4.2.7 Racket motion

Table 4-4 shows the comparison results of racket motion at the phase time T_1, T_2, T_3 and T_4, and also the phases in between: P_{BS} ($T_{1\text{-}2}$), P_{FS} ($T_{2\text{-}3}$) and P_{FT} ($T_{3\text{-}4}$). The variables include the racket centre displacement and velocity linearly in the *x*-, *y*- and *z*-directions of the global coordinate system, which are RC_x, RC_y and RC_z respectively, and angularly against *x*-*y*, *y*-*z* and *x*-*z* planes of the global coordinate system, which are RR_{xy}, RR_{yz} and RR_{xz} respectively. RC_{2D} and RC_{3D} are resultant velocity of racket centre projected on horizontal plane and in *3D* space respectively. The symbols "*H, L, O"* are used to represent the *t*-test results from the perspective of experts, as noted below the table. These tabulated results were actually processed and simplified from the original *t*-test results: two examples are shown for velocity for RC_x and RR_{xz} respectively in *Figure 4-5*. For example, the racket centre velocity RC_x varies from *L* to *O* to *H* during $T_{2\text{-}3}$ (refer to *Table 4-4*: *L*-*O*-*H*), which is a representation of the change that experts have a significantly lower velocity at T_2 but increase to no significance, and finally to significantly higher at T_3 (refer to *Figure 4-5* a). For convenience, the prefix "*D*" or "*V*" is added before a variable to

distinguish the displacement and velocity respectively (e.g. DRC_x represents the displacement of RC_x and VRC_x represents the velocity of RC_x).

Table 4-4 Comparison of different variables of racket motion on different phase time

Variables		Phase time						
		1	1-2	2	2-3	3	3-4	4
Centre displacement (D)	RC_x	O	O	O	O	O	O	O
	RC_y	L	L	L	L-O	O	O-H-O	O
	RC_z	L	L	L	L-O	O	O-L	L
Centre velocity (V)	RC_x	L	L	L	L-O-H	H	H-O-L-O	H
	RC_y	O	O-H	H	H-O-H	H	H-O	O
	RC_z	O	O	H	H-O	O	L-O	O
	RC_{2D}	H	H	H	H	H	H-O	O
	RC_{3D}	H	H	H	H	H	H-O	O
Angular displacement (D)	RR_{xy}	O	O	O	O-L-O	O	O-H-O	O
	RR_{yz}	O	O-H	H	H-O	O	O-H-O	O
	RR_{xz}	O	H	H	H	H	H-O	O
Angular velocity (V)	RR_{xy}	O	O-L	L	L-O-H	H	H-O	O
	RR_{yz}	O	O	O	O-L-O	O	O-H-O	O
	RR_{xz}	O	O	O	O-L-O	O	O-L	L

Note: "H": experts significantly higher; "L": experts significantly lower; "O": no significant difference; "-": tendency of change within a phase

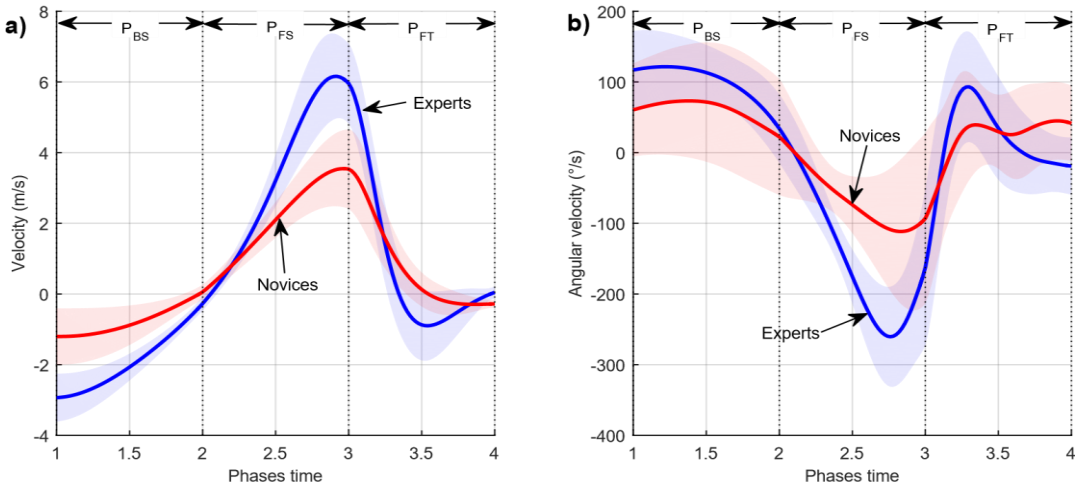

Figure 4-5 Comparison result of a) racket centre velocity RCx and b) racket angular velocity RRxz

The racket motion data was also visualized for better understanding the *Table 4-4* by implementing the kinematic model, as pictorially shown in *Figure* 4-6. The racket centre trajectory for the expert group and novice group during T_1 to T_4 are displayed in the plan view (global -*y* direction, *Figure 4-6 a*), side view (global -*z* direction, *Figure 4-6 b*), front view (global *x* direction, *Figure* 4-6 *c*) and 3D view (*Figure* 4-6 *d*). The racket centre velocity is added for T_1 to T_4 respectively, where the arrows represent the directions and the length represent the magnitudes of the velocity. The solid black bars in *a-c* are projected racket plane at T_1 to T_4 as corresponding to the racket angular displacement respectively.

The descriptions of the results are mainly based on *Table 4-4*, therefore not all the shared results, which could be identified from *Figure* 4-6, are highlighted. On the other hand, *Figure* 4-6 is less quantitative without information of variability: for example, DRC_x presents difference in *Figure* 4-6 but no significance in *Table 4-4*. There were little difference in the location of the racket when the participant hit the balls (DRC_x, DRC_y, DRC_z at phase time T_3) from *Table 4-4*. This can be visually seen from *Figure* 4-6 as the rackets are quite close at T_3, and would of course be expected for a consistent ball feeding machine. However, it can be observed that experts generally moved their racket more downward (DRC_y at phase $T_{1\text{-}2}$) and leftward (DRC_z at phase $T_{1\text{-}2}$) during backswing, and had a larger range of movement (DRC_z at phase $T_{1\text{-}2}$) when they ended their stroke. Experts also generally had much faster backswings (VRC_x at $T_{1\text{-}2}$ of experts is smaller because of the negative sign, also the velocity can be seen from *Figure 4-6*) and produced much higher speed in the forward (VRC_x at T_3) and upward (VRC_y at T_3) directions at ball-racket contact. There was, however, little difference in the leftward (VRC_z at T_3) direction at the contact moment. The resultant velocities of the experts were significantly higher than the novices during almost all the phases as shown in the table (VRC_{2D} and VRC_{3D}).

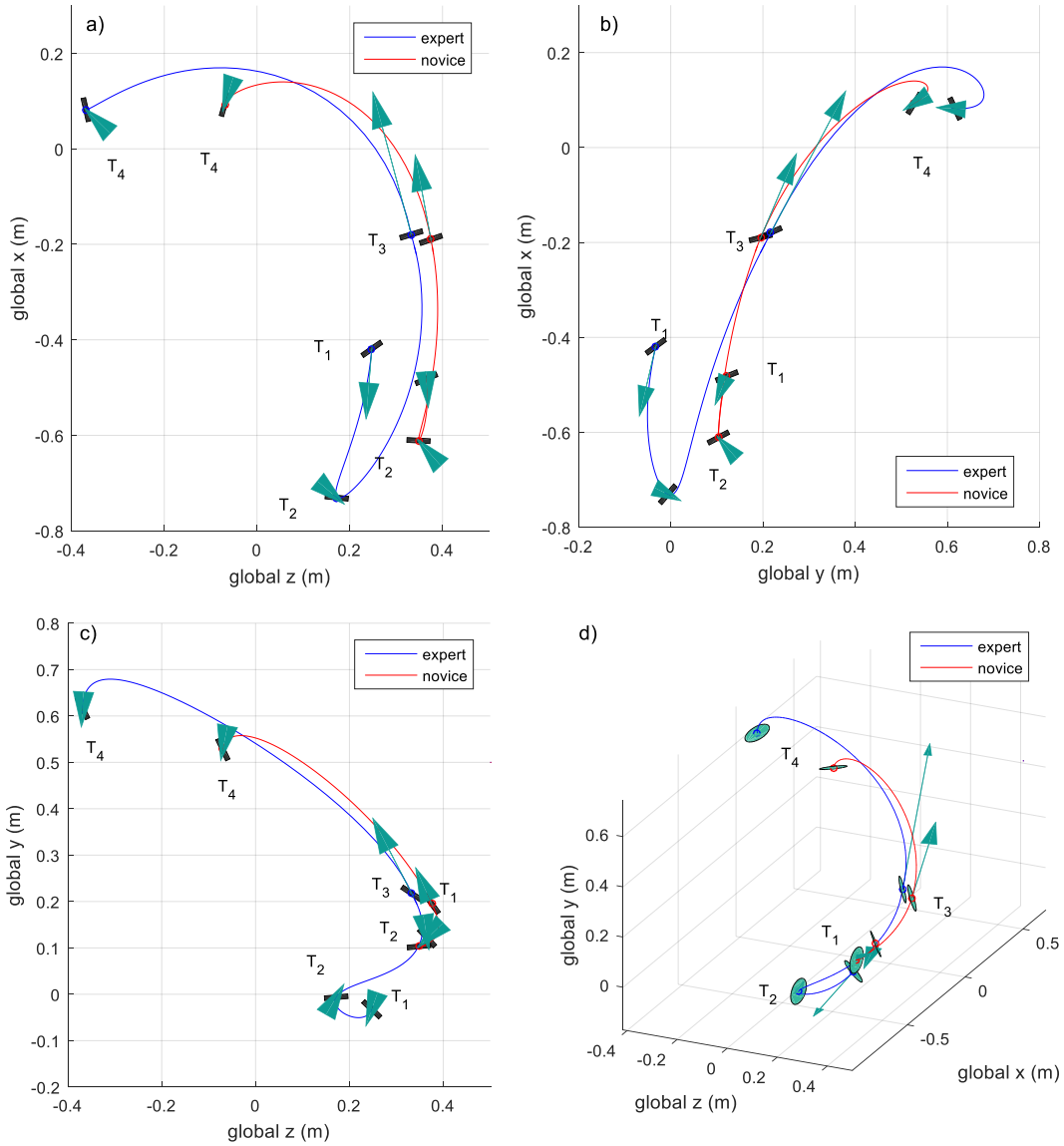

Figure 4-6 Visualized racket centre trajectory with velocity and racket orientation for T_1-T_4

Regarding the spatial direction of their rackets, the experts exhibited more downward facing of the racket face (DRR_{xz} at $T_{1\text{-}2}$) during the backswing and the forward swing phases. In the angular speed of the racket direction against *x*-*y* plane experts had lower angular speed at the beginning of forward swing but higher at the end, which indicted that expert rotated their racket with more strength (positive angular acceleration).

4.2.8 Human motion

The results for human motion are shown in

Table 4-5. The variables include trunk centre linear movement in the *x*-, *y*- and *z*-directions of the global coordinate system, which are TC_x, TC_y and TC_z respectively; the trunk rotational movement $T_{fe,}$ $T_{ll,}$ and T_{aa}; shoulder joint rotational movement $S_{pe,}$ S_e and S_{ie}; elbow joint rotational movement E_{fe} and E_{ps}; and wrist joint rotational movement W_{fe} and W_{ru}. Both of their displacement (including angular displacement) and velocity (including angular velocity) were compared. The symbols "*H, L, O"* are again used to represent the *t*-test results from perspective of experts, as noted below the table.

From the displacement results of

Table 4-5, the trunk centre of the experts were more forward ($DTCx$), downward ($DTCy$) and leftward (DTC_z) compared to the novices during almost all the phase time. There was no significant difference in the angle of trunk flexion (DT_{fe}), but experts tilted their trunk more in the lateral right direction (DT_{ll}) and axial left direction (DT_{aa}) in the backswing and forward swing phase. Experts had their shoulder directing more forward (DS_{pe} at phase $T_{1\text{-}2}$) during the backswing and downward (DS_e at phase $T_{2\text{-}3}$) during the forward swing. Experts had more pronation (DE_{ps}) during the backswing and part of forward swing. The wrist of experts had more flexion (DW_{fe}) and ulnar deviation (DW_{ru}) compared to the novices.

Table 4-5 Comparison of different variables of human motion at different phase time

Variables		Phase time						
		1	1-2	2	2-3	3	3-4	4
Displacement (D)	TC_x	H	H	H	H	H	H-O	O
	TC_y	L	L	L	L	L	L	L
	TC_z	L	L	L	L	L	L	L
	T_{fe}	O	O	O	O	O	O	O
	T_{ll}	H	H	H	H-O	O	O	O
	T_{aa}	L	L	L	L	L	L-O	O
	S_{pe}	H	H	H	H-O	O	O	O
	S_e	O	L	L	L	L	L-O	O
	S_{ie}	O	O-L	L	L-O	O	O	O
	E_{fe}	O	O	O	O	O	O-H	H
	E_{ps}	H	H	H	H-O	O	O	O
	W_{fe}	H	H	H	H	H	H	H
	W_{ru}	H	H	H	H	H	O	O
Velocity (V)	TC_x	O	O	O	O	L	L-O	O
	TC_y	O	O	O	O-H	H	H-O	O
	TC_z	O	O-L	L	L-O	O	O	O
	T_{fe}	H	H-O	O	O-L	L	L-O	O
	T_{ll}	H	H-O	O	O-L	L	L-O	O
	T_{aa}	L	L-O	O	O-H	H	H-O	O
	S_{pe}	O	O	O	O-L-O	O	O	O
	S_e	O	O-L	L	L-O	O	O-H	H
	S_{ie}	L	L-O	O	O-H	H	H-O-L	L
	E_{fe}	L	L-O	O	O-H	H	H-O-L	L
	E_{ps}	H	H	H	O-L	L	L-O	O
	W_{fe}	H	H-O	O	O-H-O	O	O-L	L
	W_{ru}	O	O	O	O-L	L	L-O	O

Note: “H”: experts significantly higher; “L”: experts significantly lower; “O”: no significant difference; “-”: tendency of change within a phase

The velocities present details on the difference of how fast the participants moved their body segments and joints. They displayed overall more complex patterns compared to displacement, as more ‘-’ are seen on velocity from

Table 4-5. On the other hand, the fact that velocities of experts changed more rapidly

than the novices indicated the experts had larger acceleration (including angular acceleration) than the novices. Note that the symbols "*H, L, O*" include the information of the sign of the values of the velocities, which means a smaller negative value may have a larger magnitude. Therefore, the displacement results and the range of motion (*Table 3-2*) and visualized kinematic model could also be taken into consideration together with the velocities. The racket-ball contact (phase time T_3) is highlighted here. At this moment, the trunk centre of the experts had a larger tendency of moving backward (VTC_x) and upward (VTC_y). In addition, the trunk had smaller velocity of extension (VT_{fe}) and lateral right rotation (VT_{ll}), but significantly larger axial rotation to left (VT_{aa}). The experts had faster velocities in shoulder internal rotation (VS_{ie}) and elbow flexion (VE_{fe}), but slower elbow pronation (VE_{ps}) and wrist ulnar deviation velocities (VW_{ru}).

4.3 Discussion

4.3.1 Summary and highlights

It is generally known that the movement of experts are faster, more precise, and more consistent than novices. In the current experiment, they were verified from the significant differences of their stroke accuracy, racket centre speed at T_3 and racket centre variability. Different from the past work which only studied limited moments (e.g. the racket-ball contact moment) and placed little work on human motion, in this chapter the controlled experiment and quantitative analysis presented results on the detailed motion pattern differences for the racket, upper arm and trunk in each continuous and unambiguous phase time. The motion of experts and novices displayed distinct patterns in the specific phase time and phases.

The experts had slightly different allocation of time spent for each phase of a stroke: they have longer backswing, and shorter forward swing and follow-through in

general. The forward swing contribute significantly to their racket centre speed at ball contact. The racket speed of experts was significantly faster during the backswing and forward swing. The experts have larger range of backswing (*Figure 4-6*) therefore has a longer acceleration path during the forward swing to generate a faster velocity at racket-ball contact (T_3). They put their racket face more downward (DRR_{xz}) and rotated the racket faster along the global *z*-axis (VRR_{xy} at T_3). The standing position of the experts was a little different from the novices: the experts were more forward (DTC_x) and leftward (DTC_z); the experts may have squatted for shorter action time as their trunks were lower (DTC_y). No significant differences were found on the elbow flexion angles (DE_{fe}), but larger range of movements was at least seen in the trunk lateral left rotation (DT_{ll}), shoulder plane of elevation (DS_{pe}) and internal rotation (DS_{ie}), and elbow supination (DE_{ps}). Most of the rotational speeds play significant roles in the contribution to the racket velocity based on their differences, including the trunk rotations, shoulder internal rotation, elbow rotations and wrist radial flexion. The shoulder plane of elevation (VS_{pe}), elevation (VS_e) and elbow flexion (VE_{fe}), however, did not differ between the experts and novices at ball-racket contact (T_3).

4.3.2 For the novice players

From the novice players' perspective, an approach to improving their performance is to help them avoid common errors by mimicking the movement of expert players. To move the racket according to the experts' pattern as the ultimate target, it is indeed the resultant movement of the kinematic chain from the trunk to the shoulder, elbow, wrist and finally the racket. The coordination of the segments and joints is essential to improve the overall performance. The kinematic model shows visually the differences between experts and novices, thus providing a good tool for novice players. Based on the results of the analysis, some discussions on the posture and

speed are given.

Firstly, novice players will need to pay careful attention to the body and racket position during a stroke. They need to squat a little to move the centre of mass lower (i.e. DTC_y), and also stand a little back and left with reference to the ball. These may give them a little more extra time to react and get ready to return the ball. The trunk may rotate more axially clockwise during the backswing, which can help them obtain a better range of motion during the forward swing. The elbow can be higher and its pronation needs to be smaller. The wrist flexion should be smaller. The racket should have smaller angle against the *x*-*z* (i.e. horizontal) plane.

Secondly, novice players should swing their racket a bit faster according to the comparison. However, they may have reached their maximum otherwise their accuracy may be reduced. In fact, this can be solved partly through the adjustment of the posture as described above. The larger range of motion of certain joint may help them have larger trajectory of acceleration, therefore improving their speed. The speed of trunk rotation, shoulder internal rotation, elbow rotation and wrist rotation are also important.

4.3.3 Further to individual

The statistical analysis has good practice in the investigating the overall motion pattern differences between novices and experts. The results were generated based on the analysis upon the two groups of data. This can provide an overall assessment on the entire novice group. However, the results may not necessarily be true for each individual novice for an individual assessment, since each individual pattern within the novice group may differ from each other.

There are several concerns if the *t*-test is to be applied for a further evaluation on an

individual sample. Though both the data of a group of experts and a group of novices (*Figure 4-7*) is obtained from the experiment, a one-sample *t*-test can only be performed on the data of one particular novice and of the group of experts. In other words, the distribution of the actual data of the novice group cannot be used therefore is assumed unknown. The one-sample *t*-test is actually "deformed" since the original sample (i.e. experts) is now fixed but the one novice data is unknown. The *t*-test is able to indicate the significance of whether the novice data is statistically the same or different from the expert data. However, the novice data may still belong to (e.g. novice 2 in *Figure 4-7*) or beyond (e.g. novice 3 in *Figure 4-7*) the novice group if there is no significant difference for one-sample *t*-test. This is because only the data of the expert group is involved in the one-sample *t*-test, but the information of the novice group, which exists but assumed unknown, is not used. On the other hand, the intervals of confidence for the experts are in fact different, though both levels of significance are set to *0.05* for the one-sample *t*-test and two-sample *t*-test. An illustration is given in *Figure 4-7*. Under the condition that the data of experts (assume known and fixed) and novices (assume unknown) are normal-distributed and with equal variance, the two-sample *t*-test may have a larger confidence interval: the new one-sample *t*-test may lead to an inconsistent result of significance (e.g. novice 1 in *Figure 4-7*) compared to the two-sample *t*-test which was already applied in this chapter. In addition, there may be other problems on the combination of each result, which is from the comparison of each single pattern. Therefore, the Student's *t*-test is not appropriate for use with individual novice players.

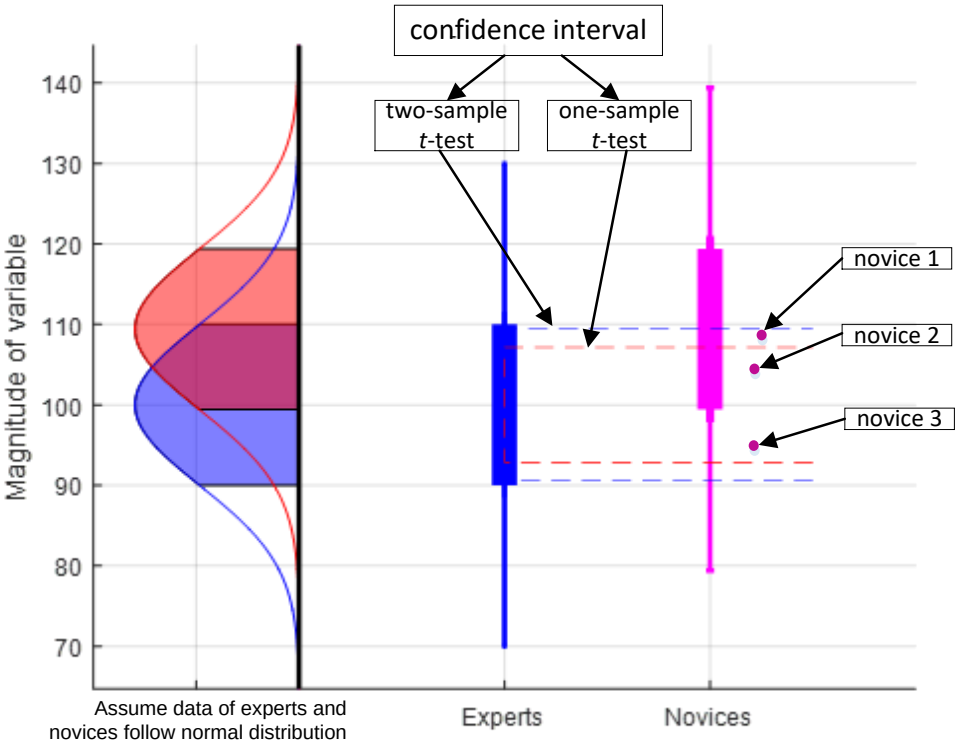

Figure 4-7 Comparison of an individual novice with an expert group

To make it convenient to apply the existing knowledge to any new individual player, a better and more convenient tool, the classification technique, is proposed. The classifier can be trained using existing data and then the classifier is used to classify new data, in the sense that the new data is compared with the existing data, therefore can be utilized to evaluate the motion of any new players. This is discussed in the next chapter.

Chapter 5 Classification model for automatic identification of motion quality

5.1 Overview of model development

In the previous chapter, the significant differences in motion pattern data of experts and novices were identified. This chapter steps further to utilize the data to develop a classification model, which has the ability to automatically identify the quality of motion patterns for an individual by classifying them into a novice or an expert. The model was created from and optimized for the dataset which was collected as described in the previous chapter. A potential application of the model is its ability to classify any new table tennis forward stroke motion data which is not part of the data set in the current research.

The flowchart in *Figure 5-1* shows the development and optimization of the model. The model was designed to use a binary Support Vector Machine (*SVM*) classifier with Nelder-Mead method to optimize parameters *C* and *K* in order to achieve the highest model performance (F_1 score), which was evaluated by cross-validation. Different sub-datasets were to be produced for the *SVM* classifier input by using different feature selection methods on the raw dataset. The proper *SVM* kernel was also to be selected. The selection of the best performing model would also result in good combinations of features that used fewer variables while maintaining good model performance.

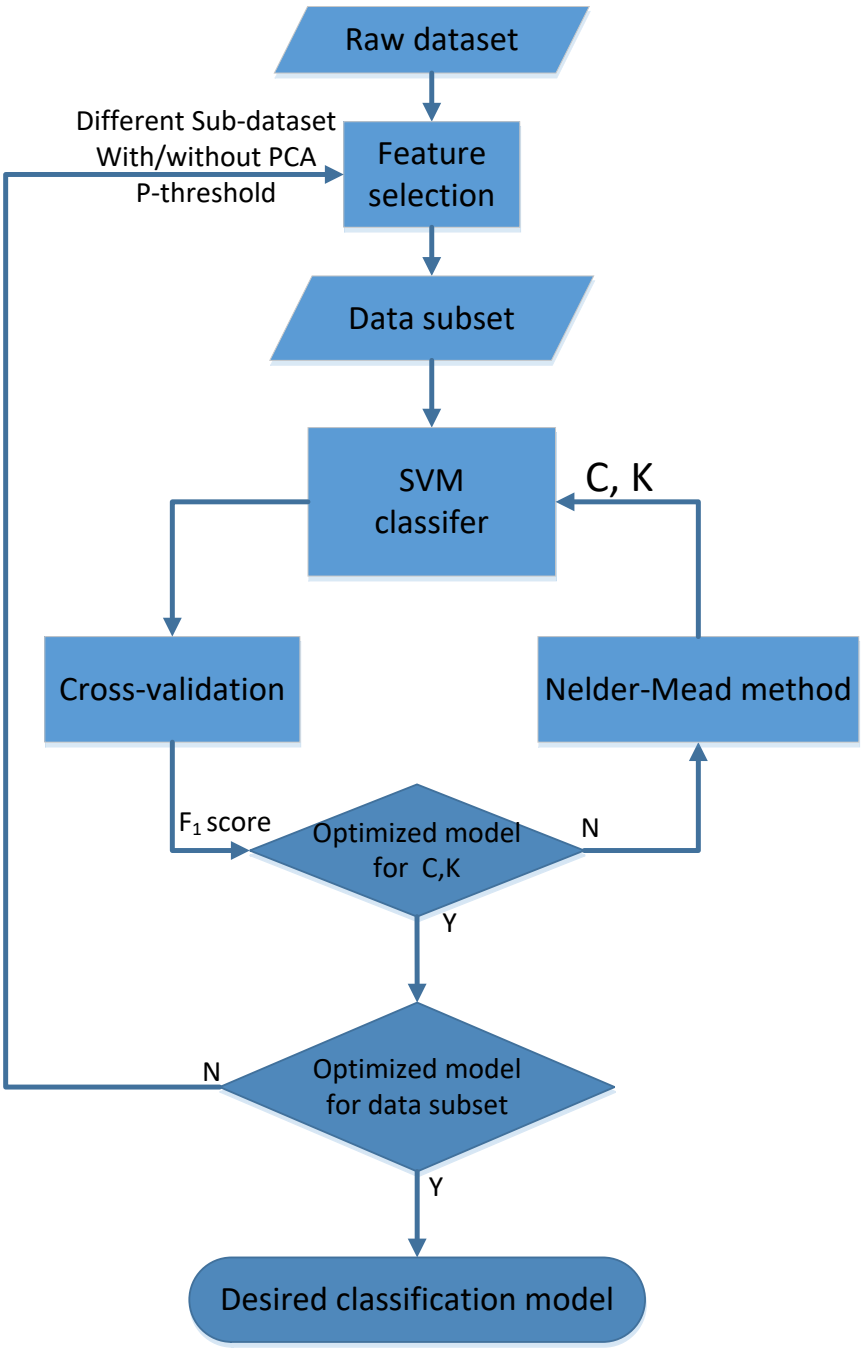

Figure 5-1 Development and optimization of the classification model

The raw data was the kinematic variables collected from the experiment as described in the previous chapter. The data subset was retrieved from the raw data by selecting different combination of the variables under the condition of *p*-threshold and either presence or absence of the Principal Component Analysis (*PCA*). The performance

of different *SVM* kernels (linear, polynomial, and *RBF*) was also to be investigated. For cross-validation, adjusted folds were used such that all the data was partitioned into the equal number of subsets to the number of participants to avoid over-fitting. In other words, there were *20* subsets for the existing data of *20* participants. Each subset contained exactly all the data of one participant. The training set and validation set were input into the *SVM* classifier. Then the performance F_1 score of the classifier were calculated based on the *20* subsets. Nelder–Mead method was used to determine the best F_1 score under the two-dimensional space constructed by *SVM* constraint *C* and kernel scale *K*.

5.2 Datasets and methodology for model development and optimization

5.2.1 Raw dataset

The processed data from the previous chapter, including those displacement and velocity data of the racket (refer to *Table 3-1*), trunk, shoulder, elbow and wrist (refer to *Table 3-2*) of final stroke data (*Table 4-1*), were the raw dataset for the model development. All of these variables were normalized time-series variables from phase time T_1 to T_4. The different *DOF*s under each segment and joint were not separated but combined as one set (e.g. displacement of RC_x, RC_y and RC_z was regarded as one set of features), though each *DOF* was regarded as one feature for the *SVM*. At each phase time, these data were formed in matrix such that each row was one observation of stroke and each column was one feature. There were *20* observations for *20* participants. To reduce the computational resources, a gap of $T_{0.1}$ was selected such that only data at *10* equal distributed phase time (e.g. T_1, $T_{1.1}$, $T_{1.2}$, …$T_{1.9}$, T_2 for P_{BS}) were used within each phase.

For brevity, the abbreviation letters (Table *5-1*) were used to represent the feature

sets and their combinations. For example, "*(RC)V*" represented the velocity data of racket centre; "*(RC+RR)(D+V)*" represented both displacement and velocity (including angular displacement and velocity) data of the racket centre translational and racket rotational motion; if a sub-dataset included all of the raw dataset, then it should be noted as "*(RC+RR+TC+T+S+E+W)(D+V)*", or "*(ALL)(D+V)*" for short specifically.

Table 5-1 Motion Abbr. for *SVM* input

Motion subjects or types	**Abbr.**
Racket centre translational motion	*RC*
Racket rotational motion	*RR*
Trunk centre translational motion	*TC*
Trunk rotational motion	*T*
Shoulder joint rotational motion	*S*
Elbow joint rotational motion	*E*
Wrist joint rotational motion	*W*
Motion of all above subjects	*ALL=(RC+RR+TC+T+S+E+W)*
Displacement or angular displacement	*D*
Velocity or angular velocity	*V*

5.2.2 Feature selection

Feature selection reduces the dimension of raw features, there would be multiple choices for features by combining or transforming the combination. In the current study, three strategies were applied to generate sub-datasets for the classification model.

The first method involved simple extractions to get a diverse range of feature combinations from the raw data set. The combinations were manually selected based

on the different physical segments and quantities, as tabulated in Table *5-2*.

Table 5-2 Basic feature combinations

Category		Displacement	Velocity	Displacement + Velocity
All	***ALL***	*(ALL)D*	*(ALL)V*	*(ALL)(D+V)*
Racket	***RC***	*(RC)D*	*(RC)V*	*RC(D+V)*
	RR	*(RR)D*	*(RR)V*	*RR(D+V)*
	RC+RR	*(RC+RR)D*	*(RC+RR)V*	*(RR+RR)(D+V)*
Human	***TC***	*(TC)D*	*(TC)V*	*TC(D+V)*
	T	*(T)D*	*(T)V*	*T(D+V)*
	S	*(S)D*	*(S)V*	*S(D+V)*
	E	*(E)D*	*(E)V*	*E(D+V)*
	W	*(W)D*	*(W)V*	*W(D+V)*
	TC+T	*(TC+T)D*	*(TC+T)V*	*(TC+T)(D+V)*
	T+S	*(T+S)D*	*(T+S)V*	*(T+S)(D+V)*
	S+E	*(S+E)D*	*(S+E)V*	*(S+E)(D+V)*
	E+W	*(E+W)D*	*(E+W)V*	*(T+W)(D+V)*
	T+S+E+W	*(T+S+E+W)D*	*(T+S+E+W)V*	*(T+S+E+W)(D+V)*
	TC+T+S+E+W	*(TC+T+S+E+W)D*	*(TC+T+S+E+W)V*	*(TC+T+S+E+W)(D+V)*

The second method implemented *PCA*, which orthogonally transformed the original features into linearly uncorrelated components and the principal components were selected. A standardization was applied before using the *PCA* so that each feature was centred to mean *0* and scaled to the standard deviation *1*. To determine the number of principal components to reserve, a threshold of *90%* was set such that at least *90%* and just above *90%* of principal components were selected. This method was applied to each sub-dataset in Table *5-2*.

An additional trial was inspired by the Student's *t*-test, such that a *p*-threshold was

set to filter the data by the significance. In other words, for a specific *p*-threshold, the Student's *t*-test was applied on the data with level of significance (type I error) equal to *p*, and only significant variables on each moment were selected for generating data subset. This *p*-threshold values were sampled from *0* to *1* manually. Specifically, when *p=1*, all the data was chosen; when *p=0.05*, it was exactly the same significant variables as those of results of the previous chapter were chosen.

5.2.3 *SVM* and cross-validation

The data subsets were input into the *SVM* and evaluated using cross-validation. The basics of the *SVM* and cross-validation have been discussed in *Section 2.3.2*. Specifically, the data of 20 participants were partitioned into a training set and a validation set, which contained the data of 19 participants and 1 participant respectively (*Figure 5-2*). Each set contained the features (i.e. selected variable sets) and their class labels (i.e. expert or novice). Given any values for the parameters — the kernel scale *K* and capacity constraint *C* (i.e. penalty for misclassification), the training set was used to train the supervised *SVM*, which was a process of optimizing the internal parameters (for details refer to Equation (2-1)). Then the testing set went through the trained *SVM* and compared the results with their class labels. This resulted in a confusion matrix, which indicated how the predictions matched the actual results (i.e. the number of true positive, false positive, false negative, and true negative).

The sampling was repeated *N* (*N=20*) times to produce different combinations of data of training sets and testing sets (*Figure 5-3*). Each combination applied the *SVM* and their output confusion matrices were combined together to calculate the precision, accuracy, recall and further the F_1 score (Section 2.3.2). This in fact covered all the combinations of training and testing datasets therefore the F_1 score reliably represented the model performance.

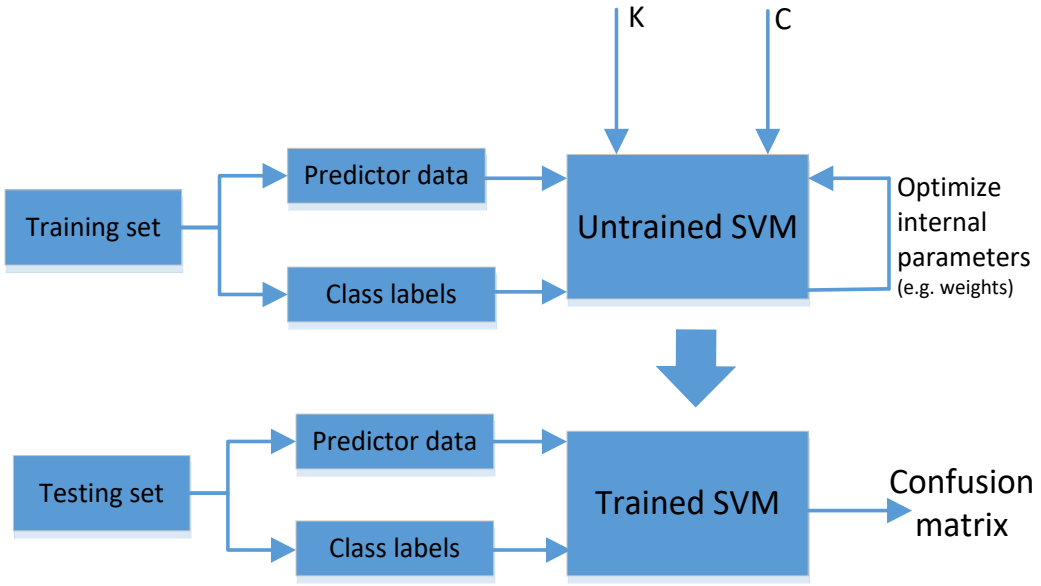

Figure 5-2 Architecture of training and testing of the *SVM* classifier

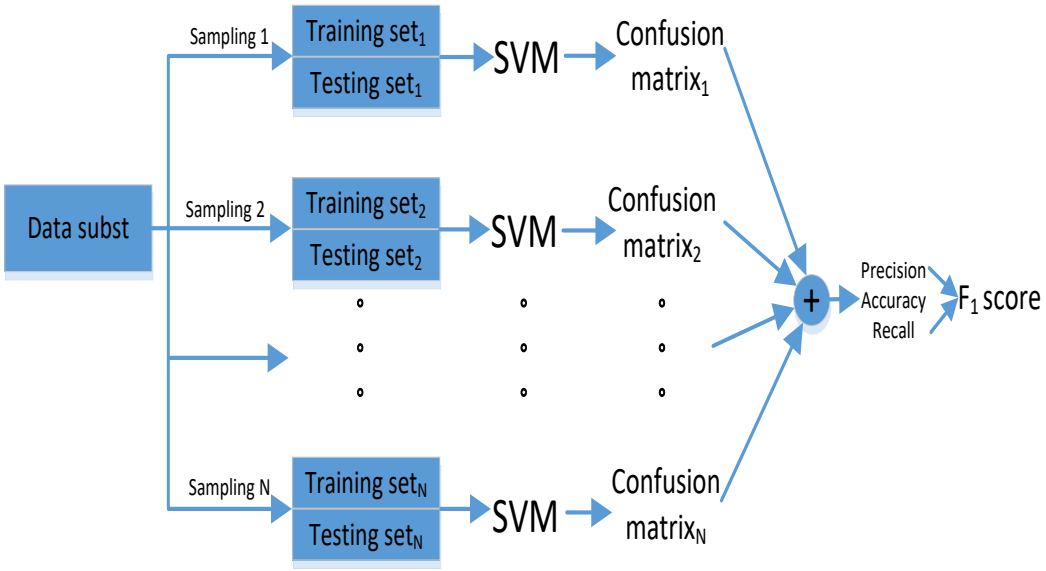

Figure 5-3 Architecture of the cross-validation

5.2.4 Tuning *SVM* parameters *C* and *K*

For the *SVM* classifier, the larger capacity constraint *C* means larger penalty on misclassification, which may theoretically lead to better model performance. On the other hand, it may have a possibility to over-train the model and it will also increase

the training time. In addition to the cross-validation which was used to avoid over-training, the Nelder-Mead method was also used to search for an approximate *C* as well as *K*.

An example for the kernel "*RBF*" is illustrated here. To apply the Nelder-Mead method, both of *C* and *K* were converted into log scale to make their range into the whole real numbers. The objective function was formulated by the model performance through cross-validation, which was calculated through numerical computation based on a selected dataset (*Equation (5-1), Figure 5-3*). Then the Nelder-Mead was used to determine the best combination of *C* and *K* to maximize the objective function.

$$\max_{C,K} F_1\left\{\sum_{i=1}^{N}\{ConMat[SVM_{C,K}(Train_i, Test_i)]\}\right\} \quad (5\text{-}1)$$

Where the function F_1 calculates the F_1 score, $ConMat$ calculate the confusion matrix, the *SVM* are the classifier trained by training set $Train_i$ and vaulted by testing set $Test_i$ under the parameters *C* and *K*. *N* is the number of SVM that Cross-Validation validates on, and *N=20* in current study.

Figure 5-4 shows the objective function in terms of *C* and *K* for the "*ALL(D+V)*" data set. From the distribution of F_1 score, it reaches maximum with quite a large range of *C* and *K*. The maximum F_1 score can be easily searched without too much concern of the local maxima problem if the initial seeds are properly selected. In fact, even a local maximum is rather close to the global optimum (also appears when infinite *C* with proper *K*). This is true for other sub-dataset based on sampled testings. Upon these tests, a pair of initial values *C=e^2* and *K=e^2* were selected for parameter tuning for all the sub-datasets.

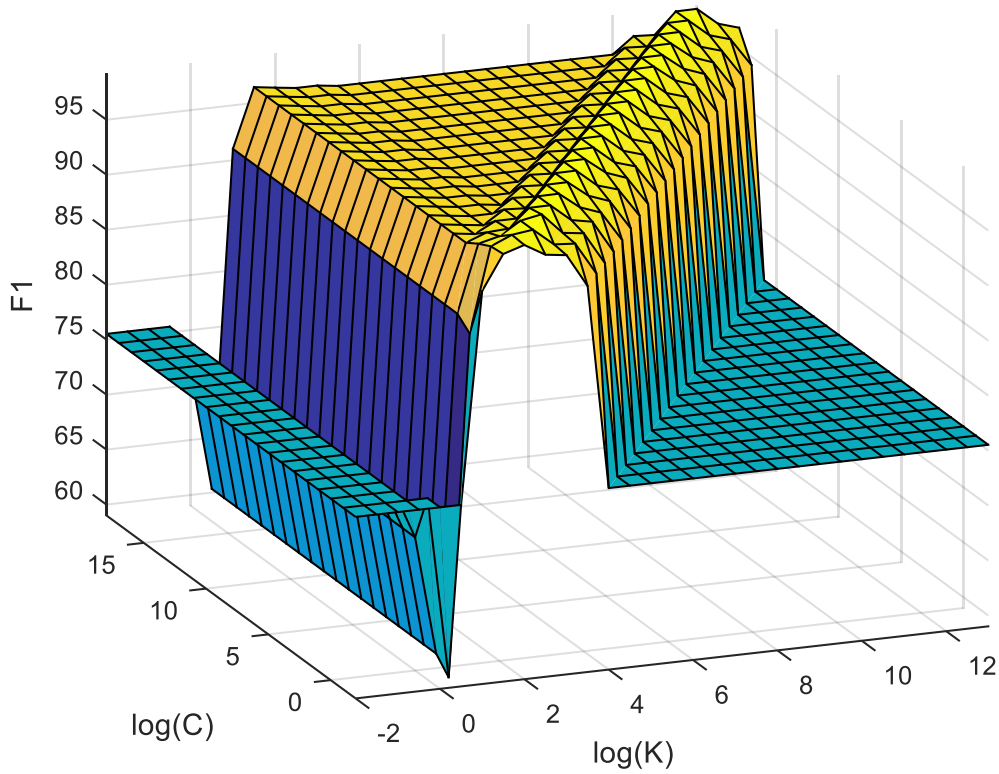

Figure 5-4 F_1 score with respect to C and K at phase time T_3 for the raw data set (*RBF* kernel)

5.3 Preliminary settings for *SVM* and results

To reduce the time and resources on the computation, some prior experiments were conducted in advance in order to optimize part of the model settings. The prior experiments here included the effects of different choices of *SVM* kernels and the *p*-threshold. These two experiments were conducted on the raw dataset only.

5.3.1 Effects of different *SVM* kernels

To make sure that a proper kernel was selected for the *SVM* classifier, the raw data was applied *SVM* with different kernels. *Figure 5-5* shows the model performance of the linear, *RBF* and polynomial (with an order of *3*) kernels for the "*ALL(D+V)*" data respectively.

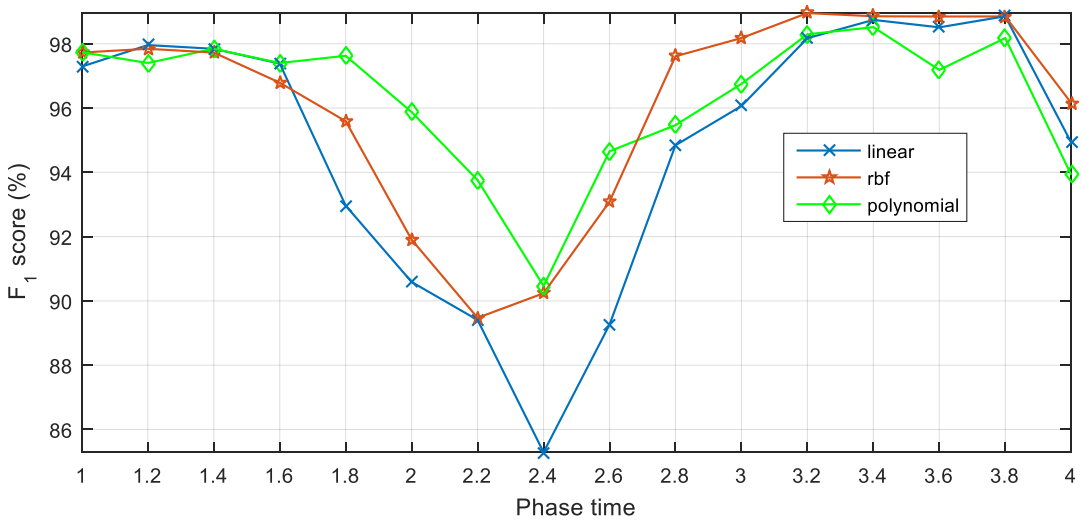

Figure 5-5 Comparison of different kernel for the raw data

Each of the kernels was able to give a relatively good performance on the all the phase time with the F_1 score of over *80%* or even over *90%*. However, the linear kernel does not seem to be able to better fit the existing datasets and presented the worst performance. The polynomial kernel gives better F_1 scores for the first half phase (around $T_{1.4}$ - $T_{2.7}$) but performed worse over the second half phase (around $T_{2.7} - T_{3.8}$) compared to the *RBF* kernel. Though a better determination of the kernel depends on the empirical experience on the data, the *RBF* kernel is the most widely used (Shanks & John, 1994). Since the subset of data varied, and *RBF* kernel had comparable performance on the raw data set, this study used the *RBF* kernel as the *SVM* kernel.

5.3.2 Effects of different *p*-threshold

An experiment was performed to investigate the effects of different *p*-threshold on the model performance. A statistical *t*-test was applied on the raw dataset by using the type *I* error equal to the specific *p*-threshold. Only significant features were selected as sub-dataset for the classification. The *p*-threshold was assigned different values varying from *0.001* to *1*.

Experiment results are shown in *Figure 5-6* and *Figure 5-7*. The former shows a distribution of the F_1 score in terms of different *p*-threshold (*0.001* to *1*) and phase time (*1* to *4*) in *3D*; the latter projects *Figure 5-6* into *2D* and the special cases where $p=0.05$ and $p=1$ are highlighted. From the figures, it can be seen that when the *p*-threshold is set to very small ($p < 0.03$), the F_1 score becomes significantly worse. On the other hand, there is not much difference when the p-threshold is larger. The lines with $p=0.05$ and $p=1$ (*Figure 5-7*) have comparable difference in-between but not too much overall.

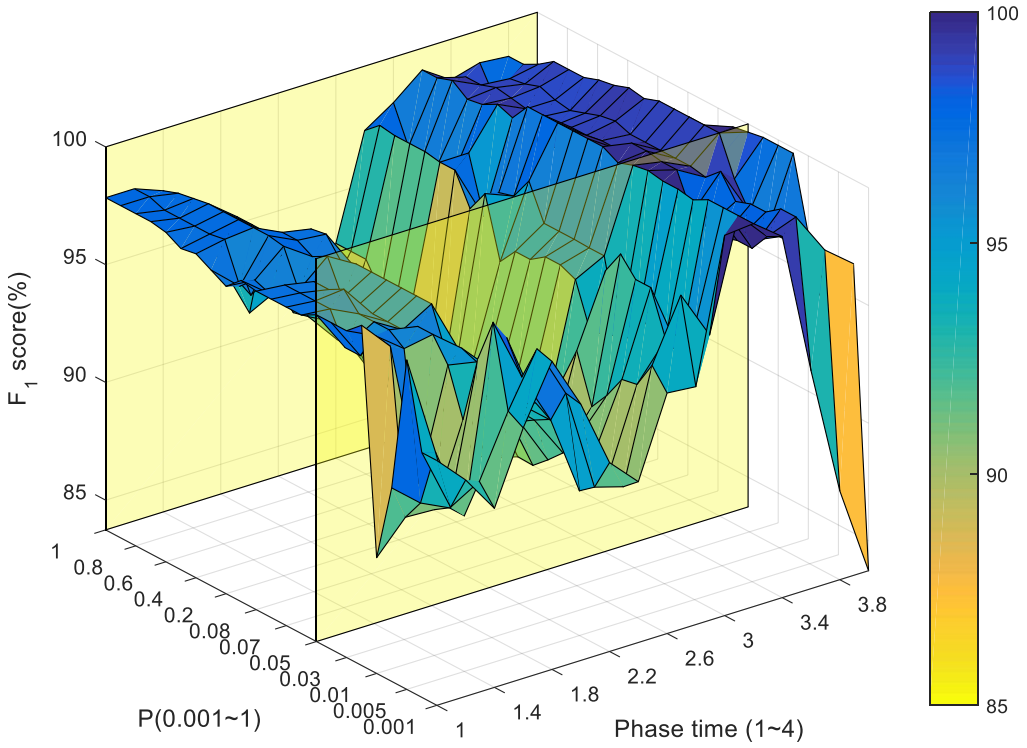

Figure 5-6 Results of raw data on different p-threshold

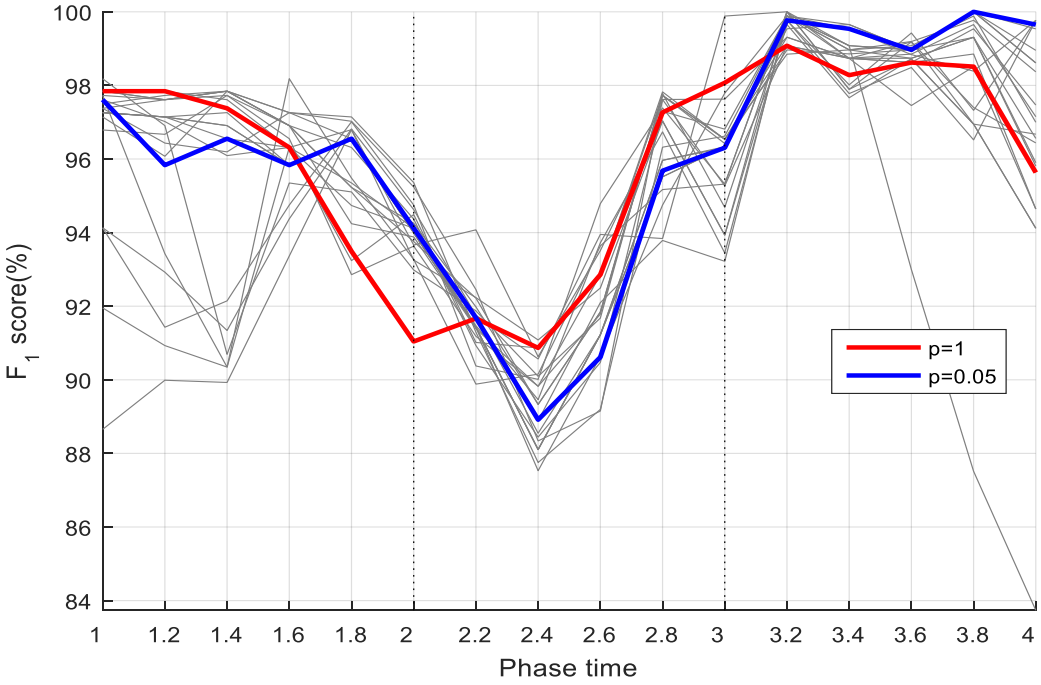

Figure 5-7 Results of raw data on different p-threshold with p=1 and p=0.05 highlighted

In fact, the implementation of the *p*-threshold on data reduced the number of features. When the *p*-threshold was set to very small (e.g. $p < 0.03$), the feature space was significantly shrunken and resulted in too many features of the original dataset were removed, including those important features which did contribute to the classification. This therefore caused the classifier performance to be unstable especially when the original dataset was not large enough. For example, results of the motion of individual segments or joints are shown in *Figure 5-8*. The number of features of the original dataset varied from *4* to *6* for these segments or joints. The *p*-threshold of *0.05* caused a lower performance, and a worse case was in some sub-datasets that their features were totally filtered out (e.g. *T(D+V)* and *S(D+V)* in *Figure 5-8*) when passing the threshold therefore caused a failure of classification.

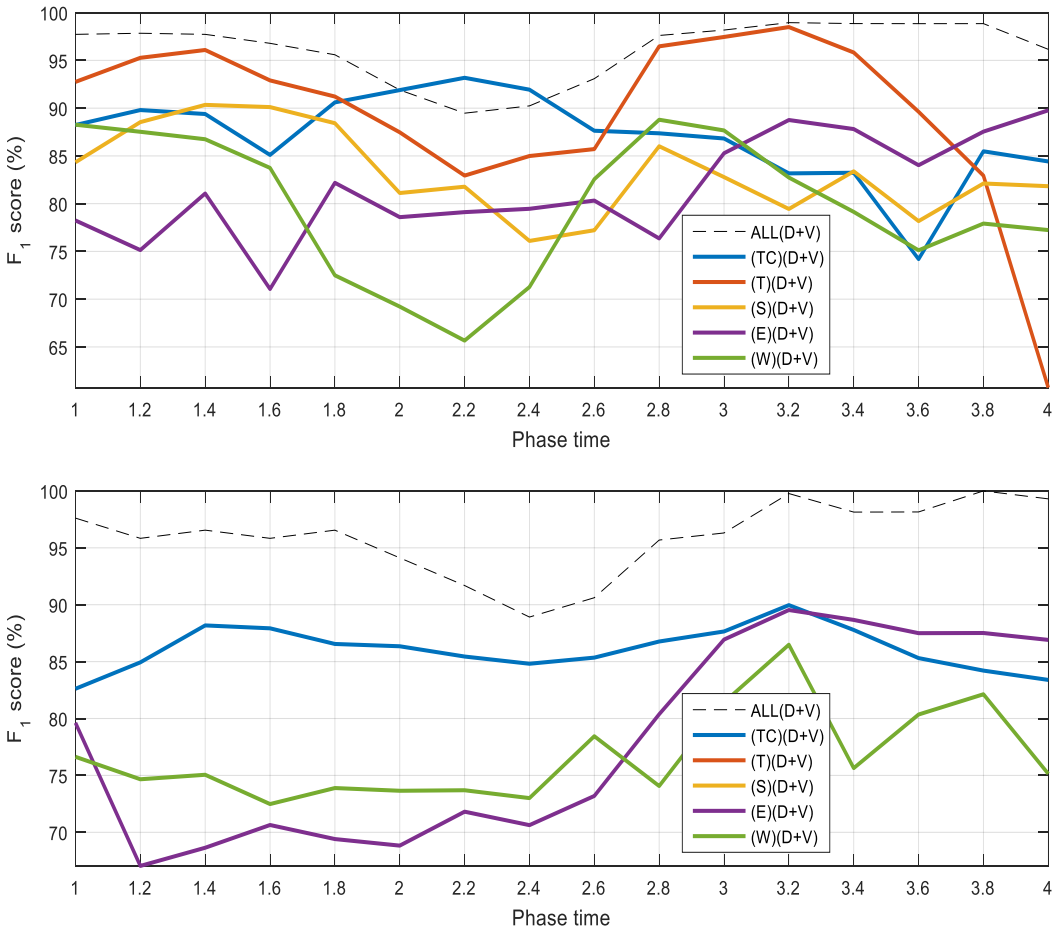

Figure 5-8 Results of different segments when p=1 (up) and p=0.05 (down)

Therefore, the *p*-threshold might improve the model performance to some extent and reduced the number of features. However, it also caused the model to become unstable. For this reason, this method was rejected.

5.4 Results

5.4.1 *PCA* on the dataset

Since *90%* of the components were selected for the classification and there was multiple phase time during a stroke, the percentage of retained principal components were calculated. Note that percentages are not final results (i.e. model performance F_1 score), yet are tabulated in *Table 5-3* for any further discussion.

Table 5-3 Percentages of retained the components

	Category	*D*	*V*	*D+V*
All	*ALL*	36.8-47.4	38.1-52.4	30.0-40.0
	RC	66.7-100.0	40.0-60.0	37.5-62.5
Racket	*RR*	66.7-100.0	66.7-100.0	50.0-83.3
	RC+RR	50.0-66.7	37.5-75.0	35.7-57.1
	TC	100.0-100.0	100.0-100.0	66.7-83.3
	T	66.7-100.0	66.7-100.0	66.7-66.7
	S	66.7-100.0	66.7-100.0	50.0-83.3
	E	100.0-100.0	100.0-100.0	75.0-100.0
	W	100.0-100.0	100.0-100.0	75.0-75.0
Human	*TC+T*	66.7-83.3	66.7-66.7	50.0-58.3
	T+S	66.7-83.3	66.7-83.3	50.0-58.3
	S+E	60.0-100.0	80.0-80.0	50.0-80.0
	E+W	75.0-75.0	75.0-100.0	62.5-75.0
	T+S+E+W	50.0-70.0	60.0-80.0	45.0-60.0
	TC+T+S+E+W	46.2-61.5	53.8-69.2	42.3-53.8

5.4.2 Results by using dataset of ALL

This section shows the performance of "*ALL*" dataset. Since "*ALL(D+V)*" had the maximum number of features, it was used as a benchmark for the results of the racket and human motions in the later sections for convenience. Both sets of results that used a basic feature selection and uses *PCA* are shown in *Figure 5-9*.

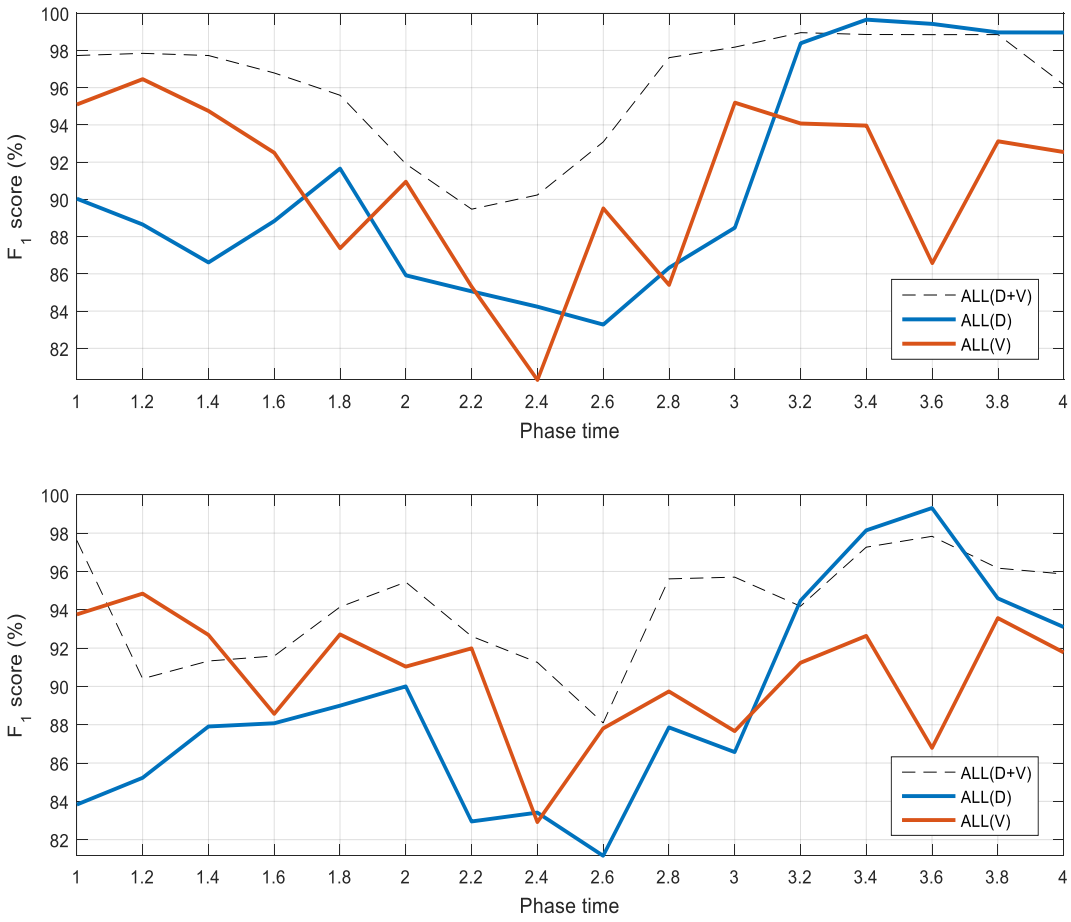

Figure 5-9 Results for using ALL dataset without PCA (up) and with PCA (down)

In addition, the respective values of the accuracy, precision and recall were also calculated for "*ALL(D+V)*" without *PCA* (*Table 5-4*) as an example to indicate that the accuracy, precision and recall of the model were also holding relative high values along with the high F_1 scores.

Table 5-4 Best performance of the model for *ALL(D+V)* without *PCA*

Phase time	**ln(*K*)**	**ln(*C*)**	***F*₁**	**Accuracy**	**Precision**	**Recall**
1	2.0	2.0	97.7	96.0	99.5	97.2
1.2	2.4	1.9	97.8	96.0	99.8	97.3
1.4	2.1	2.0	97.7	96.0	99.5	97.2
1.6	2.0	2.0	96.8	95.9	97.7	96.1

1.8	2.5	1.8	95.6	95.8	95.4	94.7
2	2.0	2.0	91.9	94.6	89.4	90.4
2.2	2.1	1.8	89.5	92.6	86.6	87.6
2.4	2.1	2.0	90.2	92.9	87.7	88.5
2.6	2.0	2.0	93.1	92.7	93.5	91.6
2.8	2.1	2.0	97.6	96.0	99.3	97.1
3	1.9	2.1	98.2	96.6	99.8	97.8
3.2	2.1	2.0	99.0	99.3	98.6	98.7
3.4	3.0	1.6	98.9	97.7	100.0	98.6
3.6	2.9	1.5	98.8	98.4	99.3	98.6
3.8	2.3	1.9	98.9	98.2	99.5	98.6
4	1.9	2.1	96.2	96.7	95.6	95.4

5.4.3 Results for all data subset with and without *PCA*

Several sample figures are shown below in *Figure 5-10*, all the results for all data subset combinations with and without *PCA* are shown in *Appendix C*. For better comparison and analysis, they were converted to a score table as discussed in the next section (*Section 5.4.4*).

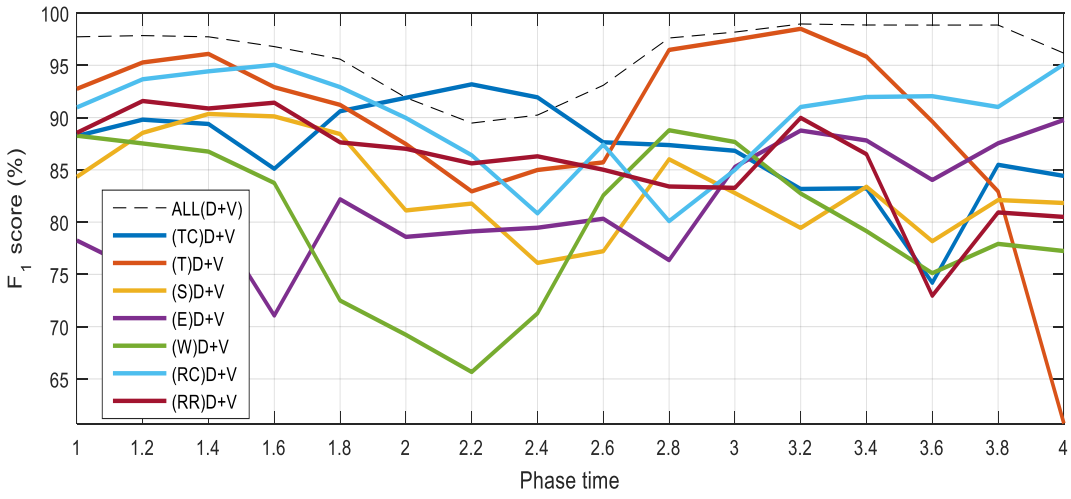

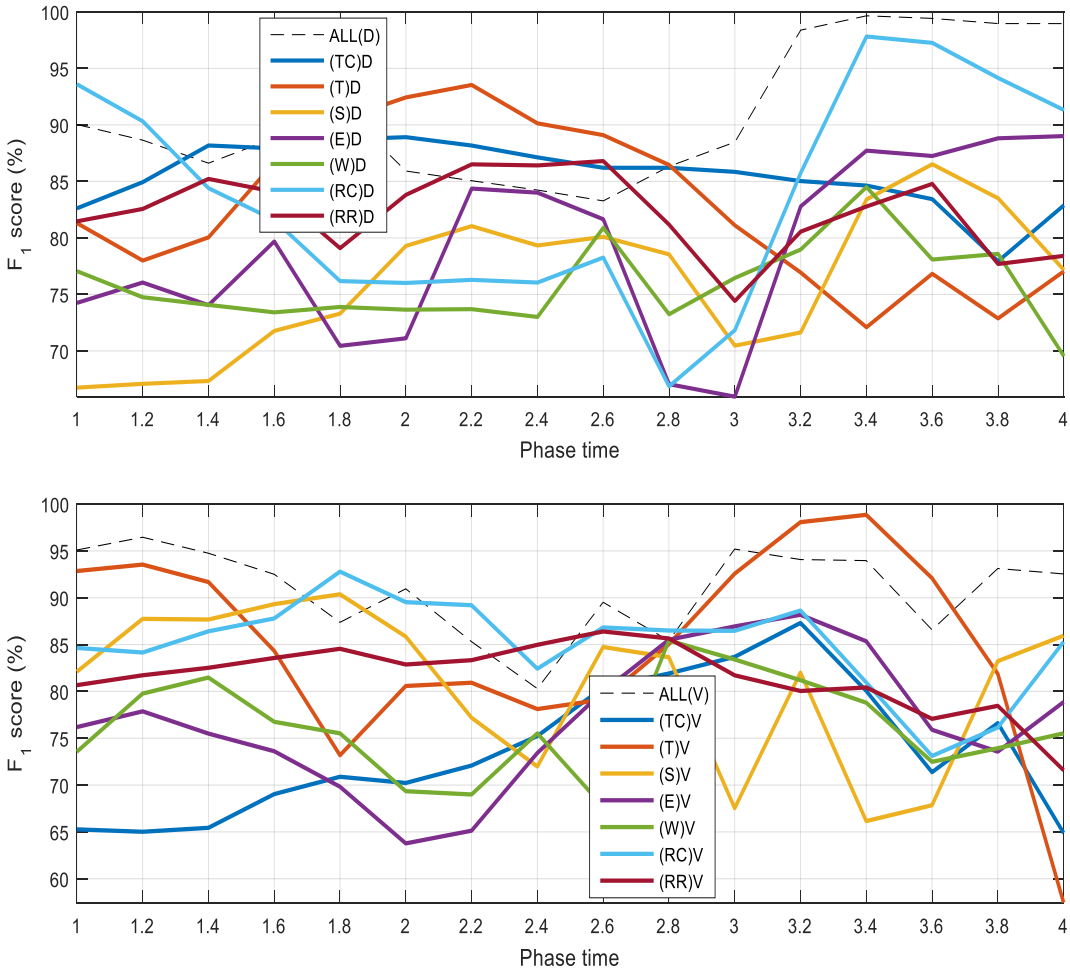

Figure 5-10 Results for some dataset (D+V) (1st), D (2nd) and V (3rd) without PCA

5.4.4 All the results on a score table

Based on the results in the previous section (*Section 5.4.3*), a score table was created to filter and better visualize the data by using a "*80% - 80%*" rule. The baseline was set to F_1 score *80%* such that if the F_1 score at a phase time or mean F_1 score during a phase was less than 80%, it was marked as "×"; otherwise if less than 80% of the phase was higher than F_1 score 80%, it was marked as "—"; otherwise the score or mean score was shown with their actual number. The results are shown in Table *5-5*. In other words, "×" highlights the worst results, "—" highlights relative good results (normally with its values varying a lot), while numbers show filtered good results. The higher the number is, the better the model performance is.

Table 5-5 F_1 score table showing all the results

	without PCA							with PCA						
	1	1—2	2	2—3	3	3—4	4	1	1—2	2	2—3	3	3—4	4
(ALL)D	90	89	86	86	88	97	99	84	87	90	85	87	94	93
(ALL)V	95	93	91	88	95	93	93	94	92	91	89	88	91	92
(ALL) (D+V)	98	96	92	93	98	98	96	98	93	95	93	96	96	96
(RC)D	94	—	×	×	×	90	91	94	—	×	×	×	90	91
(RC)V	85	88	90	87	86	—	85	89	88	89	85	87	83	86
(RC) (D+V)	91	93	90	85	85	91	95	92	92	90	—	82	92	96
(RR)D	81	83	84	83	×	×	×	82	84	86	84	×	×	×
(RR)V	81	83	83	84	82	×	×	82	84	86	85	81	×	×
(RR) (D+V)	89	90	87	85	83	82	80	89	91	88	87	83	83	×
(RC+RR)D	93	91	86	83	×	90	92	90	—	85	—	×	90	92
(RC+RR)V	87	89	90	86	83	86	98	89	90	93	88	87	87	97
(RC+RR) (D+V)	92	94	96	87	83	91	96	90	93	92	86	81	90	96
(TC)D	83	87	89	87	86	83	83	82	86	89	88	89	85	83
(TC)V	×	×	×	×	84	×	×	×	×	×	×	84	×	×
(TC) (D+V)	88	89	92	90	87	83	84	87	90	91	91	91	—	86
(T)D	81	85	92	89	81	×	×	×	×	×	—	81	×	×
(T)V	93	86	81	—	93	87	×	87	83	81	83	94	90	×
(T) (D+V)	93	93	87	89	97	88	×	×	×	×	—	92	87	×
(S)D	×	×	×	×	×	×	×	×	×	81	×	×	×	×
(S)V	82	87	86	×	×	×	86	×	×	×	×	×	×	86
(S) (D+V)	84	87	81	—	83	—	82	×	—	×	×	88	83	82
(E)D	×	×	×	×	×	84	89	×	×	×	×	×	84	89
(E)V	×	×	×	×	87	—	×	×	×	×	×	87	—	×
(E) (D+V)	×	×	×	×	85	87	90	×	×	84	84	88	88	90
(W)D	×	×	×	×	×	×	×	×	×	×	×	×	×	×
(W)V	×	×	×	×	83	×	×	×	×	×	×	83	×	×
(W) (D+V)	88	—	×	×	88	×	×	×	×	×	×	83	—	×
(TC+T)D	86	86	82	90	85	88	86	86	86	82	89	91	93	92
(TC+T)V	95	—	×	86	97	90	×	92	83	86	83	90	84	×
(TC+T) (D+V)	92	91	86	89	88	90	88	91	90	87	91	92	91	88
(T+S)D	×	—	96	91	82	×	×	×	×	×	86	80	×	81
(T+S)V	91	91	92	87	95	93	80	85	85	82	—	93	94	83
(T+S) (D+V)	90	92	93	93	99	92	×	×	91	89	89	95	91	83
(S+E)D	82	×	80	×	×	88	90	×	×	83	×	×	87	89
(S+E)V	91	88	82	—	87	83	81	91	—	×	—	89	×	×
(S+E) (D+V)	86	83	×	—	91	91	91	82	85	89	85	88	90	89
(E+W)D	82	—	82	×	×	86	91	83	—	81	×	×	85	87
(E+W)V	×	×	×	×	89	—	×	×	×	×	×	89	—	×
(E+W) (D+V)	×	×	×	—	91	90	91	81	×	×	—	87	88	90
(T+S+E+W)D	89	86	85	86	85	91	93	×	—	87	89	83	91	96
(T+S+E+W)V	95	91	80	86	96	93	84	92	—	×	85	92	93	84
(T+S+E+W) (D+V)	94	93	87	91	98	95	90	90	87	87	90	93	94	95
(TC+T+S+E+W)D	82	83	85	89	89	95	95	83	—	84	87	86	90	92
(TC+T+S+E+W)V	97	90	×	—	97	93	85	94	—	×	×	91	91	85
(TC+T+S+E+W) (D+V)	97	94	91	92	94	96	97	96	—	94	90	93	96	95

From the table, the *SVM* classification model was able to classify the existing data with relative high performance. When all the raw data "*ALL(D+V)*" was used, the model gave the best scores varying from *92%* to *98%* without *PCA* and *93%* to *98%* with *PCA*. When subset features were selected, the performance overall decreased although some may be slightly better than using all of the features.

Under the conditions that the racket, segment or joints were fixed for the features, using velocity only presented generally higher F_1 score than using displacement only. However, using both displacement and velocity would gave even better F_1 score.

The reservation of principal components varied a lot depending on the feature combinations (*Table 5-3*). In general, with higher number of features more unimportant components could be removed. This is because the larger number of features raised higher possibility of containing linearly correlated features. The reservation of the principal components could be as high as *100%* for some sub-dataset (e.g. elbow and wrist), which gave an indication that all the dimensions were important. In fact, the model performance (*Table 5-5*) shows that these principal components are insufficient and gave bad F_1 scores. Overall, the application of *PCA* generally presented comparatively similar performance compared to those without *PCA*. Therefore, the application of *PCA* may benefit if the data had more features (e.g. more kinematic variables involved), since *PCA* reduces number of features and reduce data processing time.

Besides the fact that the *ALL* dataset gave good performance, the racket centre velocity also presented good performance. However, the F_1 score for the racket centre displacement could not differentiate the experts from the novices. The racket rotations were not able to give good results by just over *80%*. When *PCA* was not applied, the trunk centre was in the opposite situation that the displacement was able to predict relatively good results but the velocity could not. Displacement and velocity of trunk rotation seemed both applicable at most phase time. The shoulder, elbow and wrist were not presenting good results. Then a combination of the trunk centre motion and trunk rotational motion showed better result in displacement. A combination of trunk and shoulder rotations showed better result in velocity. The combination of elbow and wrist were not able to predict with a good result. The

other combinations in the table (e.g.*(T+S+E+W)D*), on the other hand, were able to present good model performance.

5.5 Classification model

5.5.1 Summary

The *SVM* classification technique was applied in order to build the model for identifying the motion quality by classifying them into experts or novices. The model development included the three different feature selection methods (i.e. a diverse subset, *PCA* and *p*-threshold), three different *SVM* kernels (i.e. linear, polynomial and *RBF*) and two different *SVM* parameters (i.e. *C* and *K*) to find out the best model performance (i.e. F_1 score) through cross-validation and Nelder-Mead method. Results show that the linear kernel performed the worst on the data, the *RBF* kernel and the polynomial kernel had comparable performances and the *RBF* kernel was selected. The feature selection method of *p*-threshold did not show any advantage due to the relative small size of the data since it may over reduce the data dimensions (i.e. number of features). The application of *PCA* gave similar results against *SVM* without applying *PCA* when the data dimensions are large, but on the other hand may be worse when data size is smaller. Therefore, the model was preferred with the *RBF* kernel and basic feature selection methods (i.e. without *PCA*) for the biomechanical data of table tennis stroke; otherwise the *PCA* may be considered if the higher dimension of data was used.

Based on the model performance table (Table *5-5*), several good features combinations were selected (without *PCA*). They are tabulated in Table *5-6* . The average performance upon all the phases was calculated for these *18* combinations. Their grand average performance is 90.2%. Therefore, the *SVM* exhibited good performance in distinguishing the biomechanical motion data between expert and

novice players.

Table 5-6 Selected feature combinations

Selected combinations	Average performance (%)
RC(D+V)	89.7
RR(D+V)	85.7
(RC+RR)(D+V)	90.7
TC(D), TC(D+V)	85.7
T(D+V)	90
(TC+T)D, (TC+T)(D+V)	88.0, 90.0
(T+S)V, (T+S)(D+V)	90.3, 92.3
(T+S+E+W)D, (T+S+E+W)V, (T+S+E+W)(D+V)	87.7, 90.0, 93.0
(TC+T+S+E+W)D, (TC+T+S+E+W)(D+V)	89.0, 94.0
ALL(D), ALL(V), ALL(D+V)	90.7, 91.3, 95.7

5.5.2 Implementation of classification model

The trained *SVM* classifiers, in fact, are able to give more information than the binary classes (*Figure 5-11*). A score can be generated for describing how close a new data instance is to the two classes (*Section 2.3.2*). Given the two output of expert ($y_i = +1$) and novice ($y_i = -1$), the score can be a number in the range $[-1, +1]$ rather than the binary $\{-1, +1\}$. A score closer to +1 represents that the data has higher possibility belonging to the expert patterns; on the other hand, a smaller score close to -1 represents that the data is more like novice patterns.

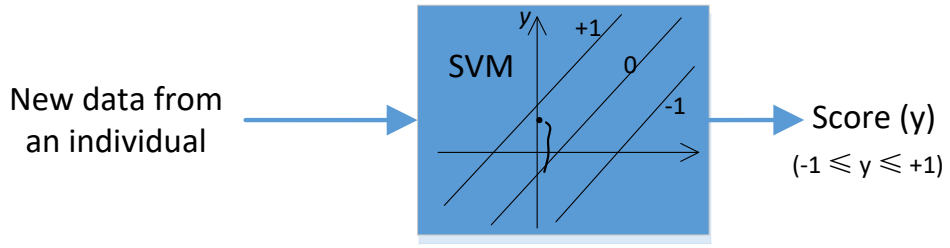

Figure 5-11 Prediction score of trained SVM model

Then the desired classification model was built as shown in *Figure 5-12*. The *SVM*s are trained models. When any new data of a player is input into the model, it processes the data and gives the prediction scores for the combinations (Table *5-6*). Each combination is able to give a performance at least over *85%* and their average performance over *90%*, then results can be used for further usage (e.g. generation of feedbacks for the novice player).

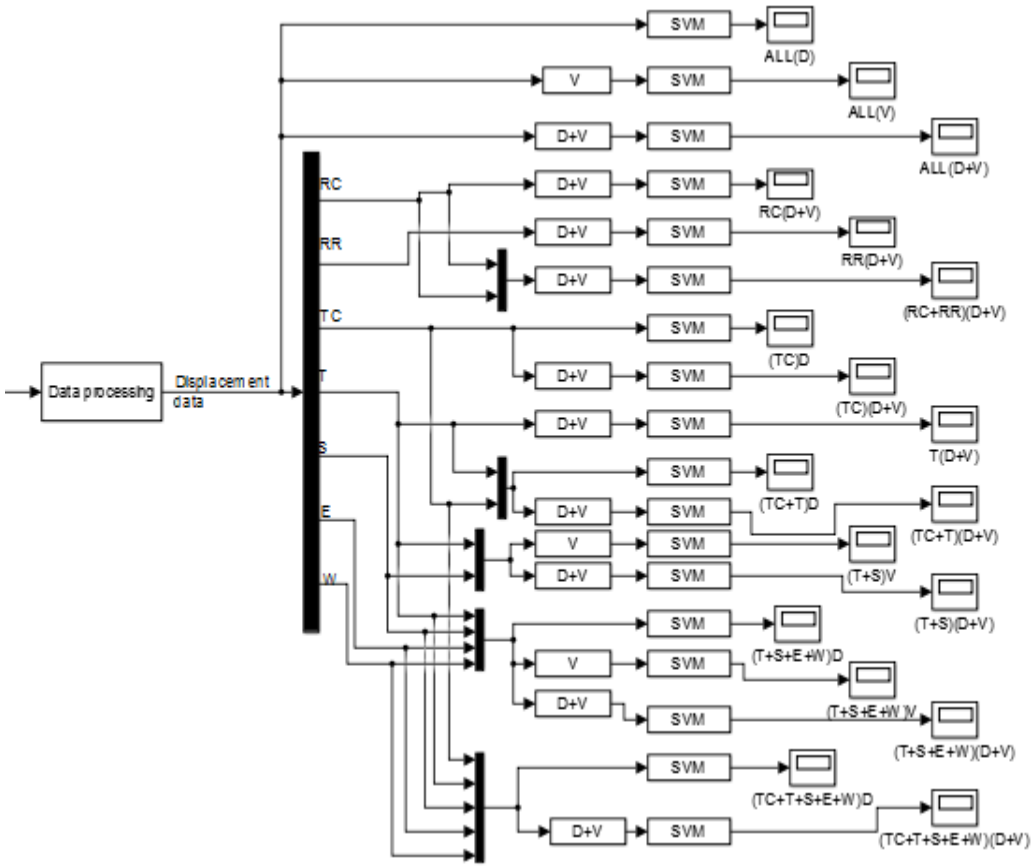

Figure 5-12 Desired classification model

5.5.3 Framework for coaching system

A potential future application of the classification model is the development of a table tennis coaching system, which will be able to monitor and provide feedback to novice players like a coach. The *SVM* model functions as the computational kernel of the system to deal with the motion data processing and evaluation. The framework of the coaching system is illustrated in *Figure 5-13*. It can be developed to continuously monitor and timely correct motion patterns for novice table tennis players, and offer useful information on the status of players' training progress.

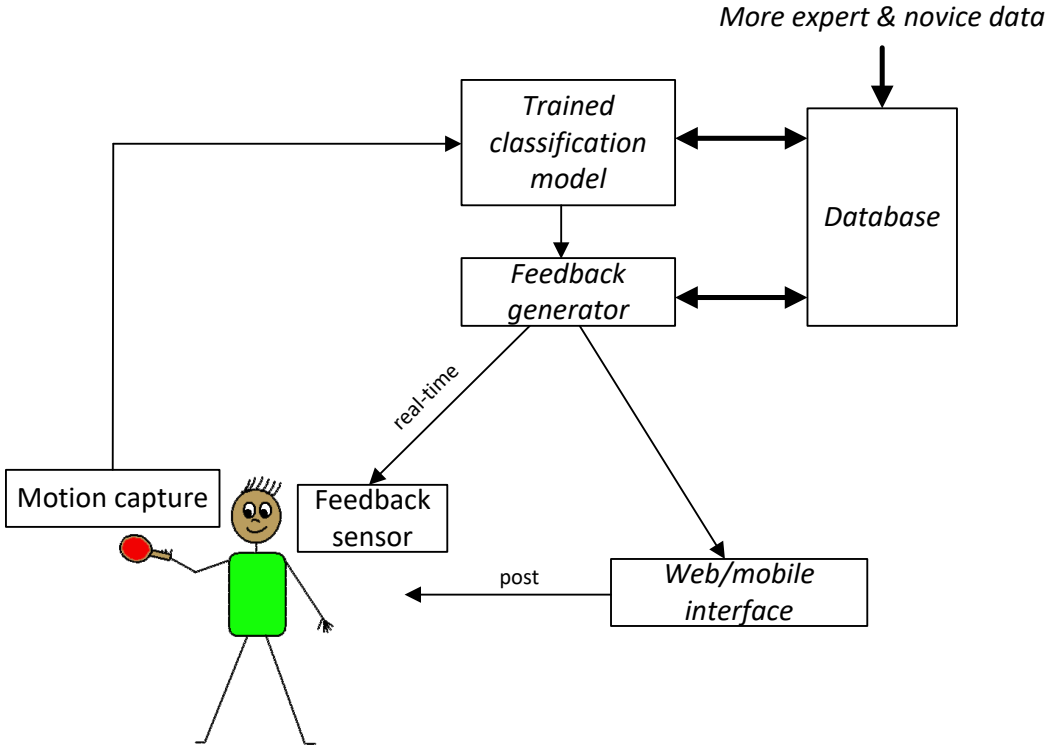

Figure 5-13 Framework of the coaching system

The system should be made up of several necessary components: the motion capture component, the classification model, the database component, and the feedback component. The motion capture component captures the data from the player by sensors in real-time and send the data to the classification model. It could be an optical motion capture system (e.g. markerless motion capture system) or a portable

inertial measure system (e.g. inertial measurement units). The classification model processes the data by phase alignment, normalization, feature selection and then classifies the data into expert patterns or novice patterns by giving a score. The feedback component generates feedback to the player either by real time feedback sensor (e.g. *LED*, voice, vibrators), or the post overview of performances through web/mobile interfaces. The database stores the results of training, and allows the progressive analysis and feedback to the players. In addition, the database should have the ability to include more data of experts and novices, therefore increase or update the training dataset of classification model to improve the model performance by itself.

Chapter 6 Conclusions and contributions

6.1 Conclusions

This research applied biomechanical analysis and model development to the assessment of the motion patterns of table tennis strokes. The major objectives of this thesis are threefold: to quantify the movement of table tennis forehand strokes, to identify the different motion patterns between novice and expert players, and to develop a model for automatic evaluation of the motion quality for an individual.

Chapter 3 introduced the kinematic model for the quantification of the motion of racket, human trunk, shoulder, elbow, and wrist. The definitions of human body motion *DOF* were based on *ISB*. The measurement and calculation methods for these variables from motion capture were then proposed. The measured variables can be segmented and piecewise-normalized with a method based on racket centre velocity profile. In addition, the kinematic model can be visualized using normalized kinematic variable values to be an assistive tool for data analysis. The methodology described in this chapter is the basis for data processing and quantified comparison in the subsequent chapters.

Chapter 4 involved a controlled experiment to capture the motion data (*60* forehand strokes per person) from *10* expert and *10* novice table tennis players. Successful strokes were picked out for data processing based on the kinematic model. Then statistical analyses were performed on an exhaustive set of motion pattern variables to determine the motion differences between the two groups. The significant differences in different phase time were comprehensively addressed. For example, the experts represented larger range of racket movement, faster racket centre velocity, smaller racket plane angle against horizontal plane, different posture in the majority of the joints while not including elbow flexion angle, and joint angle velocity in

trunk, shoulder internal rotation, elbow, and wrist radial flexion etc.

Chapter 5 proposed a classification model for the evaluation of motion quality when given new data of an individual. The model was built using a binary *SVM* classifier and the raw data set was the normalized data from the preceding experiment in *Chapter 4*. Three different feature selection methods were applied to the raw data set, including a diverse subset, *PCA* and *p*-threshold. Different *SVM* kernels (linear, polynomial, *RBF*) were also investigated. With parameter tuning for capacity constraint *C* and kernel scale *K* by cross-validation and Nelder-Mead method, the model was optimized to achieve the best model performance (F_1 score). The final classification model was built upon selected good feature combinations with *RBF* kernel and without *PCA*, with the average performance above *90%*.

6.2 Contributions

The quantification for the variables is comprehensive and unambiguous. The phase segmentation and normalization method for the table tennis stroke is novel with smaller errors and is more straightforward than displacement-based methods. It helped identify the movement within a phase and provide feasible comparison of motion between different strokes and/or different players.

The quantitative comparison and comprehensive differences of racket and human body in different phases of a forehand stroke are novel to the academic literature. The results provide insights into the mechanisms regarding how experts operate and coordinate their body segments to achieve better performance, and how novice players could correct their motion patterns by imitating experts.

The classification model has the potential to be implemented into the framework of a coaching system, which gives feedback to trainees and help improve their technical

skills. This work is novel and demonstrate the feasibility and potentiality in applying the classification technique to table tennis biomechanics. The classification model was an attempt to apply classification techniques to table tennis biomechanics, and can be applied to automatically evaluate (the data processing also needs no human interaction) the motion pattern qualities of table tennis players.

This research found a way of biomechanically and quantitatively analyze the kinematic variables of table tennis strokes. This research has the potential to be applied to other racket sports other than table tennis for assistive analysis of sport performance, and further to help players improve skills during their technical practices.

6.3 Future work

Future work to extend the research may be multi-fold. Firstly, the human kinematic model in the thesis includes the kinematic chain from upper trunk to racket. The lower trunk and legs may also be considered for more comprehensive results. Secondly, this thesis focused on the controlled forehand stroke. Other strokes, like backhands and forehands under different settings (e.g. ball spin), could be included. Thirdly, the motion capture and feedback generator (*Figure 5-13*) may be designed to make a working coaching system for real application, which would need more efforts.

References

Ahmadi, A., Rowlands, D., & James, D. A. (2009). Towards a wearable device for skill assessment and skill acquisition of a tennis player during the first serve. *Sports Technology, 2*(3-4), 129-136.

Aldrich, V. C. (1937). A theory of ball-play. *Psychological Review, 44*(5), 395-403.

Alexander, M., & Honish, A. (2009). Table Tennis: A Brief Overview of Biomechanical Aspects of the Game for Coaches and Players: Faculty of Kinesiology and Recreation Management, University of Manitoba.

Allen, J. B. (1996). Table tennis and motor development. *International Journal of table Tennis Sciences, 3*.

Anglin, C., & Wyss, U. (2000). Review of arm motion analyses. *Proceedings of the Institution of Mechanical Engineers, Part H: Journal of Engineering in Medicine, 214*(5), 541-555.

Baca, A., Dabnichki, P., Heller, M., & Kornfeind, P. (2009). Ubiquitous computing in sports: A review and analysis. *Journal of Sports Sciences, 27*(12), 1335-1346.

Barchukova, G., & Voronov, A. (1998). Biomechanical analysis of attacking strokes as a prerequisite for the development of technical and tactical actions in table tennis. *Journal of Sport Sciences, 16*(5), 407-408.

Bartlett, R. (2001). *Performance Analysis: is it the Bringing Together of Biomechanics and Notational Analysis or an Illusion?* Paper presented at the ISBS-Conference Proceedings Archive.

Bartlett, R. (2006). Artificial intelligence in sports biomechanics: New dawn or false hope. *Journal of Sports Science and Medicine, 5*(443), 474-479.

Bartlett, R. (2007). *Introduction to sports biomechanics: Analysing human movement patterns*: Routledge.

Bartlett, R. (2013). *Sports biomechanics: reducing injury and improving performance*: Routledge.

Bartlett, R., Wheat, J., & Robins, M. (2007). Is movement variability important for

sports biomechanists? *Sports Biomechanics, 6*(2), 224-243.

Begg, R., & Kamruzzaman, J. (2005). A machine learning approach for automated recognition of movement patterns using basic, kinetic and kinematic gait data. *Journal of Biomechanics, 38*(3), 401-408.

Bernstein, N. A. (1967). The co-ordination and regulation of movements. *Journal of Neuropathology & Experimental Neurology, 27*(2), 348.

Boone, D. C., & Azen, S. P. (1979). Normal range of motion of joints in male subjects. *J Bone Joint Surg Am, 61*(5), 756-759.

Bootsma, R. (1988). The timing of rapid interceptive actions: Perception-action coupling in the control and acquisition of skill. *Free University Press*.

Bootsma, R., den Brinker, B., & Whiting, H. (1986). Complex Motor Action in Sport. *Netherlands Journal of Psychology*.

Bootsma, R., & Van Wieringen, P. C. (1990). Timing an attacking forehand drive in table tennis. *Journal of Experimental Psychology: Human Perception and Performance, 16*(1), 21-29.

Buchanan, B. G., Barstow, D., Bechtal, R., Bennett, J., Clancey, W., Kulikowski, C., . . . Waterman, D. A. (1983). Constructing an expert system. *Building expert systems, 50*, 127-167.

Bunn, J. W. (1972). *Scientific principles of coaching*. Englewood Cliffs, NJ: Prentice-Hall.

Butterworth, S. (1930). On the theory of filter amplifiers. *Wireless Engineer, 7*(6), 536-541.

Campos, J., Brizuela, G., & Ramón, V. (2004). Three-dimensional kinematic analysis of elite javelin throwers at the 1999 IAAF World Championships in Athletics. *New studies in Athletics, 19*(2), 47-57.

Cheung, S., Fitzpatrick, M., & Lee, T. Q. (2009). Effects of shoulder position on axillary nerve positions during the split lateral deltoid approach. *Journal of shoulder and elbow surgery, 18*(5), 748-755.

Cortes, C., & Vapnik, V. (1995). Support-vector networks. *Machine learning, 20*(3), 273-297.

Davey, N., Anderson, M., & James, D. A. (2008). Validation trial of an accelerometer‐based sensor platform for swimming. *Sports Technology, 1*(4‐5), 202-207.

Davids, K., Glazier, P., Araujo, D., & Bartlett, R. (2003). Movement systems as dynamical systems. *Sports Medicine, 33*(4), 245-260.

DeLeo, A. T., Dierks, T. A., Ferber, R., & Davis, I. S. (2004). Lower extremity joint coupling during running: a current update. *Clinical Biomechanics, 19*(10), 983-991.

Ebrahim, H. (2010). *The Mechanical Contribution of the Arm Movement During the Performance of the Back Hand Topspin Table Tennis Players.* (Doctor of Social Sciences), University of Konstanz.

Elliott, B., Marshall, R. N., & Noffal, G. (1996a). The role of upper limb segment rotations in the development of racket‐head speed in the squash forehand. *Journal of Sports Sciences, 14*(2), 159-165.

Elliott, B., Marshall, R. N., & Noffal, G. J. (1995). Contributions of upper limb segment rotations during the power serve in tennis. *Journal of Applied Biomechanics, 11*, 433-442.

Elliott, B., Takahashi, K., & Marshall, R. N. (1996b). *Internal Rotation of the Upper Arm: the Missing Link in the Kinematic Chain.* Paper presented at the ISBS-Conference Proceedings Archive.

Feltner, M. E. (1989). Three-dimensional interactions in a two-segment kinetic chain. Part II: Application to the throwing arm in baseball pitching. *Int. J. Sport Biomech., 5*, 420-450.

Foroud, A., & Whishaw, I. Q. (2006). Changes in the kinematic structure and non-kinematic features of movements during skilled reaching after stroke: A laban movement analysis in two case studies. *Journal of Neuroscience Methods, 158*(1), 137-149.

Franks, I. M., & Miller, G. (1986). Eyewitness testimony in sport. *Journal of sport behavior*.

Fukuchi, R. K., Eskofier, B. M., Duarte, M., & Ferber, R. (2011). Support vector machines for detecting age-related changes in running kinematics. *Journal of Biomechanics, 44*(3), 540-542.

Günal, I., Köse, N., Erdogan, O., Göktürk, E., & Seber, S. (1996). Normal Range of Motion of the Joints of the Upper Extremity in Male Subjects, with Special Reference to Side*. *The Journal of Bone & Joint Surgery, 78*(9), 1401-1404.

Gavin, H. P. (2013). The Nelder-Mead Algorithm in Two Dimensions. *CEE 201L. Duke U*.

Ghasemzadeh, H., Loseu, V., Guenterberg, E., & Jafari, R. (2009). *Sport training using body sensor networks: A statistical approach to measure wrist rotation for golf swing.* Paper presented at the Proceedings of the Fourth International Conference on Body Area Networks.

Glazier, P., Davids, K., & Bartlett, R. (2003). Dynamical systems theory: a relevant framework for performance-oriented sports biomechanics research. *Sportscience, 7*(retrieved from sportsci. org/jour/03/psg. htm).

Gowitzke, B., & Waddell, D. (1991). Biomechanical studies of badminton underarm power strokes, court movement and flexibility–a review. *Biomechanics in Sports IX*, 273-277.

Guggenmos, C. (2007). *Towards a Wearable: Snowboarding Assistant.* (Diploma Thesis), Computer Science Department, RWTH Aachen University.

Hamill, J., McDermott, W. J., & Haddad, J. M. (2000). Issues in quantifying variability from a dynamical systems perspective. *Journal of Applied Biomechanics, 16*(4), 407-418.

Han, J., Kamber, M., & Pei, J. (2006). *Data mining: concepts and techniques* (Second Edition ed.): Morgan kaufmann.

Harris, C. M., & Wolpert, D. M. (1998). Signal-dependent noise determines motor planning. *Nature, 394*(6695), 780-784.

Hughes, M. D., & Bartlett, R. M. (2002). The use of performance indicators in performance analysis. *Journal of Sports Sciences, 20*(10), 739-754.

Hughes, M. D., & Franks, I. M. (2004). *Notational Analysis of Sport: Systems for Better Coaching and Performance in Sport*: Psychology Press.

Iino, Y., & Kojima, T. (2009). Kinematics of table tennis topspin forehands: effects of performance level and ball spin. *Journal of Sports Sciences, 27*(12),

1311-1321.

Iino, Y., Mori, T., & Kojima, T. (2008). Contributions of upper limb rotations to racket velocity in table tennis backhands against topspin and backspin. *Journal of Sports Sciences, 26*(3), 287-293.

Ivan, M. L., Rocco, D. M., & Franco, M. (2011). *Performance indicators in table tennis: a review of the literature*. Paper presented at the The 12th Sports Science Congress.

James, C. (2004). Considerations of movement variability in biomechanics research. *Innovative analyses of human movement*, 29-62.

Jolliffe, I. (2005). *Principal component analysis*: Wiley Online Library.

Kohavi, R., & Provost, F. (1998). Glossary of terms. *Machine learning, 30*(2-3), 271-274.

Kotsiantis, S. B., Zaharakis, I., & Pintelas, P. (2007). Supervised machine learning: A review of classification techniques.

Kwan, M., Andersen, M. S., Cheng, C.-L., Tang, W.-T., & Rasmussen, J. (2011). Investigation of high-speed badminton racket kinematics by motion capture. *Sports Engineering, 13*(2), 57-63.

Lapham, A., & Bartlett, R. (1995). The use of artificial intelligence in the analysis of sports performance: a review of applications in human gait analysis and future directions for sports biomechanics. *Journal of Sports Sciences, 13*(3), 229-237.

Lee, T. (2001). *A Beginner's Guide for Junior Players*.

Lees, A. (2002). Technique analysis in sports: a critical review. *Journal of Sports Sciences, 20*(10), 813-828.

Lees, A. (2003). Science and the major racket sports: a review. *Journal of Sports Sciences, 21*(9), 707-732.

Liu, H., Leigh, S., & Yu, B. (2010). *Effects of Movement Sequence on the Performance of Javelin Throwing.* Paper presented at the ISBS-Conference Proceedings Archive.

Liu, X., Kim, W., & Tan, J. (2009). An analysis of the biomechanics of arm

movement during a badminton smash. Singapore: Nanyang Technological University.

Mülling, K., & Peters, J. (2009). A computational model of human table tennis for robot application *Autonome Mobile Systeme 2009* (pp. 57-64): Springer.

Mullineaux, D. R. (2000). Methods for quantifying the variability in data. *In Proceedings of the 18th International Symposium of Biomechanics in Sport (edited by Y. Hong and D.P. Johns)*, pp. 684-688.

Mullineaux, D. R., Bartlett, R. M., & Bennett, S. (2001). Research design and statistics in biomechanics and motor control. *Journal of Sports Sciences, 19*(10), 739-760.

Neal, R. J. (1991). The mechanics of the forehand loop and smash shots in table tennis. *Australian Journal of Science and Medicine in Sport (AJSMS), 23*(1), 3-11.

Nelder, J. A., & Mead, R. (1965). A simplex method for function minimization. *The computer journal, 7*(4), 308-313.

Nevill, A., Atkinson, G., & Hughes, M. (2008). Twenty-five years of sport performance research in the Journal of Sports Sciences. *Journal of Sports Sciences, 26*(4), 413-426.

O'Donoghue, P. (2009). *Research methods for sports performance analysis*: Routledge.

Pavlov, I. P. (1927). *Conditioned reflexes*: Courier Dover Publications.

Pezzack, J., Norman, R., & Winter, D. (1977). An assessment of derivative determining techniques used for motion analysis. *Journal of Biomechanics, 10*(5), 377-382.

Poole, D., Mackworth, A., & Goebel, R. (1998). *Computational Intelligence*: Oxford University Press Oxford.

Powers, D. (2011). Evaluation: From precision, recall and f-measure to roc., informedness, markedness & correlation. *Journal of Machine Learning Technologies, 2*(1), 37-63.

Putnam, C. A. (1993). Sequential motions of body segments in striking and

throwing skills: Descriptions and explanations. *Journal of Biomechanics, 26, Supplement 1*(0), 125-135.

Ramanantsoa, M., & Durey, A. (1994). Towards a stroke construction model. *International Journal of Table Tennis Science, 2*(2), 97-114.

Rambely, A. S., & Osman, N. A. A. (2008). *The contribution of upper limb joints in the development of racket velocity in the badminton smash.* Paper presented at the ISBS-Conference Proceedings Archive.

Rodrigues, S. T., Vickers, J. N., & Williams, A. M. (2002). Head, eye and arm coordination in table tennis. *Journal of Sports Sciences, 20*(3), 187-200.

Ruiz-Gonzalez, R., Gomez-Gil, J., Gomez-Gil, F. J., & Martínez-Martínez, V. (2014). An SVM-Based Classifier for Estimating the State of Various Rotating Components in Agro-Industrial Machinery with a Vibration Signal Acquired from a Single Point on the Machine Chassis. *Sensors, 14*(11), 20713-20735.

Russell, S. J., Norvig, P., Canny, J. F., Malik, J. M., & Edwards, D. D. (2003). *Artificial intelligence: a modern approach* (Vol. 2): Prentice hall Upper Saddle River.

Sørensen, V., Ingvaldsen, R., & Whiting, H. (2001). The application of co-ordination dynamics to the analysis of discrete movements using table-tennis as a paradigm skill. *Biological Cybernetics, 85*(1), 27-38.

Sakurai, S., Ikegami, Y., Okamoto, A., Yabe, K., & Toyoshima, S. (1993). A 3-dimensional cinematographic analysis of upper limb movement during fastball and curveball baseball pitches. *Journal of Applied Biomechanics, 9*(1), 47-65.

Schmidt, R., Sherwood, D., Zelaznik, H., & Leikind, B. (1985). Speed-accuracy trade-offs in motor behavior: Theories of impulse variability *Motor Behavior* (pp. 79-123): Springer.

Shanks, D. R., & John, M. F. S. (1994). Characteristics of dissociable human learning systems. *Behavioral and brain sciences, 17*(03), 367-395.

Sheppard, A., & Li, F. X. (2007). Expertise and the control of interception in table tennis. *European Journal of Sport Science, 7*(4), 213-222.

Sidaway, B., Heise, G., & SchoenfelderZohdi, B. (1995). Quantifying the variability of angle-angle plots. *Journal of Human Movement Studies, 29*(4), 181-197.

Singer, S., & Nelder, J. (2009). Nelder-mead algorithm. *Scholarpedia, 4*(7), 2928.

Singley, M. K. (1989). *The transfer of cognitive skill*: Harvard University Press.

Sprigings, E., Marshall, R. N., Elliott, B., & Jennings, L. (1994). A three-dimensional kinematic method for determining the effectiveness of arm segment rotations in producing racquet-head speed. *Journal of Biomechanics, 27*(3), 245-254.

Tanabe, S., & Ito, A. (2007). A three-dimensional analysis of the contributions of upper limb joint movements to horizontal racket head velocity at ball impact during tennis serving. *Sports Biomechanics, 6*(3), 418-433.

Temprado, J., Della-Grasta, M., Farrell, M., & Laurent, M. (1997). A novice-expert comparison of (intra-limb) coordination subserving the volleyball serve. *Human Movement Science, 16*(5), 653-676.

Tepavac, D., & Field-Fote, E. C. (2001). Vector coding: a technique for quantification of intersegmental coupling in multicyclic behaviors. *Journal of Applied Biomechanics, 17*(3), 259-270.

Tsai, C.-L., Huang, C., Lin, D.-C., & Chang, S. S. (2000). *Biomechanical Analysis of the Upper Extremity in Three Different Badminton Overhead Strokes.* Paper presented at the ISBS-Conference Proceedings Archive.

Tyldesley, D., & Whiting, H. (1975). Operational timing. *Journal of Human Movement Studies*.

Van Gheluwe, B., De Ruysscher, I., & Craenhals, J. (1987). Pronation and endorotation of the racket arm in a tennis serve. *Biomechanics XB*, 666-672.

Van Gheluwe, B., & Hebbelinck, M. (1985). The kinematics of the service movement in tennis: A three-dimensional cinematographical approach. *Biomechanics IX-B*, 521-526.

Waterman, D. (1986). *A guide to expert systems*.

Wheat, J. S., & Glazier, P. S. (2005). Measuring coordination and variability in coordination *Movement system variability* (pp. 167-181): Centre for Sports Engineering Research.

Wu, G., Van Der Helm, F. C. T., Veeger, H. E. J., Makhsous, M., Van Roy, P., Anglin, C., . . . Buchholz, B. (2005). ISB recommendation on definitions of joint coordinate systems of various joints for the reporting of human joint motion - Part II: Shoulder, elbow, wrist and hand. *Journal of Biomechanics, 38*(5), 981-992.

Wu, J., & Wang, J. (2008). PCA-based SVM for automatic recognition of gait patterns. *Journal of Applied Biomechanics, 24*(1), 83.

Xiao, D., Su, P., & Hu, Z. (2006). Application and outlook about Sports Biomechanics in table tennis. *Journal of Beijing Sport University, 10*(2007), 029.

Zhang, H., Yu, L., & Hu, J. (2011). computer-aided game analysis of net sports in preparation of chinese teams for Beijing Olympics. *Int J Comp Sci Sport, 9*(3), 53-69.

Zhang, Z., Halkon, B., Chou, S. M., & Qu, X. (2016). A novel phase-aligned analysis on motion patterns of table tennis strokes. *International Journal of Performance Analysis in Sport, 16*(1), 305-316.

Appendix A: Definitions of human motion based on ISB

In current research, human body segments and joints of interest include trunk, shoulder (upper arm), elbow (lower arm), and wrist (hand). The coordinate systems and motions of human kinematic model were defined mathematically with reference to *ISB* recommendation (G. Wu et al., 2005).

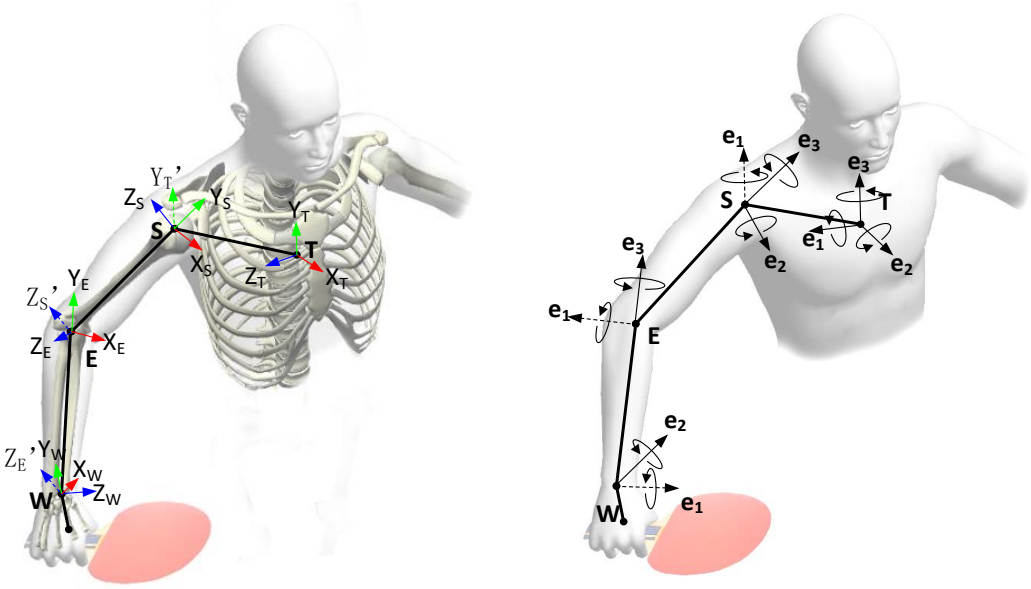

Figure 1 Kinematic model definition: coordinate systems (left) and trunk/joint rotation (right)

Trunk/Joints

T: Thorax centre (incisura jugularis)

S: Shoulder joint centre (glenohumeral rotation centre)

E: Elbow joint centre (centre of lateral epicondyle and medial epicondyle)

W: Wrist joint centre (centre of radial styloid and ulnar styloid)

Definition of trunk/joint coordinate systems

The coordinate systems were defined for trunk and right arm. All the defined rotations have a value of zero under human initial anatomical posture: the human stands with his right arm vertical down at the side, and the palm of right hand facing

forward (x_+ direction of the global coordinate system). Note the descriptions of axis directions (e.g. leftward, upward) below are only for reference based on the anatomical posture situation.

1. Trunk

X_T : perpendicular to frontal plane of human body, pointing to the front of human body

Y_T : perpendicular to transverse plane of human body, pointing to the up of human body

Z_T : perpendicular to sagittal plane of human body, pointing to the right of human body

2. Shoulder joint

X_S : line perpendicular to Y_S and Z_S, pointing forward

Y_S : line connecting *S* and *E*, pointing to *S*

Z_S : line perpendicular to plane formed by S, E, and W, pointing rightward

* The above method is used as against the other method described below, which has larger errors (both can be found in *ISB*):

X_S : line perpendicular to plane formed by S, lateral epicondyle and medial epicondyle, pointing forward

Y_S : line connecting *S* and *E*, pointing to *S*

Z_S : line perpendicular to X_S and Y_S, pointing rightward

3. Elbow joint

X_E : line perpendicular to plane formed by *E*, radial styloid and ulnar styloid, pointing forward

Y_E : line connecting *E* and *W*, pointing to *E*

Z_E : line perpendicular to X_E and Y_E, pointing rightward

4. Wrist

X_W : line perpendicular to Y_W and Z_W, pointing forward

Y_W : line parallel to long shaft of the radius to intersect with the ridge of bone between the radioscaphoid fossa and the radiolunate fossa, pointing upward

Z_W : line perpendicular to X_W , and in a plane defined by the tip of radial styloid, the base of the concavity of the sigmoid notch and the specified origin, pointing rightward

Definition of trunk/joint motions

1. Trunk

Displacement and rotation of thorax relative to the global coordinate system (*Z*-*X*-*Y*

order)

displacement : corresponds to motion with respect to the global coordinate system

e1 : axis coincident with *z*-axis of the global coordinate system (also the initial Z_T, which is parallel to global *z*-axis)

T_{fe} — flexion (negative) / extension(positive)

e2 : axis coincident with X_T

T_{ll} — lateral flexion to the right (positive) /lateral flexion to the left (negative)

e3 : axis coincident with Y_T

T_{aa} — axial rotation to the left (positive) /axis rotation to the right (negative)

2. Shoulder joint

Rotation of humerus relative to thorax (*Y-X-Y* order)

e1 : axis coincident with Y_T (also Y'_T ,which is parallel to Y_T)

S_{pe} — plane of elevation, 0° is abduction. 90° is forward flexion

e2 : axis coincident with X_S

S_e — elevation (negative)

e3 : axis coincident with Y_S

S_{ie} — internal rotation (positive) /external rotation (negative)

3. Elbow joint

Rotation of lower arm relative to upper arm (*Z-X-Y* order)

e1 : axis coincident with Z_S (also Z'_S ,which is parallel to Z_S)

E_{fe} — flexion (positive) / hyperextension (negative)

e2 : axis coincident with X_E

Not defined

e3 : axis coincident with Y_E

E_{ps} — pronation (positive) / supination (negative)

4. Wrist joint

Rotation of hand relative to lower arm (*Z-X-Y* order)

e1 : axis coincident with Z_E (also Z'_E ,which is parallel to Z_E)

W_{fe} — flexion (positive) / extension (negative)

e2 : axis coincident with X_E

W_{ru} — radial deviation (negative) / ulnar deviation (positive)

e3 : axis coincident with Y_E

Not defined

Appendix B: Motion pattern differences (part)

Among the large amount of comparison results for Chapter 2, only those at phase time T_1, T_2, T_3 and T_4 are tabulated here with units *m*, *m/s*, ° or °/*s* for the respective variables.

Variables		T_1			T_2			T_3			T_4		
		Experts	Novices	p	Experts	Novices	p	Experts	Novices	p	Experts	Novices	p
Displacement	RC_x	-0.4 ±0.1	-0.5 ±0.2	0.40	-0.7 ±0.1	-0.6 ±0.2	0.14	-0.2 ±0.1	-0.2 ±0.1	0.86	0.1 ±0.2	0.1 ±0.2	0.90
	RC_y	-0.0 ±0.1	0.1 ±0.1	0.00	-0.0 ±0.1	0.1 ±0.1	0.00	0.2 ±0.1	0.2 ±0.0	0.48	0.6 ±0.1	0.5 ±0.2	0.28
	RC_Z	0.2 ±0.1	0.4 ±0.1	0.00	0.2 ±0.1	0.3 ±0.1	0.00	0.3 ±0.0	0.4 ±0.1	0.13	-0.4 ±0.1	-0.1 ±0.2	0.00
	RR_{xy}	118.7 ±6.5	109.8 ±18.2	0.17	86.3 ±10.4	87.5 ±12.6	0.83	104.9 ±7.9	107.8 ±7.7	0.42	146.3 ±11.8	136.2 ±11.3	0.07
	RR_{yz}	45.3 ±9.3	34.7 ±15.9	0.09	49.4 ±7.9	30.9 ±18.0	0.01	29.1 ±6.5	24.7 ±5.5	0.12	101.3 ±16.4	77.7 ±32.5	0.06
	RR_{xz}	120.4 ±9.0	108.3 ±16.6	0.06	137.0 ±7.8	116.1 ±19.3	0.01	112.5 ±5.8	102.8 ±9.2	0.01	114.1 ±15.4	109.9 ±17.2	0.57
Velocity	RC_x	-2.9 ±0.7	-1.2 ±0.8	0.00	-0.3 ±0.2	0.1 ±0.2	0.00	6.0 ±1.1	3.5 ±1.1	0.00	0.0 ±0.2	-0.3 ±0.1	0.00
	RC_y	-0.7 ±0.4	-0.5 ±0.7	0.43	0.6 ±0.2	-0.1 ±0.2	0.00	3.2 ±1.2	1.6 ±0.9	0.00	-0.8 ±0.4	-0.5 ±0.3	0.06
	RC_Z	-0.2 ±0.5	0.1 ±0.8	0.27	0.3 ±0.3	-0.1 ±0.3	0.01	-1.7 ±1.9	-0.7 ±1.1	0.17	-0.1 ±0.1	-0.1 ±0.3	0.70
	RC_{2D}	3.0 ±0.7	1.4 ±0.8	0.00	0.6 ±0.2	0.3 ±0.2	0.01	6.5 ±1.4	3.8 ±1.0	0.00	0.2 ±0.1	0.4 ±0.2	0.05
	RC_{3D}	3.1 ±0.8	1.6 ±0.8	0.00	0.8 ±0.2	0.4 ±0.2	0.00	7.3 ±1.7	4.2 ±1.1	0.00	0.9 ±0.4	0.7 ±0.3	0.25
	RR_{xy}	-214.3 ±68.6	-183.0 ±93.8	0.41	-164.5 ±42.4	-91.0 ±67.1	0.01	501.6 ±81.9	294.3 ±135.4	0.00	-10.4 ±39.9	4.1 ±50.0	0.48
	RR_{yz}	-83.2 ±64.2	-110.3 ±146.7	0.60	53.8 ±59.1	19.5 ±43.4	0.16	135.8 ±190.0	150.2 ±224.0	0.88	67.7 ±27.4	68.7 ±51.3	0.96
	RR_{xz}	116.8 ±55.3	60.5 ±66.0	0.05	34.0 ±48.7	22.3 ±82.3	0.70	-162.2 ±110.7	-92.8 ±120.7	0.20	-19.0 ±40.5	41.4 ±53.4	0.01
Displacement	T_x	-0.3 ±0.1	-0.5 ±0.1	0.01	-0.3 ±0.1	-0.4 ±0.1	0.01	-0.3 ±0.1	-0.4 ±0.1	0.04	-0.3 ±0.1	-0.4 ±0.1	0.09
	T_y	0.4 ±0.1	0.5 ±0.0	0.00	0.4 ±0.1	0.5 ±0.0	0.00	0.4 ±0.1	0.5 ±0.0	0.00	0.4 ±0.1	0.5 ±0.0	0.00
	T_z	-0.2 ±0.1	-0.1 ±0.0	0.02	-0.2 ±0.1	-0.1 ±0.0	0.00	-0.2 ±0.1	-0.1 ±0.1	0.00	-0.3 ±0.1	-0.2 ±0.1	0.00
	T_{fe}	-10.2 ±7.2	-12.7 ±9.6	0.52	-9.0 ±7.4	-14.7 ±11.6	0.21	-12.6 ±8.3	-16.2 ±12.4	0.46	-14.4 ±9.1	-15.7 ±10.7	0.77
	T_{ll}	22.7 ±6.5	13.3 ±7.0	0.01	25.6 ±7.6	14.7 ±7.7	0.00	15.3 ±4.8	9.6 ±9.9	0.13	-3.0 ±7.5	0.6 ±10.8	0.40
	T_{aa}	-48.4 ±9.6	-28.9 ±11.1	0.00	-59.6 ±9.9	-29.6 ±11.8	0.00	-34.0 ±7.7	-16.8 ±11.8	0.00	14.8 ±10.8	2.4 ±16.6	0.06
	S_{pe}	19.1 ±32.1	-7.3 ±20.4	0.04	14.2 ±28.3	-13.4 ±20.8	0.02	53.0 ±17.3	51.5 ±15.8	0.84	75.1 ±12.4	67.2 ±20.0	0.30
	S_e	-26.9 ±8.8	-20.2 ±5.2	0.05	-30.7 ±7.3	-19.6 ±6.2	0.00	-44.9 ±12.8	-30.8 ±6.2	0.01	-71.1 ±19.8	-61.3 ±27.8	0.37
	S_{ie}	-29.0 ±37.2	-11.4 ±20.5	0.21	-52.1 ±32.4	-16.8 ±24.5	0.01	-74.3 ±20.1	-69.9 ±14.7	0.58	-53.4 ±9.1	-54.1 ±17.2	0.90
	E_{fe}	63.9 ±10.4	67.6 ±16.0	0.56	55.3 ±13.0	63.1 ±16.6	0.26	67.7 ±11.1	61.6 ±11.6	0.24	92.8 ±10.7	65.9 ±18.0	0.00
	E_{ps}	115.4 ±17.5	99.9 ±15.3	0.05	118.3 ±25.5	94.7 ±16.1	0.03	116.3 ±21.4	99.5 ±16.4	0.06	108.9 ±15.3	111.0 ±17.2	0.78
	W_{fe}	-0.2 ±12.5	-15.5 ±10.0	0.01	-1.6 ±16.3	-22.0 ±11.9	0.00	-0.9 ±16.1	-24.7 ±11.2	0.00	2.0 ±12.8	-16.2 ±10.6	0.00
	W_{ru}	19.4 ±5.6	10.0 ±6.8	0	23.7 ±5.8	14.6 ±7.6	0.01	23.6 ±5.5	16.3 ±7.9	0.03	18.8 ±5.0	14.1 ±9.3	0.18
Velocity	T_x	0.1 ±0.1	0.2 ±0.2	0.25	0.2 ±0.2	0.2 ±0.1	0.89	-0.1 ±0.1	0.0 ±0.1	0.05	-0.0 ±0.1	-0.1 ±0.1	0.19
	T_y	-0.1 ±0.1	-0.1 ±0.1	0.28	-0.1 ±0.1	-0.0 ±0.1	0.65	0.2 ±0.1	0.1 ±0.0	0.04	-0.0 ±0.1	0.0 ±0.0	0.36
	T_z	-0.1 ±0.1	-0.1 ±0.1	0.59	-0.3 ±0.1	-0.2 ±0.1	0.02	-0.2 ±0.1	-0.2 ±0.1	0.12	0.0 ±0.1	0.0 ±0.0	0.75
	T_{fe}	18.9 ±27.2	-16.3 ±22.3	0.01	-9.7 ±14.8	-13.1 ±15.4	0.61	-22.3 ±28.0	-1.1 ±9.4	0.04	-4.0 ±15.9	4.8 ±13.0	0.19
	T_{ll}	44.9 ±25.9	20.5 ±12.8	0.02	-17.3 ±7.1	-5.3 ±24.8	0.16	-86.5 ±48.2	-31.4 ±29.7	0.01	-17.7 ±22.8	-9.5 ±10.1	0.32
	T_{aa}	-129.7 ±40.9	-18.6 ±35.3	0.00	27.5 ±44.1	28.0 ±24.6	0.98	219.1 ±60.1	70.2 ±49.9	0.00	33.9 ±45.8	2.3 ±24.0	0.07
	S_{pe}	-90.0 ±80.0	-90.5 ±78.3	0.99	95.0 ±87.1	69.4 ±110.5	0.57	283.9 ±134.5	287.6 ±128.2	0.95	-36.0 ±33.8	-54.0 ±48.3	0.35
	S_e	-12.9 ±47.8	3.3 ±20.9	0.34	-33.2 ±39.2	17.2 ±16.0	0.00	-202.6 ±73.7	-206.7 ±104.9	0.92	102.4 ±37.3	63.6 ±27.6	0.02
	S_{ie}	-90.0 ±86.9	6.9 ±67.2	0.01	-219.0 ±110.0	-111.2 ±139.8	0.07	83.0 ±201.3	-135.7 ±166.5	0.02	11.0 ±49.6	75.9 ±52.3	0.01
	E_{fe}	-105.6 ±65.1	-45.2 ±42.1	0.02	-10.8 ±39.8	-12.2 ±26.2	0.93	136.0 ±85.2	-26.3 ±90.4	0.00	11.2 ±25.4	47.1 ±29.1	0.01
	E_{ps}	21.2 ±71.5	-48.4 ±29.9	0.01	22.8 ±52.1	-17.2 ±26.6	0.04	-54.7 ±90.5	44.8 ±29.6	0.00	-22.5 ±20.0	-15.5 ±45.1	0.66
	W_{fe}	5.5 ±28.8	-39.0 ±30.3	0.00	-33.1 ±56.9	-50.3 ±32.9	0.42	44.6 ±44.8	26.9 ±43.8	0.38	-3.4 ±16.8	17.3 ±18.6	0.02
	W_{ru}	30.9 ±13.8	37.3 ±38.1	0.63	22.3 ±14.3	25.5 ±21.8	0.70	-30.5 ±15.4	4.5 ±14.6	0.00	-5.8 ±6.0	-10.3 ±10.9	0.27

Appendix C: Classification model performance

Without *PCA*

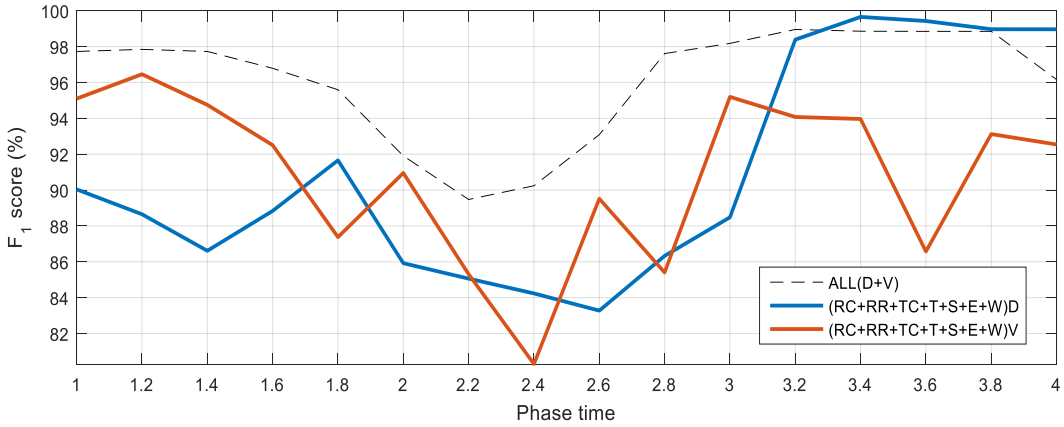

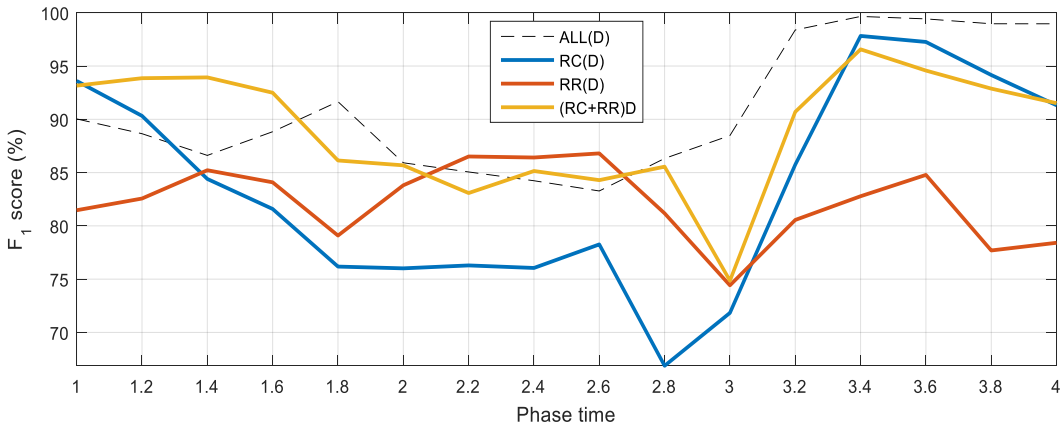

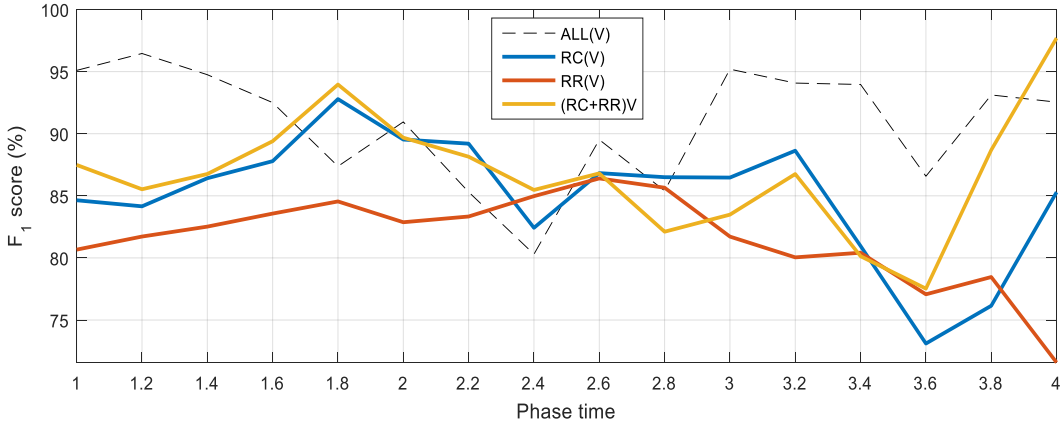

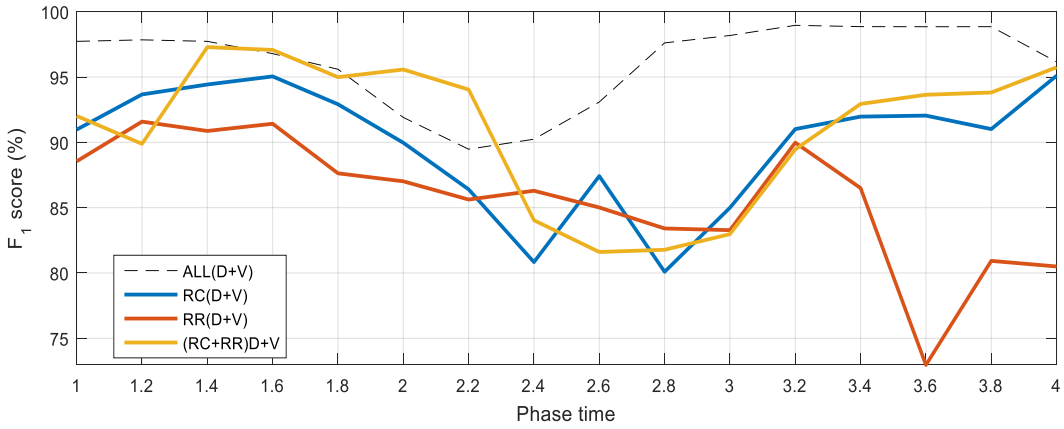
F1 score (%)
Phase time
ALL(D+V)
RC(D+V)
RR(D+V)
(RC+RR)D+V

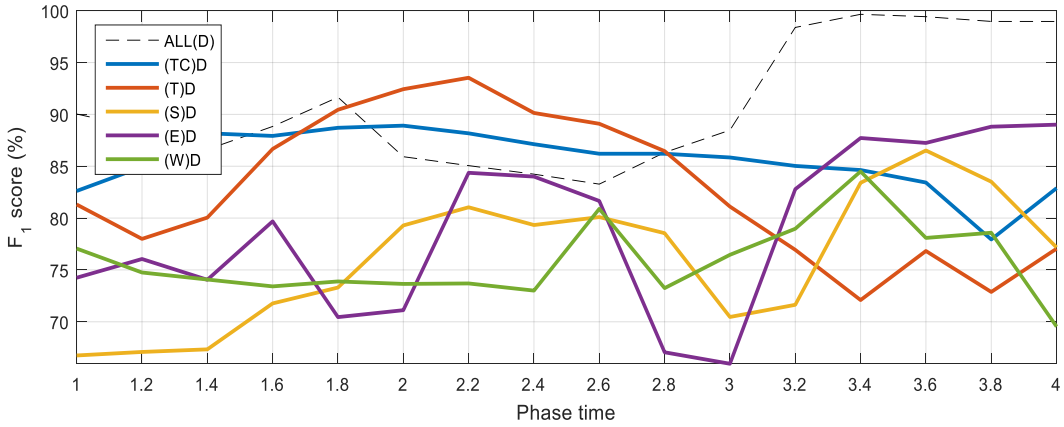
F1 score (%)
Phase time
ALL(D)
(TC)D
(T)D
(S)D
(E)D
(W)D

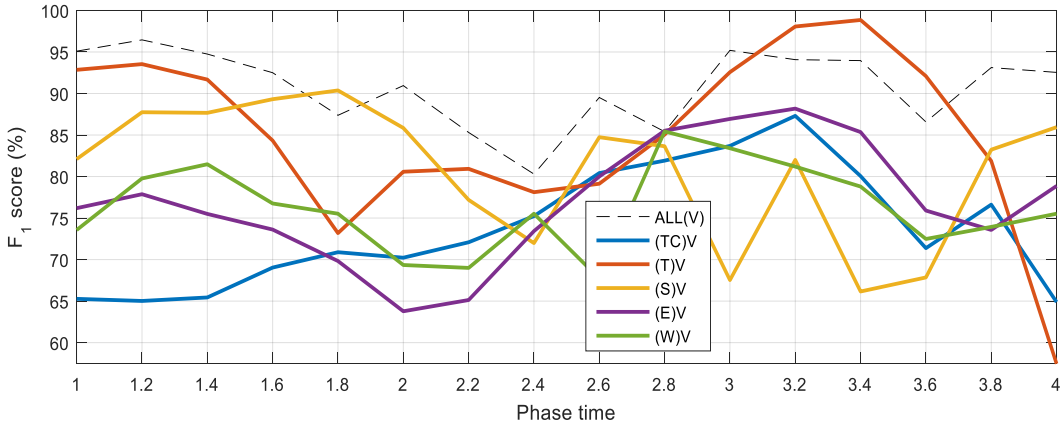
F1 score (%)
Phase time
ALL(V)
(TC)V
(T)V
(S)V
(E)V
(W)V

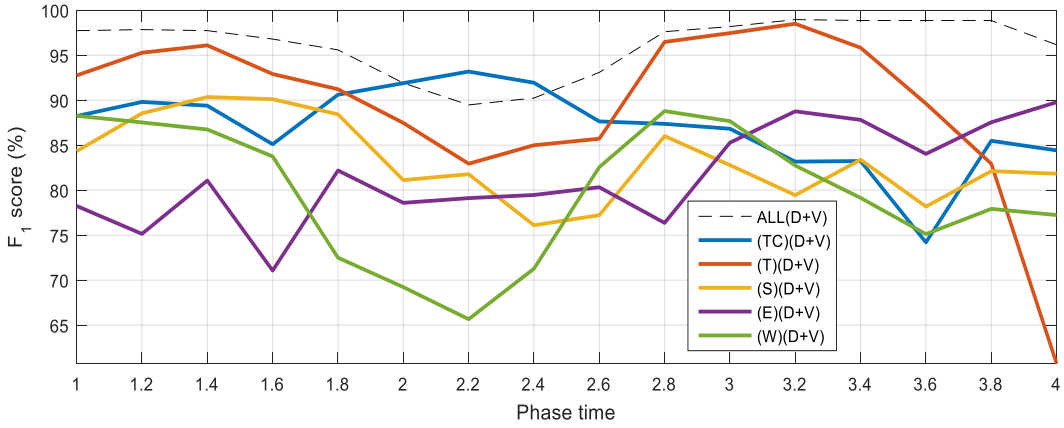
F1 score (%)
Phase time
ALL(D+V)
(TC)(D+V)
(T)(D+V)
(S)(D+V)
(E)(D+V)
(W)(D+V)

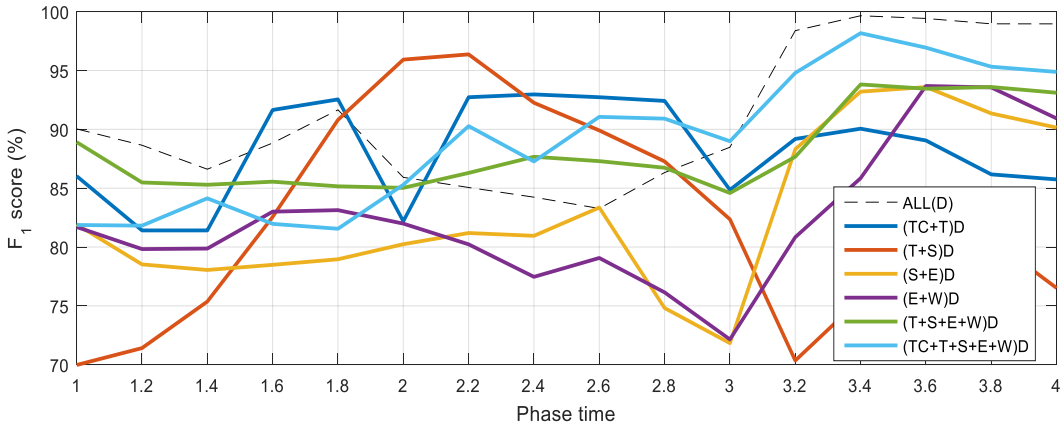
F1 score (%)
Phase time
ALL(D)
(TC+T)D
(T+S)D
(S+E)D
(E+W)D
(T+S+E+W)D
(TC+T+S+E+W)D

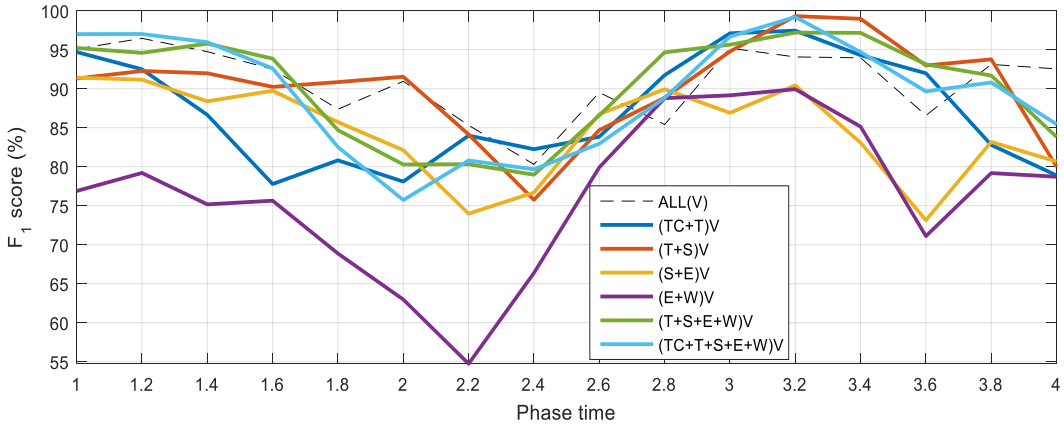
F1 score (%)
Phase time
ALL(V)
(TC+T)V
(T+S)V
(S+E)V
(E+W)V
(T+S+E+W)V
(TC+T+S+E+W)V

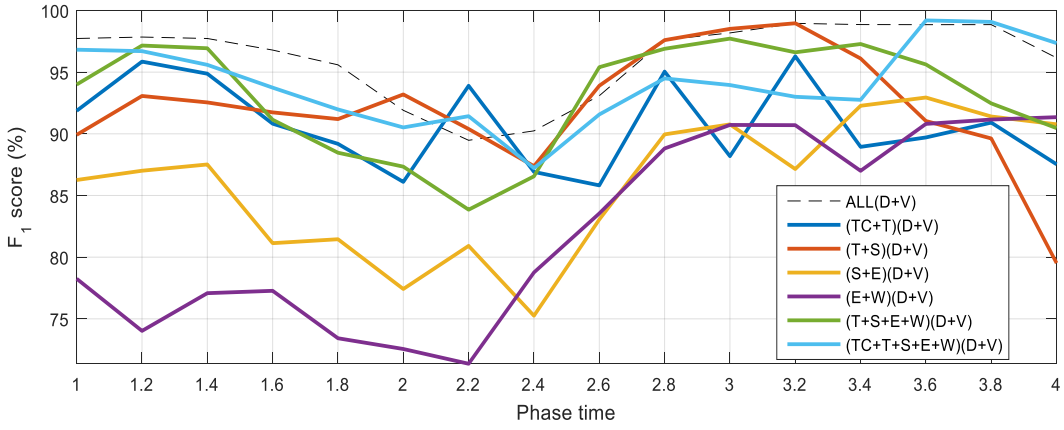
F1 score (%)
Phase time
ALL(D+V)
(TC+T)(D+V)
(T+S)(D+V)
(S+E)(D+V)
(E+W)(D+V)
(T+S+E+W)(D+V)
(TC+T+S+E+W)(D+V)

With *PCA*

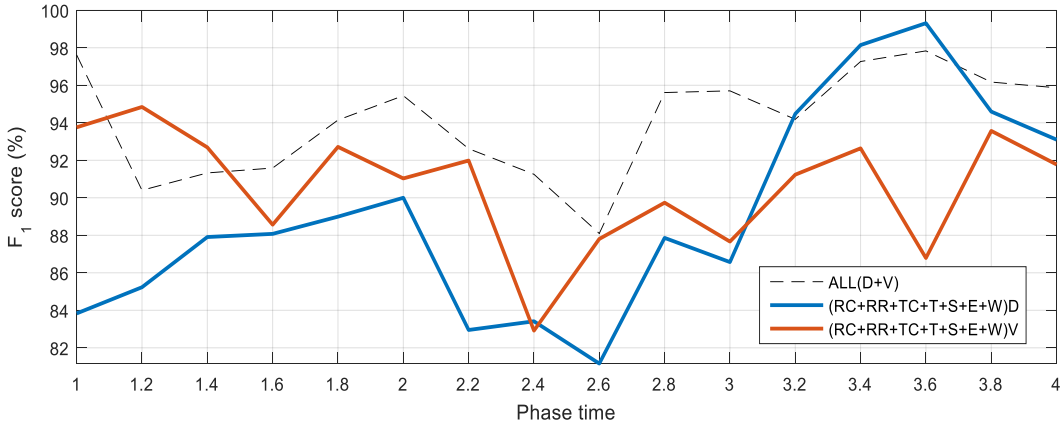
F1 score (%)
Phase time
ALL(D+V)
(RC+RR+TC+T+S+E+W)D
(RC+RR+TC+T+S+E+W)V

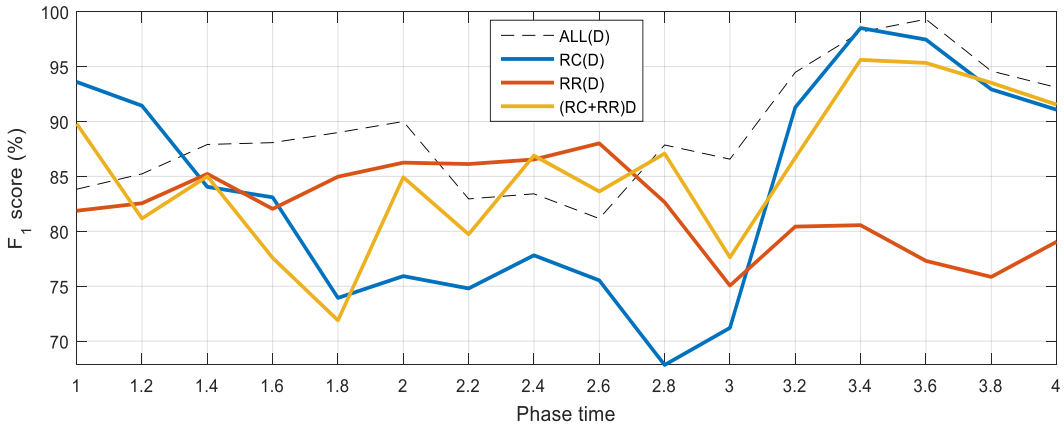
ALL(D)
RC(D)
RR(D)
(RC+RR)D
F 1 score (%)
Phase time

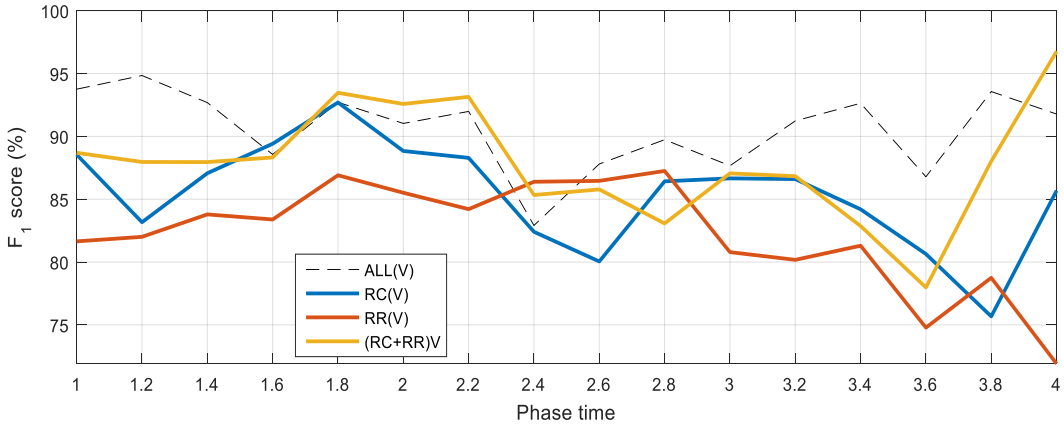
ALL(V)
RC(V)
RR(V)
(RC+RR)V
F 1 score (%)
Phase time

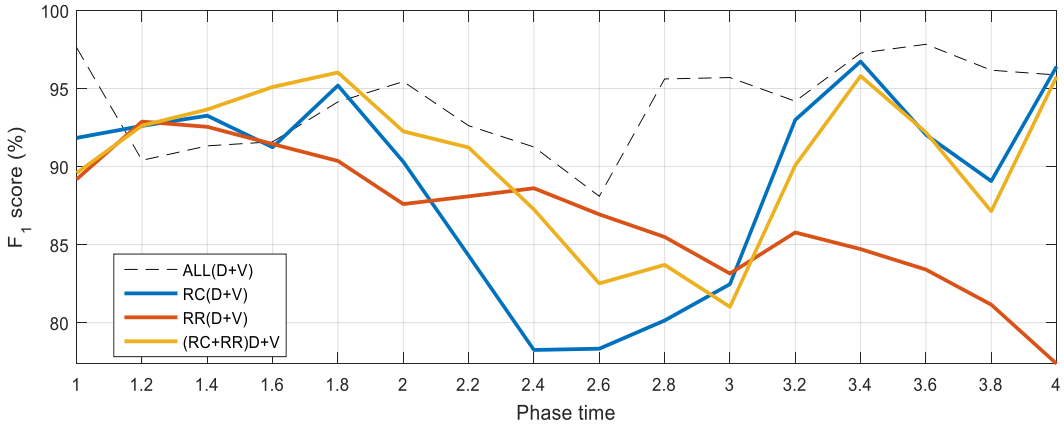
ALL(D+V)
RC(D+V)
RR(D+V)
(RC+RR)D+V
F 1 score (%)
Phase time

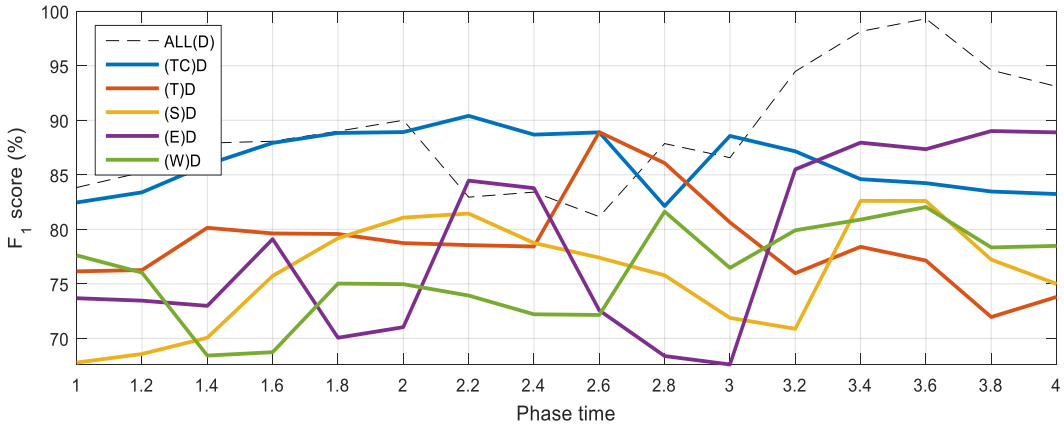
ALL(D)
(TC)D
(T)D
(S)D
(E)D
(W)D
F 1 score (%)
Phase time

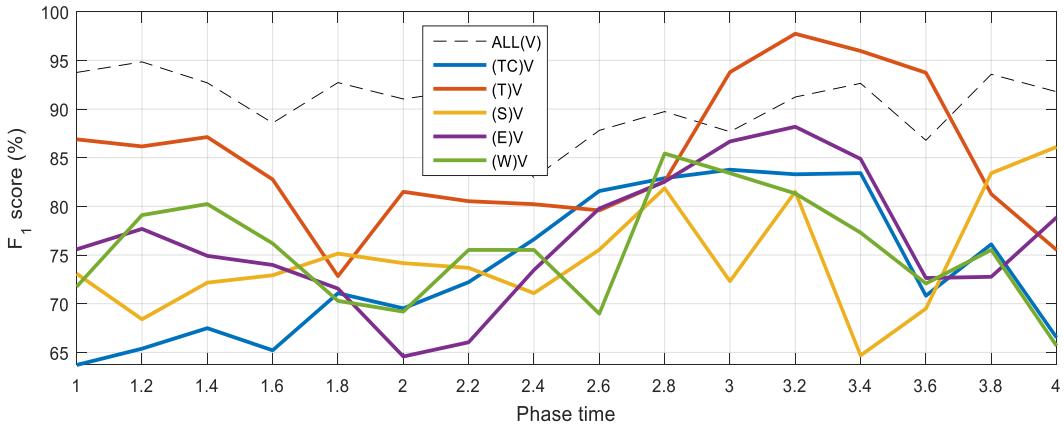
ALL(V)
(TC)V
(T)V
(S)V
(E)V
(W)V
F1 score (%)
Phase time

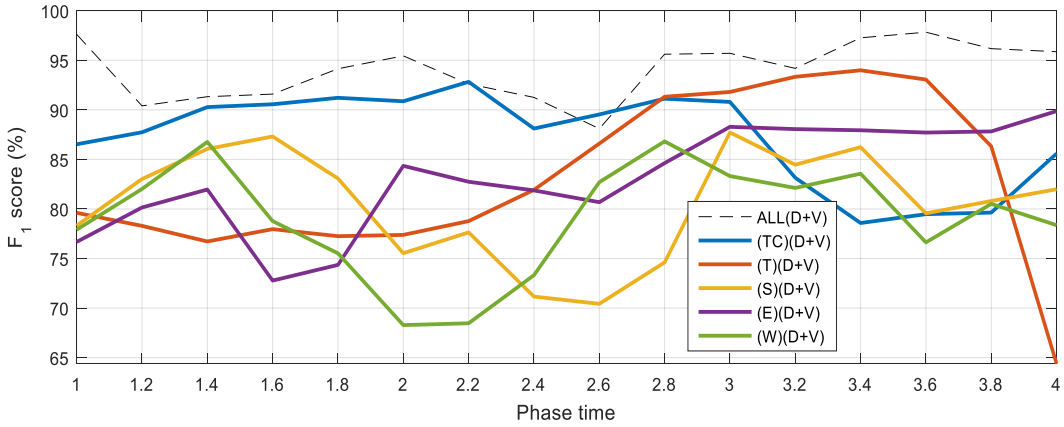
ALL(D+V)
(TC)(D+V)
(T)(D+V)
(S)(D+V)
(E)(D+V)
(W)(D+V)
F1 score (%)
Phase time

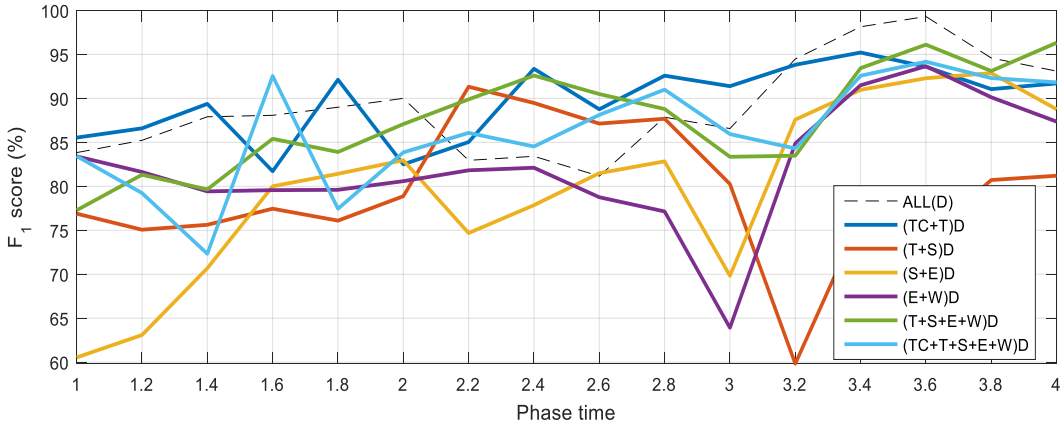
ALL(D)
(TC+T)D
(T+S)D
(S+E)D
(E+W)D
(T+S+E+W)D
(TC+T+S+E+W)D
F1 score (%)
Phase time

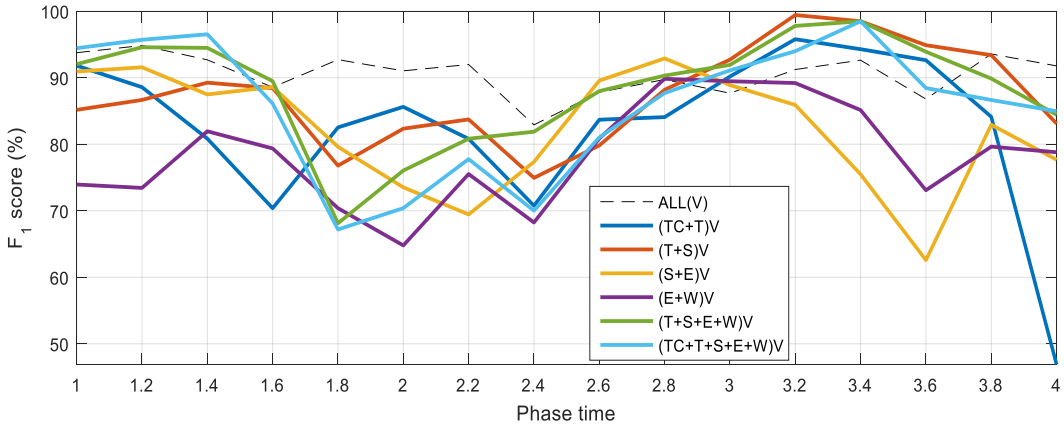
ALL(V)
(TC+T)V
(T+S)V
(S+E)V
(E+W)V
(T+S+E+W)V
(TC+T+S+E+W)V
F1 score (%)
Phase time

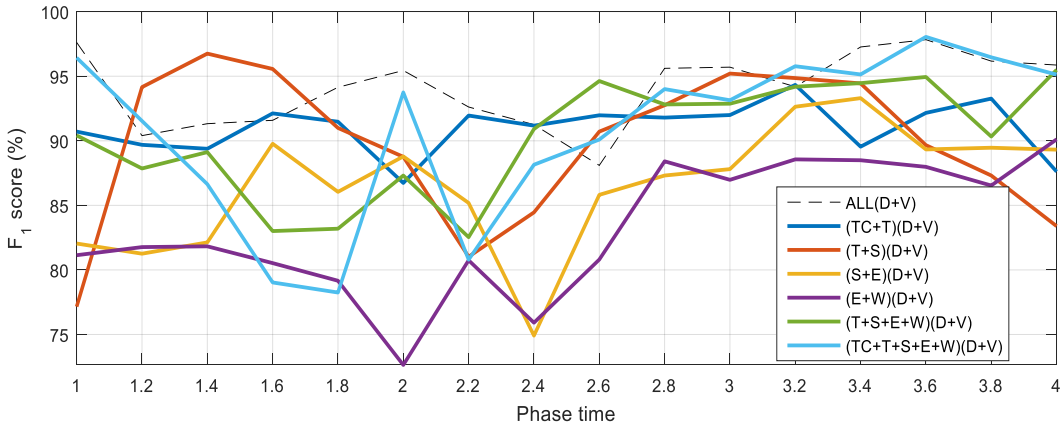
100
95
90
85
80
75
F 1 score (%)
1
1.2
1.4
1.6
1.8
2
2.2
2.4
2.6
2.8
3
3.2
3.4
3.6
3.8
4
Phase time
ALL(D+V)
(TC+T)(D+V)
(T+S)(D+V)
(S+E)(D+V)
(E+W)(D+V)
(T+S+E+W)(D+V)
(TC+T+S+E+W)(D+V)